No. 12885

United States Court of Appeals for the Ninth Circuit.

CONSOLIDATED VULTEE AIRCRAFT CORPORATION and AMERICAN AIR LINES, INC.,

Appellants,

vs.

MAURICE A. GARBELL, INC., and GARBELL RESEARCH FOUNDATION,

Appellees.

Transcript of Record

Volume IV

Book of Exhibits
(Pages 835 to 1005)

Appeal from the United States District Court,
Southern District of California,
Central Division.

Phillips & Van Orden Co., 870 Brannan Street, San Francisco, Calif.

DEFENDANTS' EXHIBIT FF

Engineering Report
Date: November, 1941

No. 1484, Vol. I
No. Pages, 185

The Glenn L. Martin Company
Baltimore

Model B-26 B1 & C

Detail Specification GLM Spec. #88B Contract
DA-W535AC-46
DA-W535AC-19342

Stress Analysis
of Wing

Prepared By:

/s/ VINCENT COUDELLO,
/s/ PETER N. LAYTON, III,
/s/ F. LEIGH NOYES.

Checked By:

/s/ RICHARD K. WENTZ,
/s/ C. H. RIS,
/s/ LEON R. COBAUGH.

Approved By:

/s/ P. C. MEDINA,
A Project Stress Engineer,
/s/ G. N. MANGURIAN,
A Structural Design Engr.,
/s/ G. L. BRYAN, JR.,
Chief Structural Engr.

Revisions

Date	Pages Affected	By	Remarks

. . . .

Defendants' Exhibit FF—(Continued)

Analysis of Wing

Table of Contents

Defendants' Exhibit FF—(Continued)

Defendants' Exhibit FF—(Continued)

References—Volume I

(a) U. S. Army Air Corps "Spec. No. X-1803-A, Stress Analysis Criteria," dated Nov. 15, 1938.

(b) G.L.M. Spec. No. 88; "Detail Specification for Air Corps, Model B-26 Bombardment Airplane, Twin Engine."

(c) Army - Navy - Commerce Bulletin, ANC-1(1); April, 1938, "Spanwise Air Load Distribution."

(d) N.A.C.A. Confidential Memo. Report of Oct. 3, 1939, "Wing Tunnel Tests of a 1/8 Scale Model of Martin 179 Bomber."

(e) N.A.C.A. Confidential Memo. Report of Oct. 7, 1939, "Additional Tests of 1/8 Scale Model of Martin 179 Bomber."

(f) G.L.M. Engineering Report No. 1483, "Stress Analysis of Basic Flight Criteria, Model B-26, B1 & C."

(g) G.L.M. Model B-26, B1 & C Data Book.

(h) G.L.M. Engineering Report No. 1499, "Weight and Balance Report, Model B-26, B1 & C."

(i) U. S. Army Air Corps "Handbook of Instructions for Airplane Designers," 8th Edition, revised to July 1, 1939.

(j) Letter to G. L. Martin Co. from U. S. Army Material Division, CKM-rf-51, October 28, 1939.

Defendants' Exhibit FF—(Continued)

(k) G.L.M. Engineering Report No. 1486, "Stress Analysis of Landing Gear, Model B-26, B1 & C."

(l) G.L.M. Engineering Report No. 1485, "Stress Analysis of Fuselage, Model B-26, B1 & C."

(m) G.L.M. Engineering Report No. 1154, "Stress Analysis of Wing, Model B-26."

(n) Army-Navy-Civil Bulletin, ANC-1(2), "Chordwise Airload Distribution"—Feb., 1939.

Introduction

The stress analysis of the wing for Air Corps Bomber Model B-26-B1&C (Martin Model 179-15) consists of three volumes. Volume I contains the computations of the basic design loads, Volume II contains the stress analysis of the wing box, and Volume III contains the stress analysis of the ribs and structural details. The analysis of the fittings is made in G.L.M. Engineering Report No. 1488.

Volume I Consists of Five Parts:

Part 1—General Data.

Part 2—Spanwise and Chordwise Air Load Distribution.

Part 3—Air Load Computations—Shears, Bending Moments, and Torsional Moments.

Part 4—Unit Load Computations—Dead Weight, Shears, Bending Moments, and Torsional Moments.

Part 5—Net Design Load Computations—Shears, Bending Moments, and Torsional Moments.

Defendants' Exhibit FF—(Continued)

Part 1

General Data

Wing Geometry—Reference (f) and (g)

Span .... 71 ft.

Area .... 659 sq. ft.

Airfoil Section

Station 46.........N.A.C.A. 0016.7-64

Tip (theoretical).....Martin Revision

Root Chord (theoretical at CL).. 166.75 inches

Tip Chord (theoretical) .... 58.12 inches

Incidence (relative to thrust line)....+ 3½°

Mean Aerodynamic Chord...121.5 in. (ref. (f))

Weights

Normal Gross Weight (Ref. (f))....31,000 lbs.

Minimum Flying Weight (Ref. (f)).24,200 lbs.

Overload Gross Weight (Ref. (f))...35,500 lbs.
(Max. Range)

Sign Conventions

The planes of the wing spar webs are perpendicular to a horizontal plane through the thrust line. Forces are resolved into components parallel and normal to the thrust line. Loads and accelerations referred to as being in the "beam" direction are normal to the thrust line while those in the "chord" direction are parallel to it.

Loads and accelerations are positive when up, aft, and out.

Positive beam bending moment causes compression in the upper surface of the wing.

Defendants' Exhibit FF—(Continued)

Positive chord bending moment causes compression in the rear spar.

Positive torsional moments tend to stall the airplane.

All dimensions of lengths and areas are in inches and square inches, respectively, unless otherwise noted.

Reference Axis

A reference axis is used for the calculation of torsional moments. This axis is the intersection line of a horizontal plane through the thrust line and a plane normal to the thrust line which passes through the leading edge of the root chord. (See pages 7 and 75.)

In the detailed analysis of any section of the wing, the torsional moments are transferred from this axis to the elastic axis of the wing section under consideration.

Aerodynamic Center (a.c.)

Aerodynamic loads are assumed to be concentrated at the aerodynamic center. Although the a.c. location along the span does not actually vary linearly, the slight discrepancy introduced by assuming it so is negligible. Therefor for convenience in calculating the torsional moments, a line of aerodynamic centers is assumed, which varies from 23% C at Station 46 to 24% C at theoretical tip. (Ref. page 75.)

ANALYSIS OF WING
DIAGRAM

843

Fig. # 1 Diagramatic Sketch of Wing Ref. (9), F. W.-1

(In True Chord Plane)

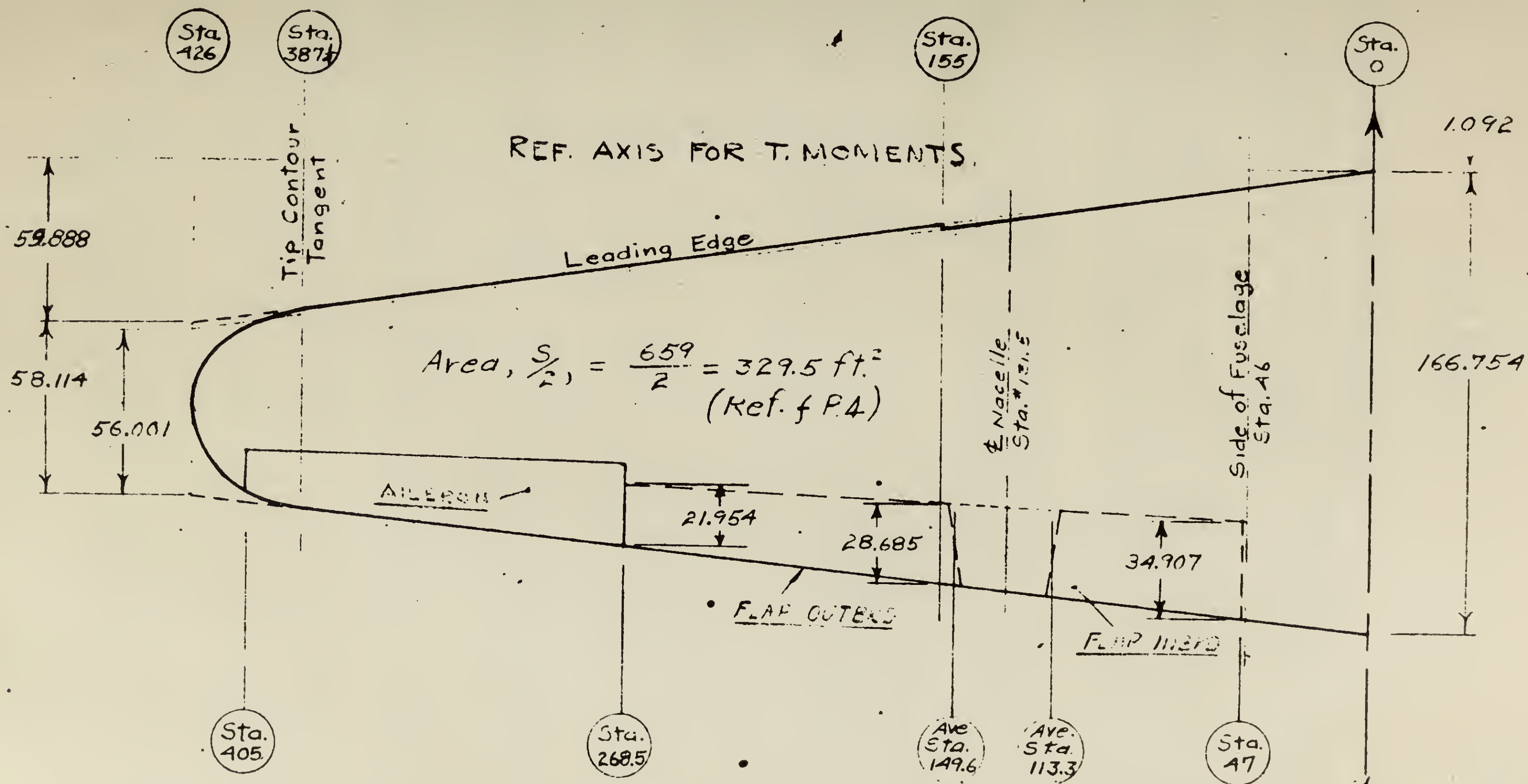

"True" Chords (Inboard of Sta. # 387¼)

Inboard of Sta. # 155:

$$C = 166.754 - \left(\frac{166.754 - 56.001}{426}\right) \times \text{Sta.}$$
$$= 166.764 - .25998(\text{Sta.})$$

Outboard of Sta. # 155:

$$C = 167.846 - \left(\frac{167.846 - 58.114}{426}\right) \text{Sta.}$$
$$= 167.846 - .25759(\text{Sta.})$$

PART No. 2

Span-wise Distribution of Wing Coefficients

The span-wise distribution of wing coefficients is obtained for two conditions:- Wing with flaps neutral (page 9 to 28) and wing with flaps deflected 45° (page 29 to 43).

Since the wing has an effective twist (drooped nose and modified trailing edge) outboard of station 155, the "general method" of Ref. (c) is used to obtain the span distribution of lift and drag coefficients. The distribution of a twisted wing requires two steps, the basic and the additional lift distribution.

The wing tapers uniformly in thickness from tip to root. The chord tapers from theoretical tip to station 155. The chord inboard of 155 is slightly reduced and is assumed to taper uniformly to ℄ airplane (see page 7).

The aerodynamic characteristics of the wing are determined from those of the airfoil sections between station 46 (NACA 0016.7-64) and the theoretical tip (NACA 0010-64 with dropped nose and modified trailing edge). The data obtained from these airfoils are correlated with the characteristics of a similarly shaped wing tested in the wind tunnel.

Wing with Flap Neutral

The basic $\frac{dC_L}{d\alpha}$ vs span (page 10) is adjusted in order to obtain the corrected slope of .072 for the actual A.R. of 7.65 (see page 15).

For the "basic lift distribution" the absolute angles of incidence are estimated (as shown on page 9) to determine the lift distribution which depends on the effective twist and is the same for all angles of attack.

The total lift distributions corresponding to the critical design flight conditions are determined by adding the basic and the additional distributions as shown on page 23 and figure 4 , page 24).

The variation of C_{D_0} is adjusted (fig. 5 p. 26) to give the average C_{D_0} = .0085 (Aerodynamic estimate) over the entire wing.

The C_{d_0} is assumed to have the same variation along the span as C_{d_i} (see page 25).

The total wing drag distribution for the critical design conditions is shown on page 27 and plotted on figure 6 , page 28.

Prepared By
Date 11-17-41
Checked Clements

THE GLENN L. MARTIN COMPANY
BALTIMORE, MD.

Page 47 51
Report No. 1434-I
Model XB-26 B1 C

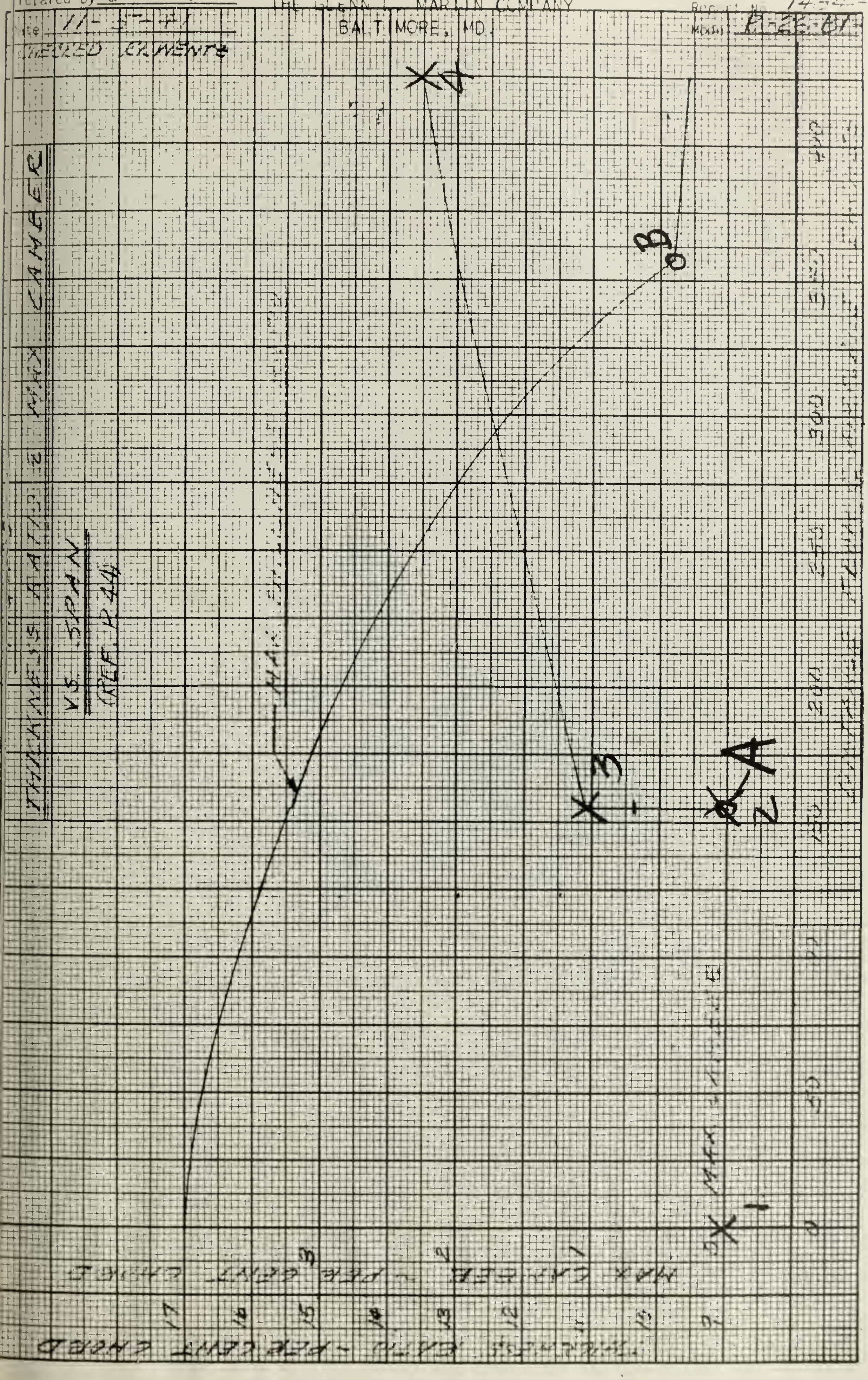

Admitted November 24, 1950.


42160 - 5-28-43

Admitted Novemb:r 24, 1950.

Defendants' Exhibit I I

SUMMARY OF CHANGES IN THE WING GEOMETRY

OF

THE PBM-3

Engineering Report No. 1339

The Glenn L. Martin Company
Baltimore, Maryland
August 16, 1940

Prepared by: J. Goddard

Checked by:

Approved by: Vernon Outman
Chief of Aerodynamics

Approved by:
Chief Research Engineer

INTRODUCTION

Certain changes have been made in the wing geometry of the PBM-3 airplane as compared to the wing of the PBM-1 airplane.

The changes listed below are discussed in the following pages indicating why the changes were made and the improvement to be achieved by each.

The changes are as follows:

1. The wing has been swept back.
2. The thickness of the wing has been increased.
3. The tip plan form has been modified.
4. The form of the leading edge forward of the spar has been changed outboard of the gull.
5. The dihedral of the outer panel has been reduced.
6. The span of the gull portion of the wing has been increased.
7. The wing taper is straight from the ship ℄ to the wing tip.

The changes are discussed individually in the following pages.

DISCUSSION OF THE CHANGES

1 - WING SWEEP-BACK

The theoretical tip chord of the PBM-3 wing has been swept back by an amount which provides a margin of 4% between the maximum rearward c.g. location in percent of the M.A.C. and the c.g. location for which the static longitudinal stability is neutral. This neutral point is at 34.6% and the most aft c.g. is at about 31.1%. Hence the prescribed sweepback gives satisfactory balance and longitudinal stability.

The wing geometry for the PBM-3 is shown in Figure 1 and the geometry for the PBM-1 is shown in Figure 2.

2 - WING THICKNESS DISTRIBUTION

The wing thickness tapers linearly from the ℄ of the ship to the theoretical wing tip. The section at the ℄ is the 23020 and, at the tip, a modified 23010. The PBM-1 wing was 23020 at the ℄ to modified 23006 at the tip.

The above change in thickness was made to provide greater structural stiffness and to improve the stall characteristics toward the wing tip through use of a thicker section which increases the section C_L maximum.

A comparison of the thickness distribution for PBM-3 and PBM-1 is shown in Figure 3.

The increase in wing thickness causes an estimated 0.5 mph top speed decrease.

3 - TIP PLAN FORM

The tip plan form has been modified from the previous Army tip used on the PBM-1 for reasons of appearance.

4 - OUTER WING LEADING EDGE

The nose section contour forward of the spar has been changed to the form shown in Figure 4. This nose section at station 668 is faired linearly into the 23019.024 section at the gull. (Station 173.5)

4 - OUTER WING LEADING EDGE - Contd.

The purpose of this change is to increase the local C_L maximum toward the tip by increasing the camber of the airfoil and moving the maximum camber forward on the cord. This change also tends to delay the angle of attack at which the tip section will stall. The nose radius of the outer wing section has been increased appreciably by this change as shown in Figure 5, where a 4410 tip has been compared with the PBM-1 and the PBM-3 nose radius variation with span. The combined effect of the blunt nose and camber increase is to produce a flat-top lift curve by moving the transition point aft on the wing surface.

Figure 6 gives a comparison of the camber distribution along the span for the PBM-1 and PBM-3 and for the same wing with a 4410 tip.

The effect of the so-called drooped-nose (Figure 4) on the total airplane drag has been estimated from wind tunnel test on a medium bomber with the same type nose section. The drag polar for this model with and without the droop -nose is shown in Figure 7. $\Delta C_{Dp} = .0002$ at $C_L = .35$. Since the droop-nose covers about 75% of the span of the PBM-3 and about 38% of the span of the medium bomber, the drag increment for the PBM-3 is estimated at $\Delta C_{Dp} = .0004$. The corresponding decrease in top speed is one mph. (1)

5 - WING DIHEDRAL

The dihedral of the top skin of the outer wing in the chord plane has been made 0° at the 30% chord stations. This was done in order to reduce the rate of change of rolling moment coefficient with angle of yaw, $\frac{dc_l}{d\psi}$, as much as possible and yet not give the wing a drooped appearance. Reducing the value of $\frac{dc_l}{d\psi}$ tends to reduce the possibility of the occurrence of a Dutch Roll condition. The combination

5 - WING DIHEDRAL - Contd.

of reduced dihedral and increased vertical tail area will materially aid this situation.

6 - GULL SPAN

The span of the inner wing (the gull) has been increased twelve inches on either side of the airplane ℄ in order to make room for the nacelle bomb bay, which holds 4-1000 lb. bombs, and still maintain the same spanwise location of the nacelle ℄ as was the case for the PBM-1.

7 - WING PLAN-FORM TAPER

The PBM-3 plan form taper is maintained straight from the ship ℄ to the tip, just as was done on PBM-1.

FIG. 1

162-B WING
PROJECTED PLAN VIEW.

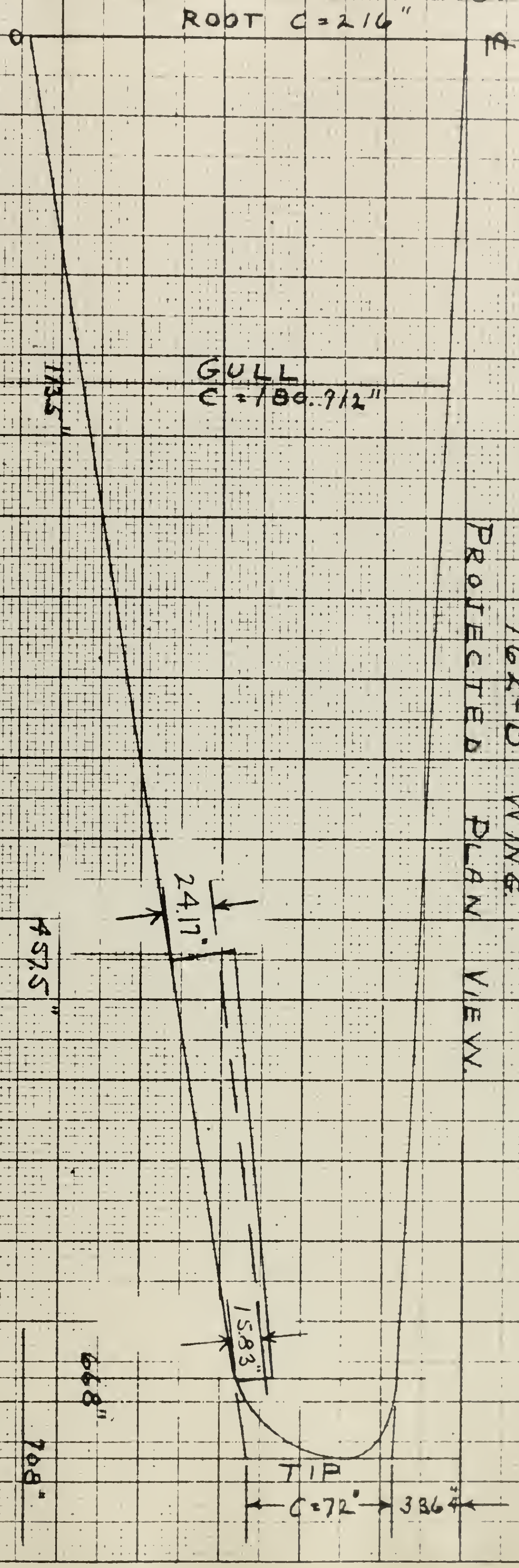

23010 TIP: (DROOPED NOSE)

THICKNESS - IN.	43.2"	34.3"	9.1"	7.2"
% THICKNESS	20	19.024	11.5	10
NOSE RADIUS - % CHORD	4.15	3.80	2.54	1.10
MAX. MEANLINE CAMBER - % THICKNESS	10.00	10.53	30.80	20.0

4410 TIP.

THICKNESS - IN.	43.2"	34.3"	9.1"	7.2"
% THICKNESS	20	19.024	11.5	10
NOSE RADIUS - % CHORD	4.15	3.80	1.45	1.10
MAX. MEANLINE CAMBER - % THICKNESS	10.00	10.53	32.10	40.0

SCALE 1:80

Prepared By
Date 7/31/40

THE GLENN L. MARTIN COMPANY
BALTIMORE, MD.

Report No. 1321
Model 162-?

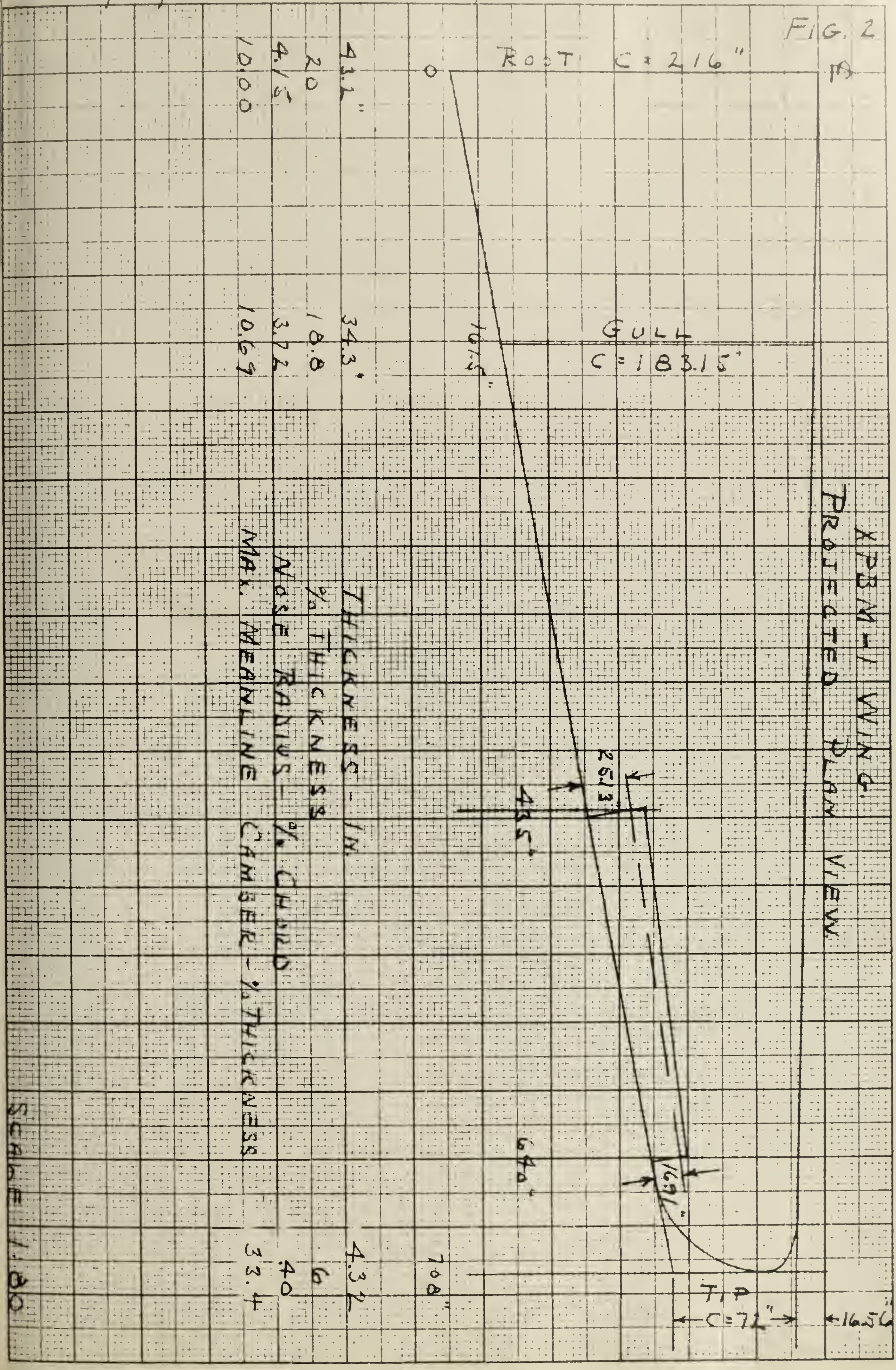

PREPARED BY Goddard — DATE 7/23/40

THE GLENN L. MARTIN COMPANY
BALTIMORE, MD.

856

REPORT NO. 1339
MODEL 162-B

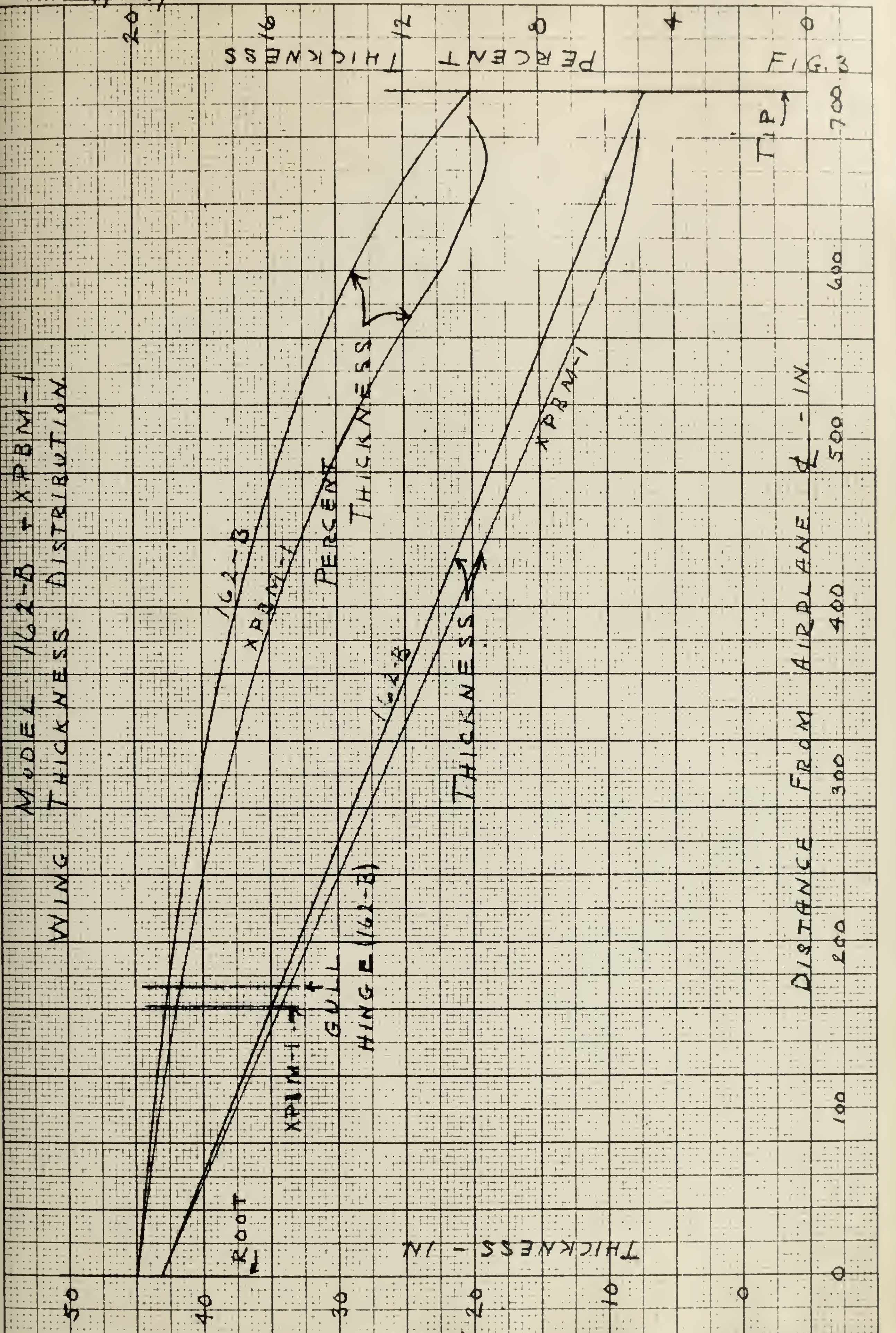

FIG. 4

MARTIN MODEL XPBM-3
WING SECTION AT 668

Prepared By Goddard
Date 8/1/40

THE GLENN L. MARTIN COMPANY
BALTIMORE, MD.

Page 85
Report No. 1339
Model 162-B

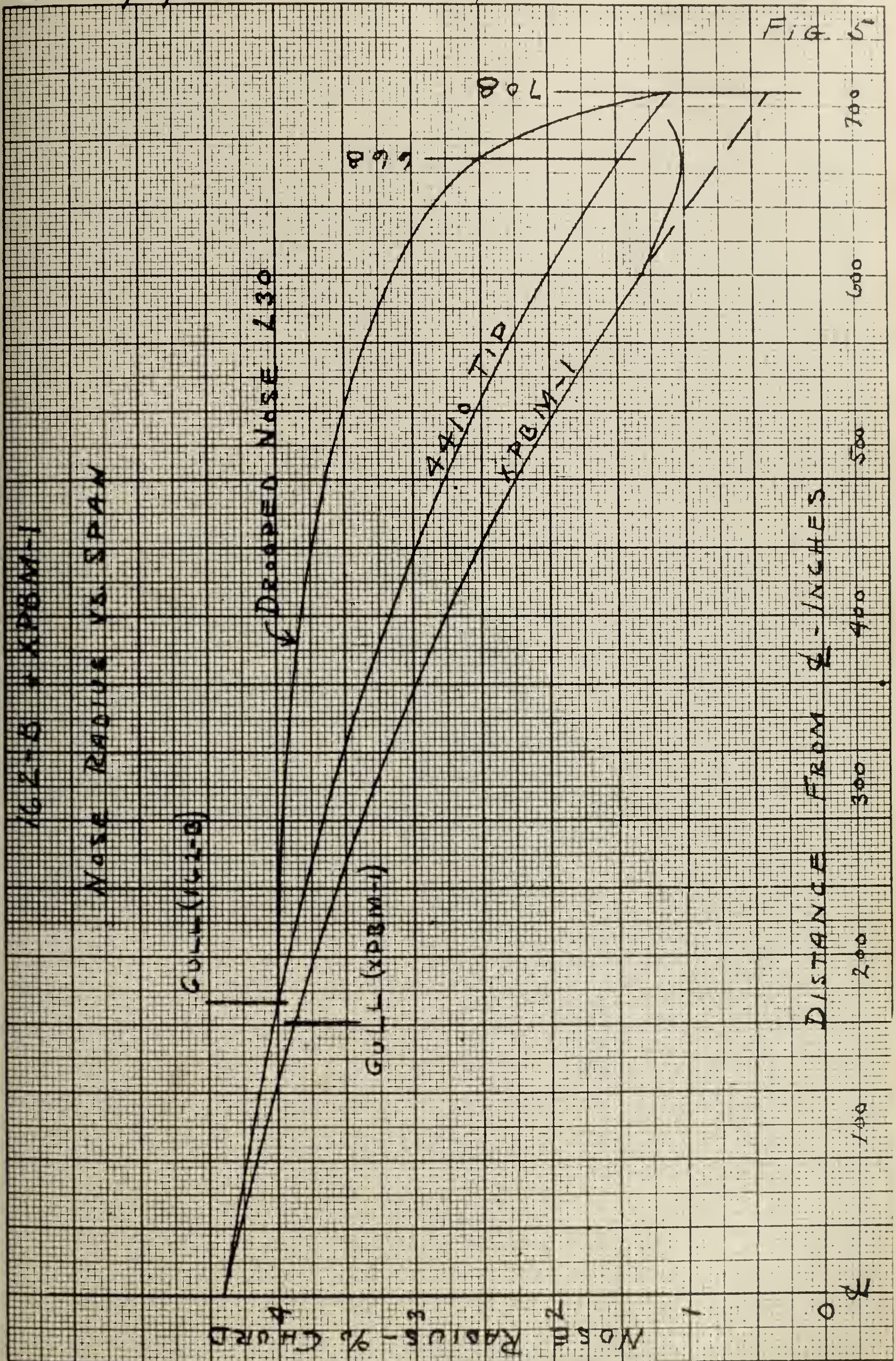

GLM FORM 738

Prepared By Godin...C
Date 8/1/40

THE GLENN L. MARTIN COMPANY
BALTIMORE, MD.

Report No. 1339
Model 162-B

FIG. 6

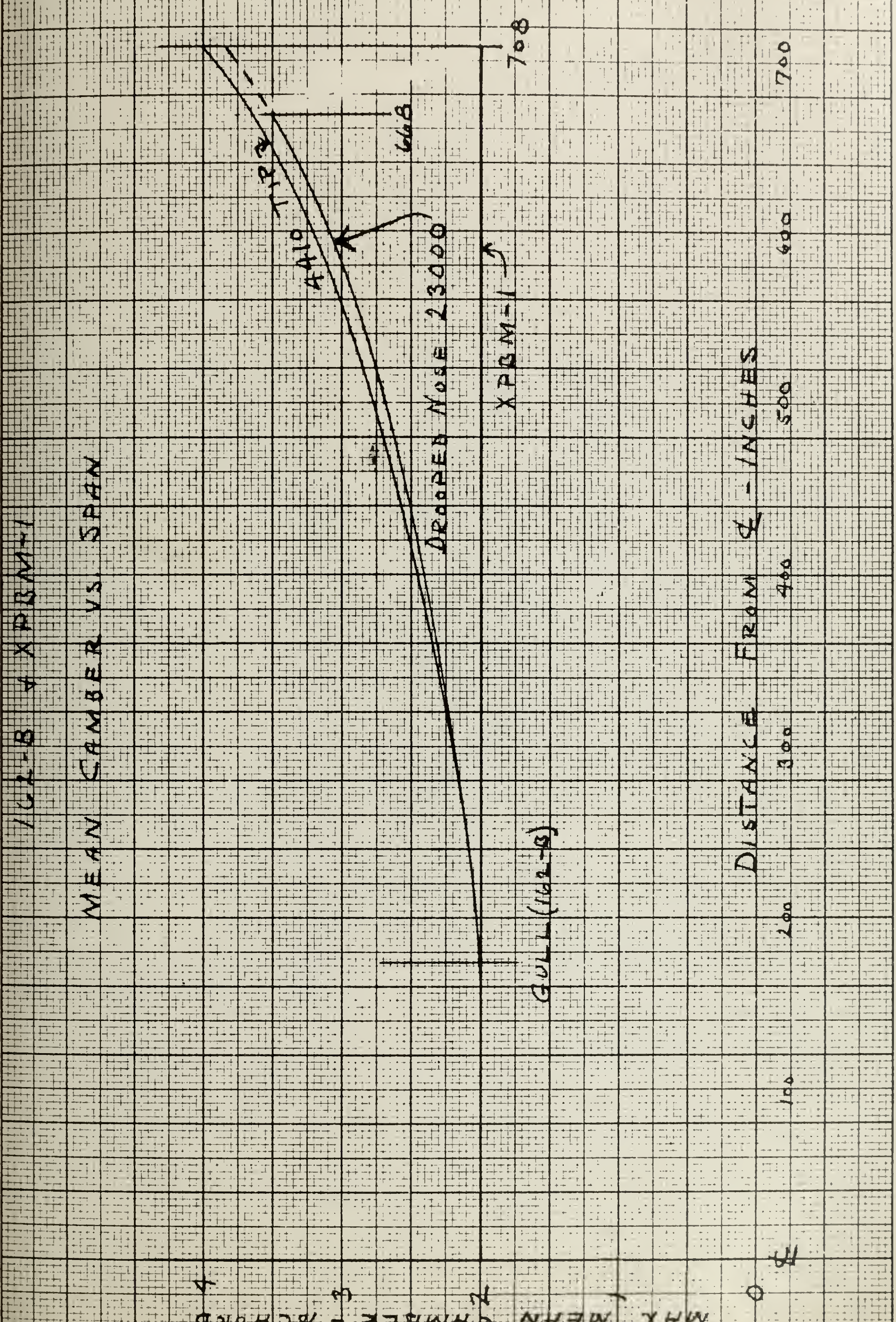

Prepared By [illegible]
Date 8/2/40

THE GLENN L. MARTIN COMPANY
BALTIMORE, MD.

860

1239

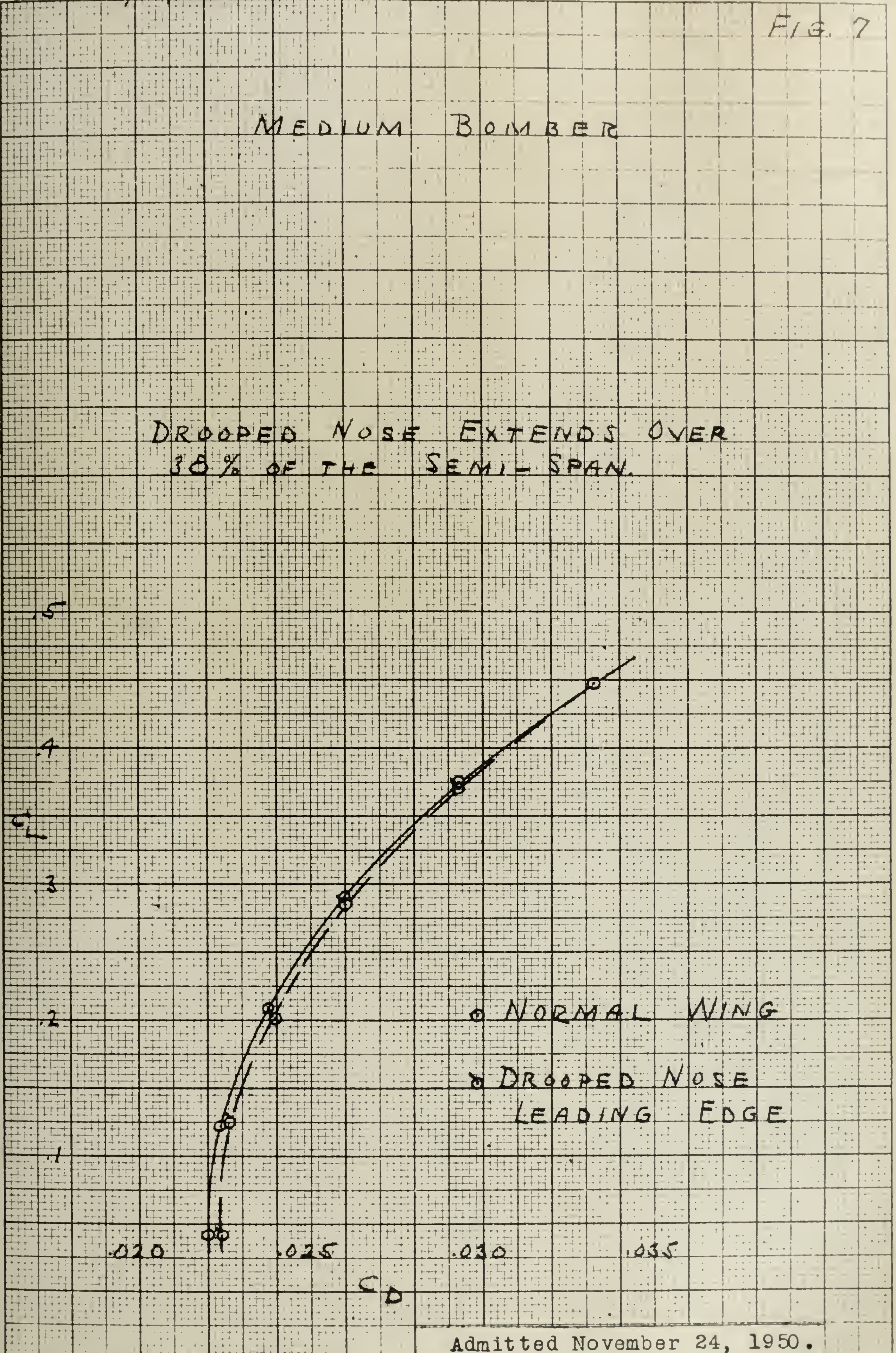

Admitted November 24, 1950.

GLM FORM 738

DEFENDANTS' EXHIBIT NN

DUPLICATE COPY

PAGE W-3

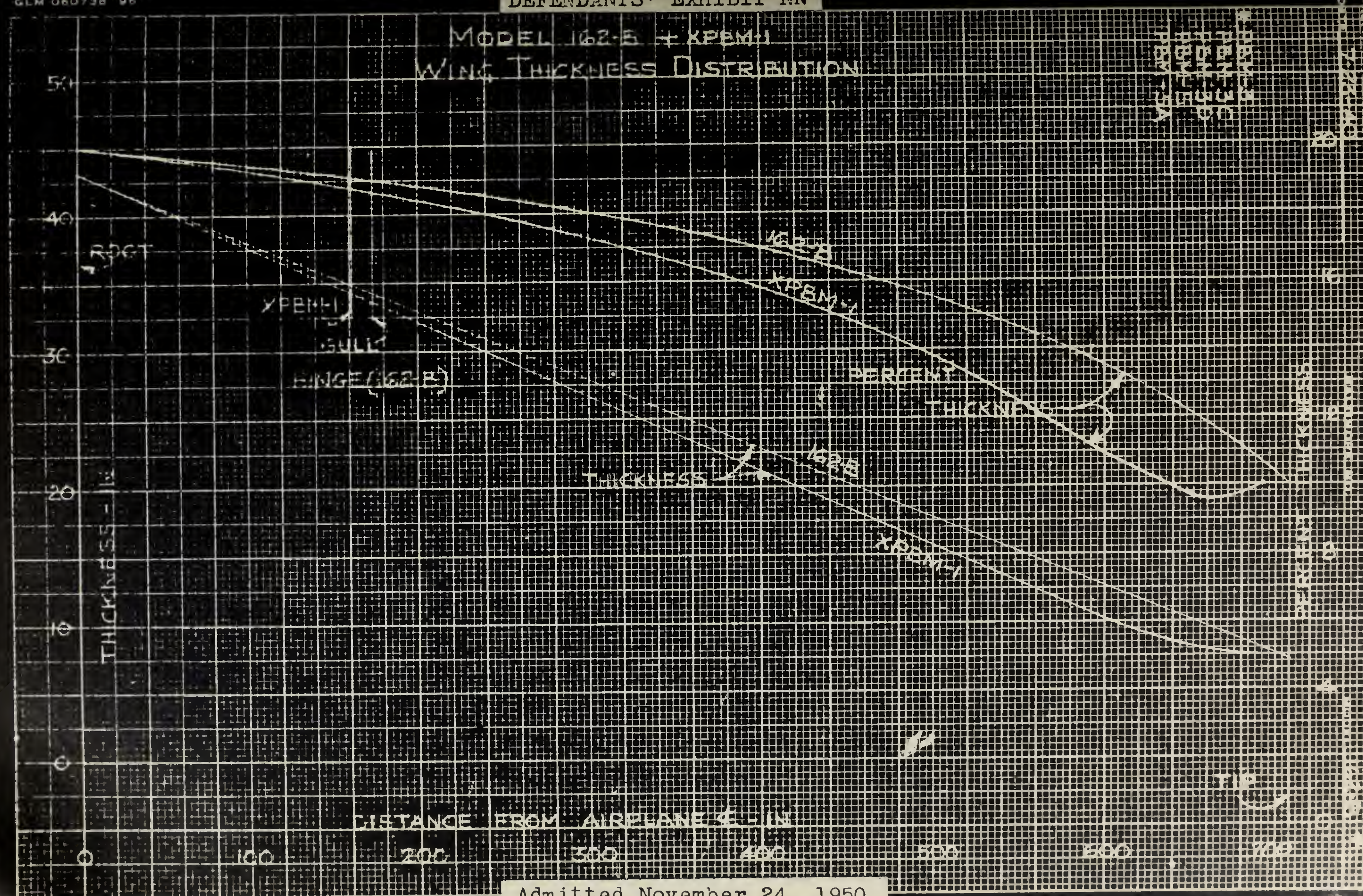

Admitted November 24, 1950.


P-6578

Admitted November 24, 1950.

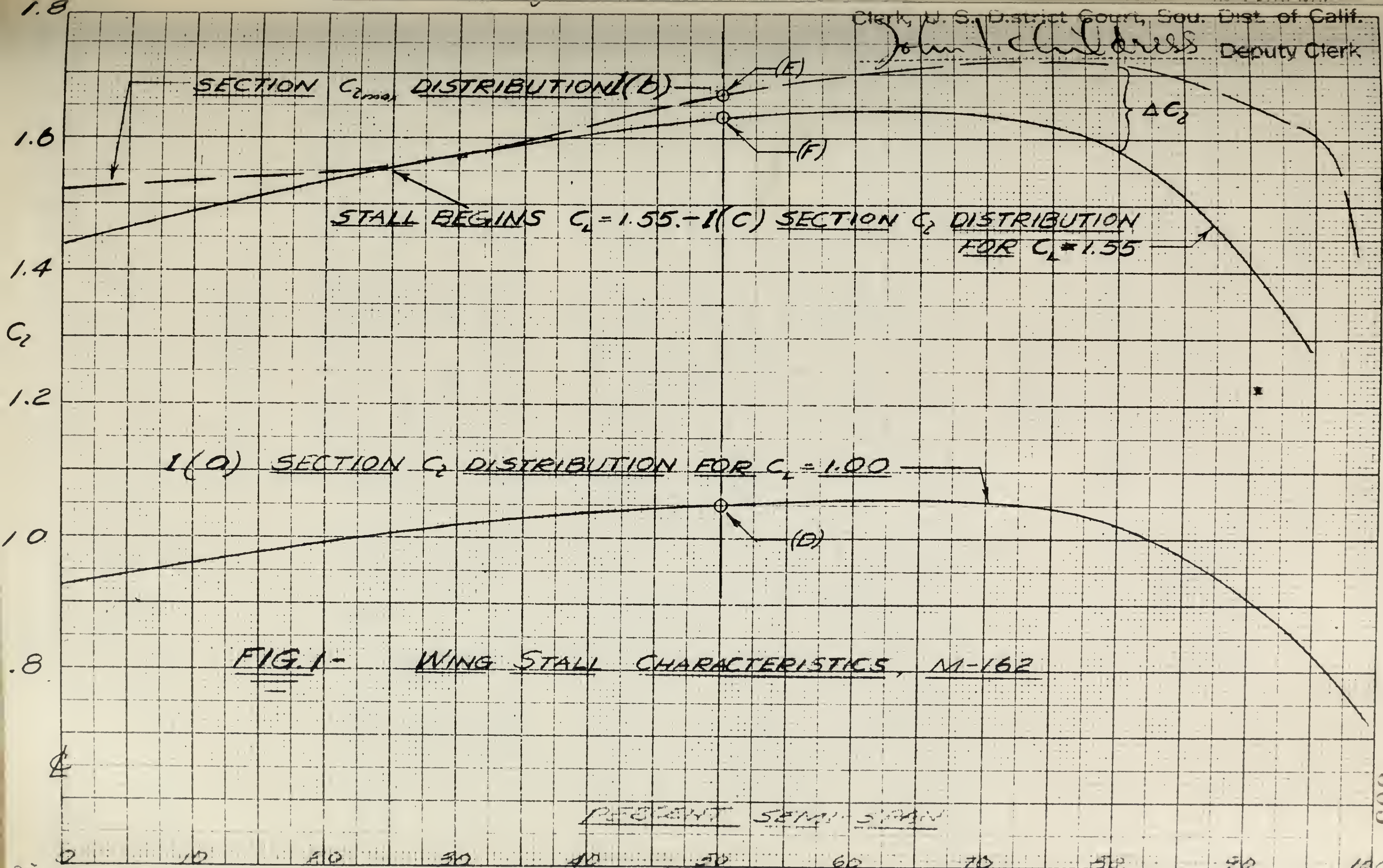

FIG. 1 – WING STALL CHARACTERISTICS, M-162

224

W. G. STREET 12-1-39

NATIONAL ADVISORY COMMITTEE FOR AERONAUTICS

TECHNICAL NOTE NO. 713

A COMPARISON OF SEVERAL TAPERED WINGS DESIGNED TO AVOID TIP STALLING

By Raymond F. Anderson

SUMMARY

Optimum proportions of tapered wings were investigat- by a method that involved a comparison of wings de- ned to be aerodynamically equal. The conditions of odynamic equality were equality in stalling speed, in uced drag at a low speed, and in the total drag at ising speed. After the wings were adjusted to aerody- ic equivalence, the weights of the wings were calcu- ed as a convenient method of indicating the optimum g. The aerodynamic characteristics were calculated m wing theory and test data for the airfoil sections. ious combinations of washout, camber increase in the foil sections from the center to the tips, and sharp ding edges at the center were used to bring about the ired equivalence of maximum lift and center-stalling racteristics.

In the calculation of the weights of the wings, a ple type of spar structure was assumed that permitted integration across the span to determine the web and flange weights. The covering and the remaining weight e taken in proportion to the wing area. The total ghts showed the wings with camber and washout to have the est weights and indicated the minimum for wings with a er ratio between 1/2 and 1/3.

INTRODUCTION

Many investigations have been made of the aerodynamic d the structural aspects of tapered wings with a view to ding the best taper ratio. Investigations of taper tio are reported in references 1 and 2. A general dis- ssion of tapered wings is given in reference 3. Although

EXHIBIT 16

ding and weight were considered in references 1 and 2, the effect of taper ratio on the maximum lift and the manner of stalling of wings was not considered. The effect of taper ratio on the maximum lift is considerable. The tip stall that usually results from the use of tapered wings, moreover, evidences itself as instability in roll at angles of attack less than that corresponding to the maximum lift coefficient. This condition is generally recognized as undesirable from the point of view of handling characteristics in low-speed flight.

It is accordingly considered herein that wings should be designed to avoid tip stalling. With this point of view, wings of different taper ratio were designed to be aerodynamically equal; that is, equal in stalling speed, in induced drag at a low speed, and in total drag at cruising speed. The weights were then calculated to indicate the "optimum" wing (the wing of lowest weight).

In the calculation of the maximum lift, the areas were so obtained that they approximate the values which would be required by wings with full-span flaps. The effect of partial-span flaps was not considered.

Wings with taper ratios of 1/2, 1/3, and 1/4 were considered for a large airplane. In the determination of the maximum lift coefficients, a margin against the stalling of the tips was specified. For the three taper ratios the stalling of three sets of wings was considered: wings with no washout or camber increase in the airfoil sections from center to tip (referred to as the "basic" series, to be described later); wings with washout; and wings with washout and camber increase from center to tips. For each of the three sets of wings, lift-spoiling devices, such as sharp leading edges, were assumed at the center of the wings to make up the required balance of the margin against stalling of the tips. This procedure is practically equivalent to increasing the lift by the use of leading-edge slots over all of the span except for a small portion of the center. The comparative effects of washout and camber should therefore be nearly independent of whether the lift is decreased at the center or increased at the tips.

ASSUMPTION FOR THE AERODYNAMIC CALCULATIONS

The wings had straight tapers and rounded tips and were of a size suitable for a four-engine airplane of 6[illegible],000 pounds gross weight with a wing loading of approximately 30 pounds per square foot. The tip chord of the trapezoid enclosing the rounded tips was used to define the taper ratio, as in reference 4. The distribution of thickness along the span and of camber and washout, when they were used, was linear. A thickness ratio of 0.09 was taken for the airfoil sections at the tips. A basic wing, used to determine the aerodynamic values to be equaled by the other wings, had a root thickness ratio of 0.14, an area of 2,200 square feet, a taper ratio of 1/3, and a span of 138.2 feet. The method of calculating the dimensions of the other wings will be given later. The symbols used are listed in an appendix.

Prevention of Tip Stalling

For the first series of wings of varying taper ratio, the method for prevention of tip stalling was the use of sharp leading edges to reduce $c_{l_{max}}$ at the center of the wings. This series of wings was called the basic series because it included the basic wing of taper ratio 1/3 used to establish the aerodynamic values. The N.A.C.A. 230 series airfoil sections listed in table I were used.

For a second series of wings, washout was used; and, for the third series, washout was combined with an increase in camber of the airfoil sections from center to tips. The increase in camber produces an increase in the $c_{l_{max}}$ of the sections near the tips and thereby causes the stalling point to move inward. For the wings with washout, small amounts of washout were used to prevent excessive increase in the induced drag. Sharp leading edges at the center of the wings were then used to make up the balance of the margin required against stalling of the tips. The case of taper ratio 1/4 was omitted for the series with washout alone because too thin a wing would have resulted.

For all the wings, in order to insure the avoidance of tip stalling, a certain c_l margin was specified at 0.7 b/2 when $C_{L_{max}}$ was reached. (See fig. 1.) The mar-

quired depended on the calculated spanwise position stalling point without sharp leading edges. This occurred where a c_l curve corresponding to the se load distribution became tangent to the $c_{l_{max}}$ as outlined in detail in reference 4. When this ng point was at or inside 0.7 b/2, the c_l margin b/2 was taken as 0.1. When it was outside 0.7 b/2, rgin was increased in the ratio of the distance from nter of the wing to 0.7 b/2. The provision of this of margin when stalling started at the center gave ulated positive damping in roll at the stall that prevent sudden dropping of a wing.

Conditions of Aerodynamic Equality

or the first of the conditions of aerodynamic equal- qual stalling speeds, plain airfoil sections were d when $C_{L_{max}}$ was computed because of the availabil- the $c_{l_{max}}$ data. The Reynolds Number at stalling was made to fall within the usual range for an air- of the size assumed by basing it on the stalling with flaps, so that the wings had approximately the reas as wings with full-span flaps. That the condi- f stalling-speed equality would not be appreciably d by considering the wings to have full-span flaps rified from figure 60 of reference 5, which gives $c_{l_{max}}$ increments produced by flaps. (The range of verage thickness of the wings was small.)

s the stalling speed V_S is equal to $\sqrt{\dfrac{2W_g}{\rho\ S\ C_{L_{max}}}}$ W_g was fixed, the stalling-speed condition required the product $SC_{L_{max}}$ for each wing be equal to the ct for the basic wing (taper ratio 1/3).

he second condition was that the induced drags should ual at a speed corresponding to a C_L of 1.0 for the wing (low-speed condition). The induced drag rather the total drag was used because the induced drag was y all of the drag and was relatively easy to calcu- The induced drag, with the effect of twist ϵ in- d, may be found from

$$D_i = \frac{W_g^2}{q\pi b^2 u} + W_g\ \epsilon\ a_0\ v + q\ S\ (\epsilon\ a_0)^2\ w \qquad (1)$$

o the spans required to make the induced drags equal may b expressed

$$\frac{b}{b_b} = \sqrt{\frac{u_b\ D_{i_b}}{u\ [D_{i_b} - W_g\ \epsilon\ a_0\ v - q\ S\ (\epsilon\ a_0)^2\ w]}} \qquad (2)$$

wcre the subscript b refers to the basic wing, and

$$D_{i_b} = \frac{W_g^2}{q\ \pi\ b_b^2\ u_b} \qquad (3)$$

Euation (3) is equation (1) with the last two terms omitt d because the basic wing has no twist. These equations wre derived from the formula for C_{D_i} given in reference

The third condition, equal cruising speeds, was satisfed by making the drags equal at cruising speed, as the pwer was assumed constant. Cruising speed corresponded to a C_L of 0.3 for the basic wing.

METHOD OF CALCULATION

Proportions and Aerodynamic Characteristics

The method used for calculating $C_{L_{max}}$, C_{D_0}, and the oher aerodynamic characteristics of the wings has been fund to give results that agree well with test results (eferences 4 and 6).

The method of calculating the maximum lift coefficient r the basic wing is illustrated in figure 1. For this wng, $c_l = c_{l_a}$ because there is no washout and therefore $c_{l_b} = 0$. Stalling was calculated to occur without any shar lading edge at 0.7 b/2; that is, c_{l_a} would reach $c_{l_{max}}$ frst at the 0.7 point. (See reference 4 for a detailed

explanation.) A value of c_{l_a} of 0.1 less than the $c_{l_{max}}$ at $y = 0.7\ b/2\ (c_{l_a}')$ was then the lift coefficient corresponding to $C_{L_{max}}$. Numerically, $C_{L_{max}} = c_{l_a}'/c_{l_{a1}}$, where $c_{l_{a1}}$ was taken at $y = 0.7\ b/2$. The values of $c_{l_{max}}$ at the center of the wing were then considered to be reduced by a sharp leading edge to the values of c_{l_a}, as shown, so that stalling would begin at the center of the wing. The values of $c_{l_{max}}$ used for calculating $C_{L_{max}}$ for this wing were taken from reference 5.

The value of the induced drag at the low-speed condition for the basic wing, D_{i_b}, to be used in finding the spans of the other wings was calculated from equation (3).

The drag of the basic wing at cruising speed was calculated in terms of q in the form

$$\frac{D}{q} = \frac{D_o}{q} + \frac{D_i}{q} \tag{4}$$

The value of D_o/q was calculated for a C_L of 0.3 and for the cruising-speed Reynolds Number (as outlined in reference 4) by a graphical integration along the span of the section drags from

$$\frac{D_o}{q} = \int_0^{b/2} c_{d_o}\ c\ dy \tag{5}$$

The values of c_{d_o} were taken from reference 7 for the basic wing as well as for the others. The value of D_i/q was calculated from equation (3) for a value of q corresponding to the cruising speed.

With the values for the basic wing established, equal values for the other wings were found by successive approximations. For the other two wings of the basic series, a root thickness and an area were assumed that, it was hoped, would produce the desired characteristics. An approximate

span was then found from equation (2) so that c and c_{l_a} could be found. For these values, $C_{L_{max}}$ was then calculated in the same manner as for the basic wing.

For the wings with washout and with washout and camber increase, airfoil sections and washout were assumed. The value of $C_{L_{max}}$ was then calculated as for the basic wing, except that c_{l_b} due to washout was combined with c_{l_a} to obtain c_l, as shown in figure 2.

From the values of $C_{L_{max}}$ for the wings, a more accurate value of S was found for each wing to obtain a product of S and $C_{L_{max}}$ equal to the value for the basic wing. The approximate span was used to calculate the aspect ratio so that the induced-drag factors u, v, and w could be found from reference 4. A more accurate value of the span to obtain the required induced drag at low speed could then be found from equation (2). A value of a_0 of 0.1 per degree was used. From S and b, more accurate values of c could be found so that D/q could be computed.

The value of D/q at cruising speed for each wing was next found from equation (4), where the value of D_0/q was calculated from equation (5) for a C_L corresponding to the cruising speed and the wing area. The value of D_i/q was then found from equation (1) for a value of q corresponding to the cruising speed. If the values of D/q calculated in this manner were not close to the value for the basic wing, new values of root thickness ratio were assumed and the calculations were repeated.

Successive approximations were repeated in this manner until the required values of $SC_{L_{max}}$, b, and D/q were obtained. Two or three approximations were usually required. The resulting dimensions and the values of D/q are given in table I. The amounts of washout required were a compromise between a high $C_{L_{max}}$ and a low induced drag. In order to investigate the effect of greater washout, calculations were made for a wing with camber increase and washout with a taper ratio of 1/3, and with $\epsilon = -4^\circ$, but the results were not included in the table because the weight was excessively increased. It should be noted that

the washout is "aerodynamic"; that is, it is measured, not from the chord, but from the zero-lift directions of the root and the tip sections.

Weight of the Wings

The load factors for calculating the weights of the wings were computed as specified in reference 8. A high speed of 240 miles per hour was used with a gust of 30 feet per second, as given for condition I in reference 8. The lift-curve slope was computed from figure 2 of reference 4. The values of the limit-load factors n, computed in this manner, are listed in table I.

The C_N to be used for calculating the load on the wings was then found from

$$C_N = \frac{n(W_g - W)}{qS} \tag{6}$$

where W_g is the gross weight; W, the assumed wing weight; and q corresponds to a speed of 240 miles per hour. The load distribution per unit length along the span, l, was then found from $l = q\, c_l\, c$ where c_l was found as in reference 4 from

$$c_l = C_N\, c_{l_{a1}} + c_{l_b} \tag{7}$$

For the wings without twist, c_{l_b} is zero.

The values of $c_{l_{a1}}$ and c_{l_b} were calculated from the load-distribution data given in reference 4 so that the variation of the load distribution with taper was taken into account. From the distribution of load across the span, the distribution of the shear and the moment could be easily found.

The shears and the moments were assumed to be carried by a single spar with a simple type of structure as shown in figure 3, so that the weights of the material could be

rl by an integration across the span. The torsion load eliminated by assuming the spar to be located at the center of each section may be considered to be carried by the skin.

The relieving loads caused by the engines and the fuse were taken into account so that the total wing hts were calculated in the form

$$W = W_W - \Delta W_W + W_F - \Delta W_F + W_C \tag{8}$$

The weights thus calculated may not agree with the hts of actual airplane wings because of the simple of structure assumed and the improbability that all material will develop the stress assumed. The effects he assumptions should, however, be similar on all the s so that the correct relative weights should be obable.

The load distributions across the semispan of the s, computed in the manner previously given, had the represented in figure 3. From the load, or $c_l c$, es, the shears and the moments at any point y along semispan were found from

$$F_S = q \int_y^{b/2} c_l c \, dy \tag{9}$$

$$M = \int_y^{b/2} F_S \, dy \tag{10}$$

shear bracing was assumed to have an angle of 45°, as n in figure 3. For a unit length along the span dy esponding to a unit length of bracing dL, the weight he web will be

$$dW_W = p \frac{f}{s} dL = p \frac{F_S}{0.707s} \frac{dy}{0.707} = \frac{2p\,F_S}{s} dy \tag{11}$$

e

p is the specific weight (assumed to be an aluminum alloy weighing 0.1 pound per cubic inch).

s, allowable stress.

f, force in a diagonal.

a factor of safety of 1.5, the web weight for both es of the wing is then

$$W_W = 4 \times 1.5 \frac{p}{s} \int_0^{b/2} F_S \, dy \tag{12}$$

nservative stress of 20,000 pounds per square inch was med in calculating W_W.

In the calculation of the weight of the flanges, the nt at any point along the span was considered to be ried by tension and compression in the flanges. If F he force in a flange (fig. 3) and if the effective kness of the beam t' is taken as 0.9 the wing thick-, then the weight of a unit length of one flange will

$$dW_F = p \frac{F}{s} dy = p \frac{M}{t's} dy \tag{13}$$

weight of upper and lower flanges for both halves of wing, with a factor of safety of 1.5, is then

$$W_F = 4 \times 1.5 \frac{p}{s} \int_0^{b/2} \frac{M}{t'} dy \tag{14}$$

n equations (12) and (14), the web and the flange ghts were found by graphical integration of curves of and M/t' along the semispan. Values of s of 20,000 nds per square inch for compression and 30,000 pounds square inch for tension were used to calculate the nge weights.

In the calculation of the weight decrements due to the ieving loads, the concentrated loads shown in figure 3 e considered, and the useful loads were omitted to be conrvative. The shear was assumed to be taken off at the

lage wall so that half the weight of the body $W_B/2$ at a distance y_B. The weight of the body consists he complete weight of the fuselage and the tail, less useful load. The nacelles and the cowling were includ- n the power-plant weights, W_{P_1} and W_{P_2}, and the ing-gear weight was included in W_{P_1}. The correct rel- e weights of the relieving loads were established by a nt analysis.

The relieving effect of each load on the web weight roportional to the load times its distance from the er. Then, from equation (11), the web-weight decrement both halves of the wing, with a factor of safety of 1.5 a limit-load factor n, may be written

$$\Delta W_W = \frac{4 \times 1.5\ pn}{s} \left(\frac{W_B}{2}\ y_B + W_{P_1}\ y_1 + W_{P_2}\ y_2\right) \qquad (15)$$

same value of s was used as in the web-weight calcu- on.

The relieving effect of each load on the flange weight roportional to the moment times the distance of the from the center. Then if t_s' is 0.9 the root thick- , the weight decrement due to the relieving loads for flanges and both halves of the wing will be, from equa- (13),

$$\Delta W_F = \frac{4 \times 1.5\ pn}{t_s'\ s} \left(\frac{W_B}{2}\ y_B^2 + W_{P_1}\ y_1^2 + W_{P_2}\ y_2^2\right) \qquad (16)$$

same values of s were used as for the flange-weight ulation.

The final weight item W_C, which included the cover- and all of the structural weight other than that of beam, was taken as a constant proportion of the wing . The net weights of the various structural parts of wing and the total weights are listed in table I. As wing weight was found, it was compared with the as- d weight used in equation (6) and the calculations repeated until the value of the weight assumed did not ct the final weight.

RESULTS AND DISCUSSION

From the dimensions and the characteristics of the wings listed in table I, the effect of changes of the taper and of the method to prevent tip stalling may be noted. The effect of a change of the taper on $C_{L_{max}}$ and on the resulting area may be explained as follows. As the taper is increased, c_l increases from the center to the tip of the wing. In addition, the Reynolds Number decreases toward the tips so that, for the usual airfoil sections, $c_{l_{max}}$ decreases. The value of $C_{L_{max}}$ is thereby reduced and stalling tends to start nearer the tips. A greater amount of the means to prevent stalling of the tips must therefore be used to obtain the desired c_l margin, as the taper is increased. The amount required may be measured in terms of the difference, at the center of the wing, between $c_{l_{max}}$ and the c_l corresponding to $C_{L_{max}}$ (shown by Δc_l in fig. 1). Thus, Δc_l increases with taper, as listed in table I. Because of the foregoing effects, the areas also tend to increase with the taper, as shown in table I.

The change in span required to obtain the desired induced drag for the low-speed condition depends only on the value of the induced-drag factor u for wings without twist. As the value of u, which is a measure of the change of induced drag with taper for wings without twist, changes only slightly with the taper, the span varies only slightly, as shown in table I. The wings with washout, however, require a greater change in span owing to the twist, as may be seen from equation (2) and as given in the table.

The increase in area with increase in taper previously mentioned requires a reduction in thickness to obtain the required low value of the profile drag at the cruising condition. The exact value of profile drag required also depends on the induced drag at cruising speed, as the total drag must have a fixed value. This induced drag tends to be adversely affected by an increase in taper or in washout. The combined effect of washout and taper is appreciable for the wings with washout and camber increase, as shown by the values of D_i/q in the table. The foregoing effects cause the required thickness to decrease with the taper.

When the thickness was changed to make another approximation in the calculation of the characteristics of the s, $C_{L_{max}}$ was affected as well as the drag. Whether change increased or decreased $C_{L_{max}}$ depended on the kness ratio near 0.7 b/2 and on the corresponding x. The effect may be predicted for any particular from figure 55 of reference 6, which shows the variaof $c_{l_{max}}$ with thickness ratio. A decrease in root kness ratio usually increased $C_{L_{max}}$.

For the wings with camber increase, the increase in er toward the tips increased $c_{l_{max}}$ and produced er $C_{L_{max}}$ values and lower areas. As some sharp leadedge was used for all the wings to obtain the desired margin, the wings should be comparable in their avoid- of tip stalling.

For the wings with washout and camber increase, the red margin could have been obtained by more washout the induced drag would have been too greatly increased. l amounts of washout were used, as listed, and the camwas increased from 3 to 4 percent of the chord as the r ratio changed from 1/2 to 1/3. No further increase amber for the wing of taper ratio 1/4 was used because would have produced no further increase in $c_{l_{max}}$.

With reference to the weights of the wings, it may be d that the lowest weights were obtained for the wings camber increase and washout. The lowest weight is inated for a taper ratio between 1/2 and 1/3, as may be from figure 4. In order to determine whether the low- weight had been approached, the case of taper ratio with washout and camber increase was investigated with ce as much washout, or 4°. The increase in washout red a reduction in thickness to obtain the desired drag cruising speed and an increase in span to maintain the ired induced drag at low speed. The result was a conorable increase in weight.

If this analysis were applied to wings of other size, ax and D_o would be affected by the change in Reynolds ber, but it is believed that considerable variation in e would be possible without altering the conclusion as the best taper ratio. The number of engines is also of

ight importance because the effect of their relieving ad on the wing weight is small. It is also believed at, for the thickness ratios in common use, the selection of a different thickness ratio for the basic wing uld not appreciably alter the conclusions.

As an aid in similar calculations and to show the effect of washout on C_{D_i}, the change in C_{D_i} due to washout has been plotted in figures 5 to 7. The increase in C_{D_i} may be considered to consist of two parts, which may be found by dividing the last two terms of equation (1) by A. The $w(\epsilon\, a_o)^2$ term is the increase in C_{D_i} for C_L = 0 and varies mainly with ϵ^2, as w does not vary much in the usual range of taper ratios. (See fig. 6 of reference 4.) The term $v\,\epsilon\, a_o\, C_L$ contributes a positive or negative increment depending on the sign of v except that, for the elliptical wing, $v = 0$ and ΔC_{D_i} does not vary with C_L. For the tapered wings, however, ΔC_{D_i} increases with C_L for taper ratios less than about 1/2, as may be seen from figures 5 to 7.

For taper ratios approaching 1, ΔC_{D_i} becomes negative for high values of C_L as shown by figure 7, which means that an elliptical span loading is approached owing to the washout. Values of ΔC_{D_i} for other aspect ratios and taper ratios, for either washin or washout, may be calculated from reference 4.

The values of ΔC_{D_i} given are for wings with linear twist distribution along the span. Wings are commonly constructed using straight-line elements between corresponding points of the root and the tip sections. For such a construction, the twist distribution is nonlinear and, for a given washout at the tip, ΔC_{D_i} is less than for a linear twist distribution. As an illustration of the order of magnitude of the difference that the type of twist distribution may produce, values of ΔC_{D_i} are given in figure 8 for wings with trapezoidal tips and with the two types of twist distribution. As may be seen, the differences are small. With reference to the effect of the type of twist distribution on the lift distribution, and hence on the margin against stalling of the tips, it may be said that the amount of washout required is substantially the

for the two types of twist distribution for taper os between 1/3 and 1.0.

From the present paper and from the data given in rence 4, similar calculations can be made for wings ny size and for any aerodynamic conditions. Analyses ld probably be made for wings with partial-span flaps other high-lift devices.

CONCLUSIONS

For wings within the range of thickness ratios comy used, designed to be aerodynamically equal, and with stalling avoided by the methods considered, the res of this analysis indicate that:

1. The optimum wings (the wings of the lowest weight) obtained when tip stalling is prevented by the use of rate washout combined with an increase in camber of airfoil sections from the center to the tip.

2. The optimum wings have a taper ratio between 1/2 1/3.

gley Memorial Aeronautical Laboratory,
National Advisory Committee for Aeronautics,
Langley Field, Va., May 3, 1939.

APPENDIX

Symbols

S, wing area.

b, span.

b_b, span of basic wing.

A, aspect ratio, b^2/S.

c, chord at any section along the span.

ϵ, aerodynamic twist, in degrees, from root to tip, measured between the zero-lift directions of the center and the tip sections, negative for washout.

y, distance along the span measured from the center.

y_s, see figure 3.

a_o, section lift-curve slope, per degree.

c_l, section lift coefficient; $c_l = c_{l_a} + c_{l_b}$.

c_{l_b}, part of lift coefficient due to aerodynamic twist (computed for $C_L = 0$); $c_{l_b} = \frac{\epsilon a_o S}{cb} L_b$.

c_{l_a}, part of lift coefficient due to angle of attack at any C_L; $c_{l_a} = C_L c_{l_{a1}}$.

$c_{l_{a1}}$, part of lift coefficient due to angle of attack for $C_L = 1.0$; $c_{l_{a1}} = \frac{S}{cb} L_a$.

L_a, L_b, additional and basic load distribution parameters (Values of L_a and L_b were taken from reference 4 to obtain the load distributions.)

$c_{l_{max}}$, airfoil section maximum lift coefficient.

c_{d_o}, airfoil section profile-drag coefficient.

882

C_N, wing normal-force coefficient (taken equal to C_L).

C_L, wing lift coefficient.

$C_{L_{max}}$, wing maximum lift coefficient.

C_{D_o}, wing profile-drag coefficient.

C_{D_i}, wing induced-drag coefficient.

ΔC_{D_i}, increase in wing induced-drag coefficient due to aerodynamic twist.

D, total wing drag.

D_o, wing profile drag.

D_i, wing induced drag.

D_{i_b}, induced drag of the basic wing.

and w, induced-drag factors (reference 4).

n, limit-load factor.

l, load distribution per unit length along the span.

W_g, airplane gross weight.

W, wing weight.

Subscripts W, F, and C refer to web, flange, and cover weights, respectively.

Δ refers to a weight decrement due to relieving loads.

F_S, shear force at any point along the span.

M, bending moment at any point along the span.

p, specific weight (of aluminum alloy, 0.1 lb./cu. in.).

s, allowable stress.

t', effective thickness of beam at any point along span.

t_s', effective thickness of beam at center of wing.

REFERENCES

1. Upson, Ralph H.: Wings - A Coordinated System of Basic Design. S.A.E. Jour., vol. XXVI, no. 1, Jan. 1930, pp. 15-30.

2. Upson, R. H., and Thompson, M. J.: The Drag of Tapered Cantilever Airfoils. Jour. Aero. Sci., vol. 1, no. 4, Oct. 1934, pp. 168-177.

3. Lachmann, G. V.: Aerodynamic and Structural Features of Tapered Wings. R.A.S. Jour., vol. XLI, no. 315, March 1937, pp. 162-212.

4. Anderson, Raymond F.: Determination of the Characteristics of Tapered Wings. T.R. No. 572, N.A.C.A., 1936.

5. Jacobs, Eastman N., Pinkerton, Robert M., and Greenberg Harry: Tests of Related Forward-Camber Airfoils in the Variable-Density Wind Tunnel. T.R. No. 610, N.A.C.A., 1937.

6. Anderson, Raymond F.: The Experimental and Calculated Characteristics of 22 Tapered Wings. T.R. No. 627, N.A.C.A., 1938.

7. Jacobs, Eastman N., and Abbott, Ira H.: Airfoil Section Data Obtained in the N.A.C.A. Variable-Density Tunnel as Affected by Support Interference and Other Corrections. T.R. No. 669, N.A.C.A., 1939.

8. Bur. Air Commerce, U. S. Dept. Commerce: Airplane Airworthiness. Pt. 04 of Civil Air Regulations, May 1938, pp. 12 [38] and 59 [85].

obtained by -	ratio	(sq.ft.)	ratio, A	(ft.)	c_s (ft.)	c_t (ft.)	section N.A.C.A.	section N.A.C.A.		(deg.)
Sharp leading edge	1/2	2,132	8.93	138.0	20.91	10.46	23015.4	23009	0.16	0
	1/3	2,200	8.68	138.2	24.20	8.07	23014	23009	.36	0
	1/4	2,350	8.16	138.5	27.29	6.82	23011	23009	.43	0
Washout and sharp leading edge	1/2	2,090	9.13	138.1	20.48	10.24	23015.5	23009	--	2
	1/3	2,194	8.77	138.8	23.89	7.96	23013.2	23009	--	1
Washout, camber increase, and sharp leading edge	1/2	2,082	9.15	138.0	20.40	10.20	23016	33009	--	1
	1/3	2,080	9.32	139.2	22.55	7.52	23014	43009	--	2
	1/4	2,149	9.16	140.2	24.62	6.16	23012	43009	--	2

([a]Sections with sharp leading edge.)

Center stall obtained by -	D_o/q	D_i/q	D/q	C_L at cruising speed	Wing loading W/S	Limit-load factor, n	Weight of flanges, $W_F-\Delta W_F$ (lb.)	Weight of web $W_W-\Delta W_W$ (lb.)	Weight of covering and bracing W_C (lb.)	Total Weight W (lb.)
Sharp leading edge	12.7	7.4	20.1	0.309	30.0	2.98	5,930	624	2,533	9,087
	12.8	7.4	20.2	.300	29.1	3.04	5,572	615	2,614	8,801
	12.7	7.4	20.1	.281	27.2	3.15	6,202	607	2,790	9,599
Washout and sharp leading edge	12.6	7.6	20.2	.316	30.6	2.93	5,465	582	2,481	8,528
	12.5	7.5	20.1	.300	29.2	3.03	5,656	592	2,606	8,854
Washout, camber increase, and sharp leading edge	12.7	7.4	20.1	.317	30.7	2.91	5,521	599	2,474	8,594
	12.4	7.8	20.2	.317	30.8	2.93	5,395	568	2,470	8,433
	12.3	7.9	20.2	.307	29.8	2.98	5,904	565	2,551	9,020

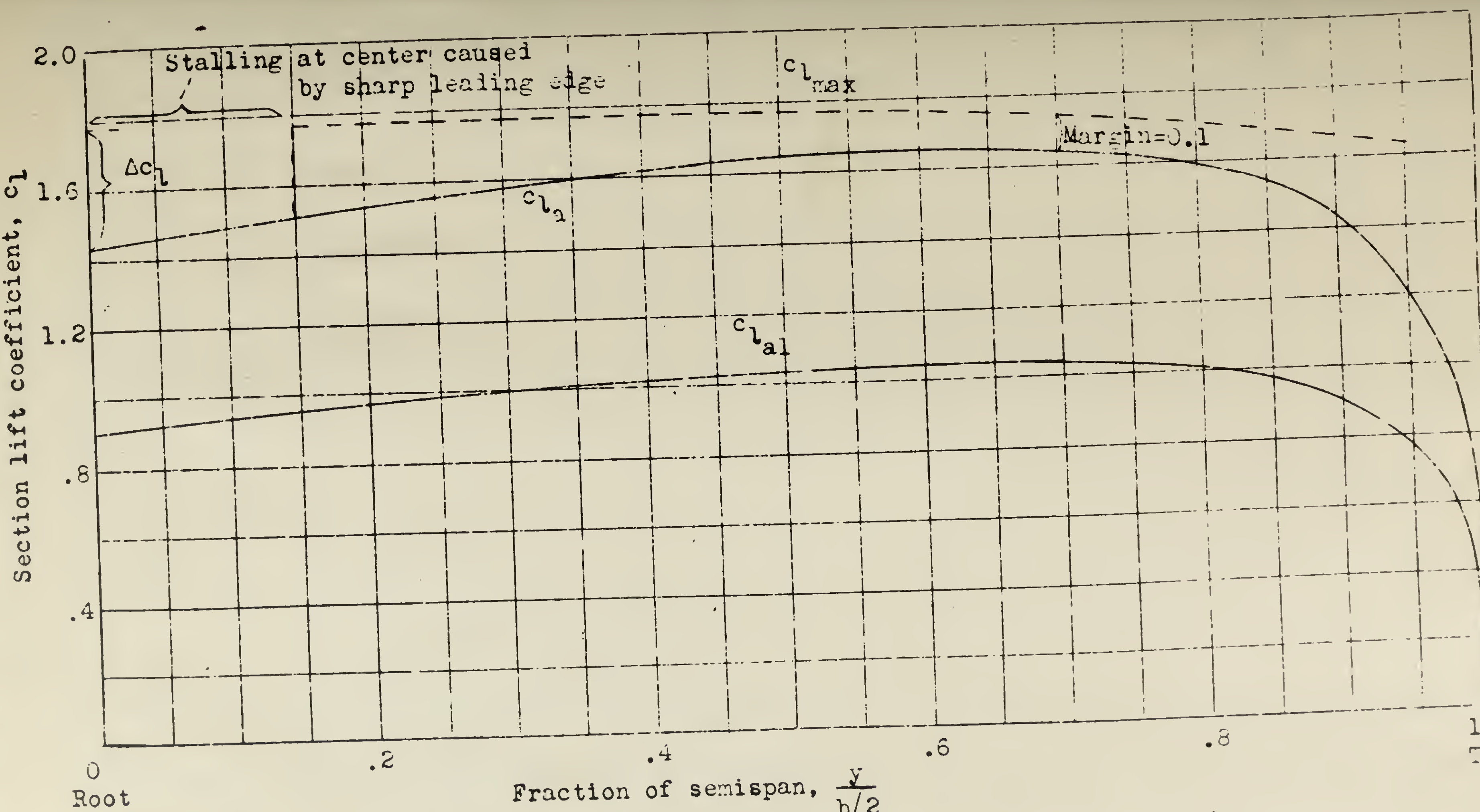

Figure 1.- Calculated stall of wing with sharp leading edge; taper ratio, 1/3 .

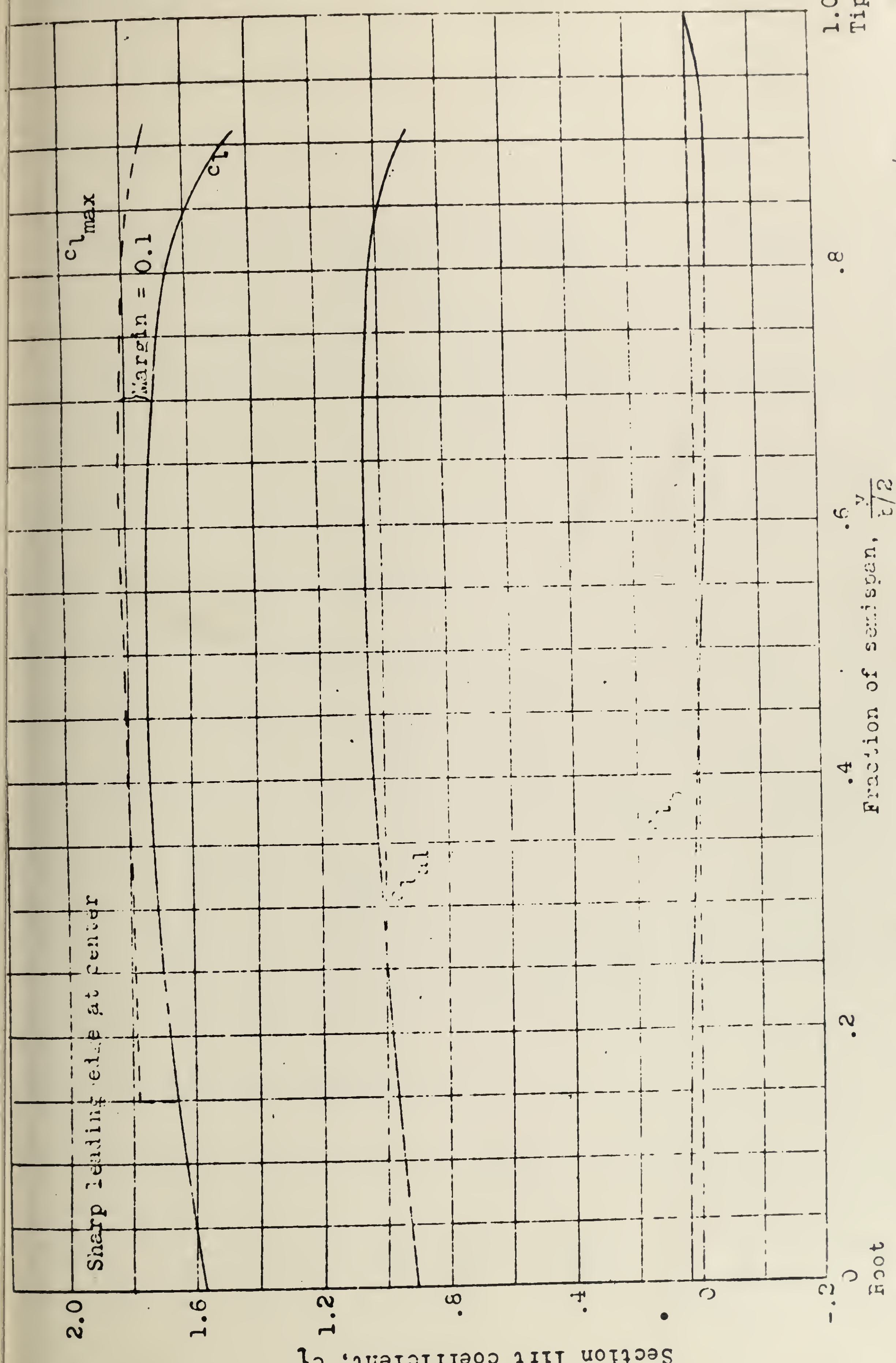

Figure 2.- Calculated stall of wing with camber increase and washout; taper ratio, 1/3.

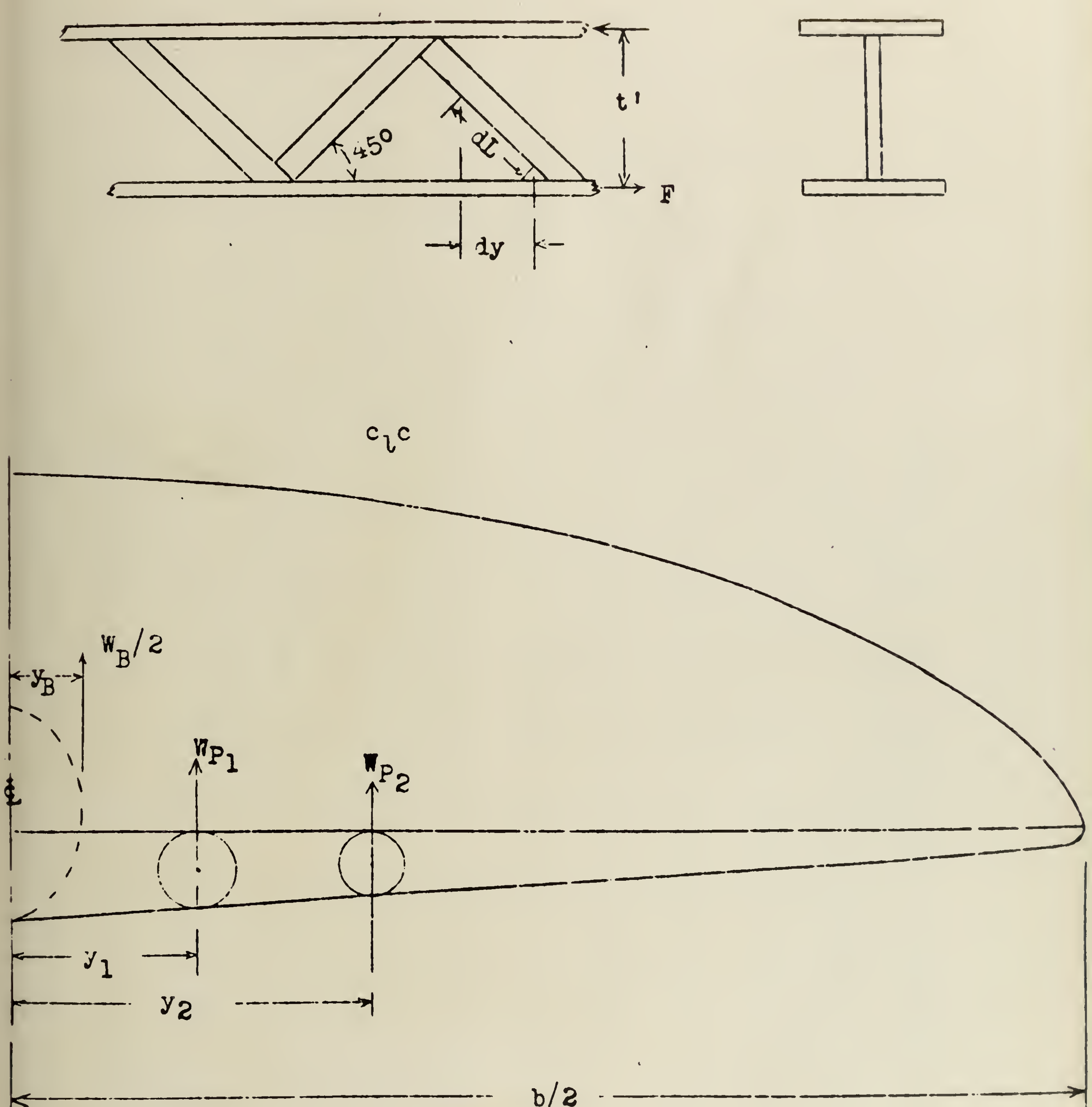

Figure 3.- Spar structure and loads on wing.

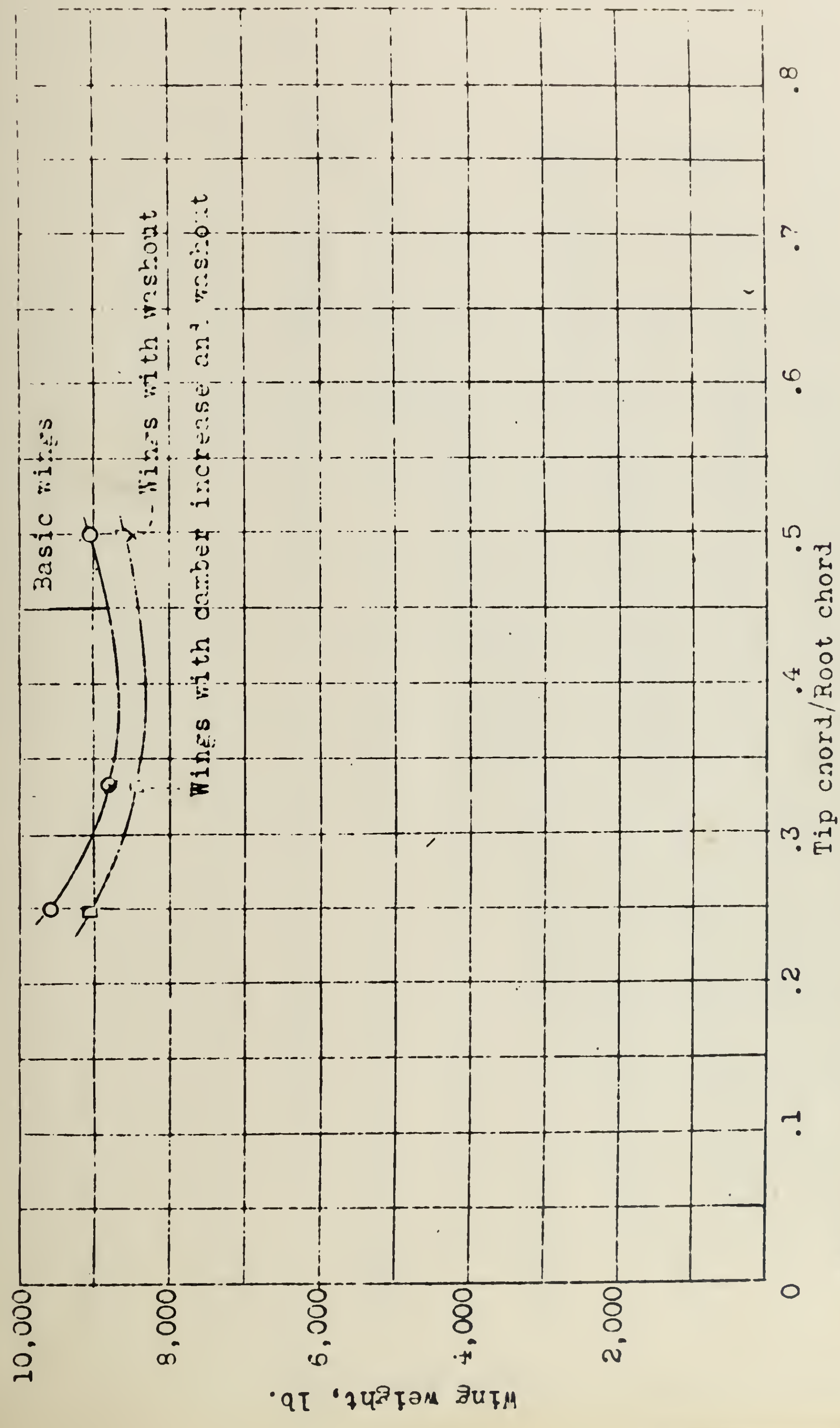

Figure 4.- Variation of wing weight with taper ratio.

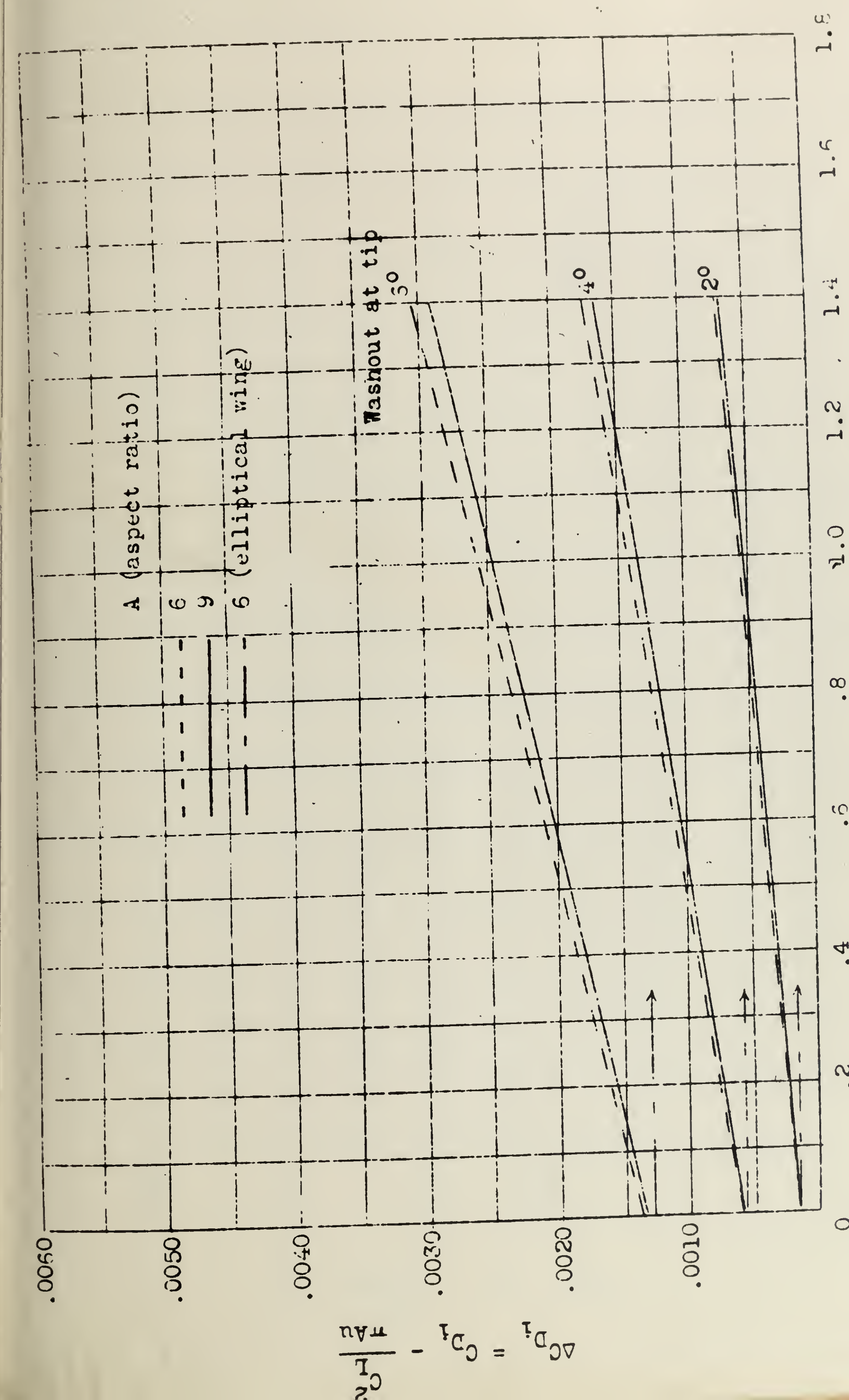

Figure 5.- Increase in induced-drag coefficient due to linear washout; rounded-tip wings; taper ratio, 1/3.

890

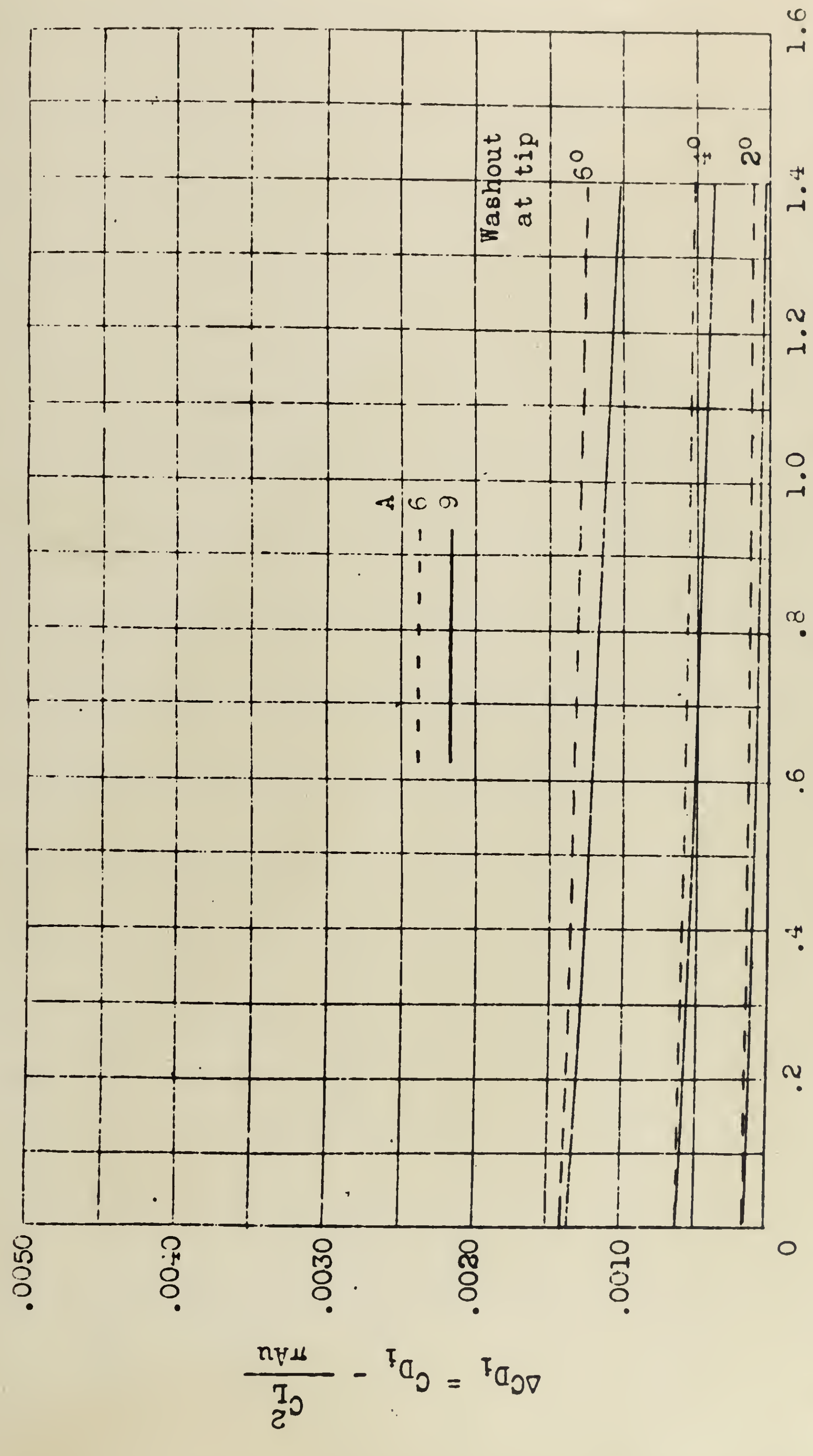

Figure 6.- Increase in induced-drag coefficient due to linear washout; rounded-tip wings; taper ratio, 1/2 .

244

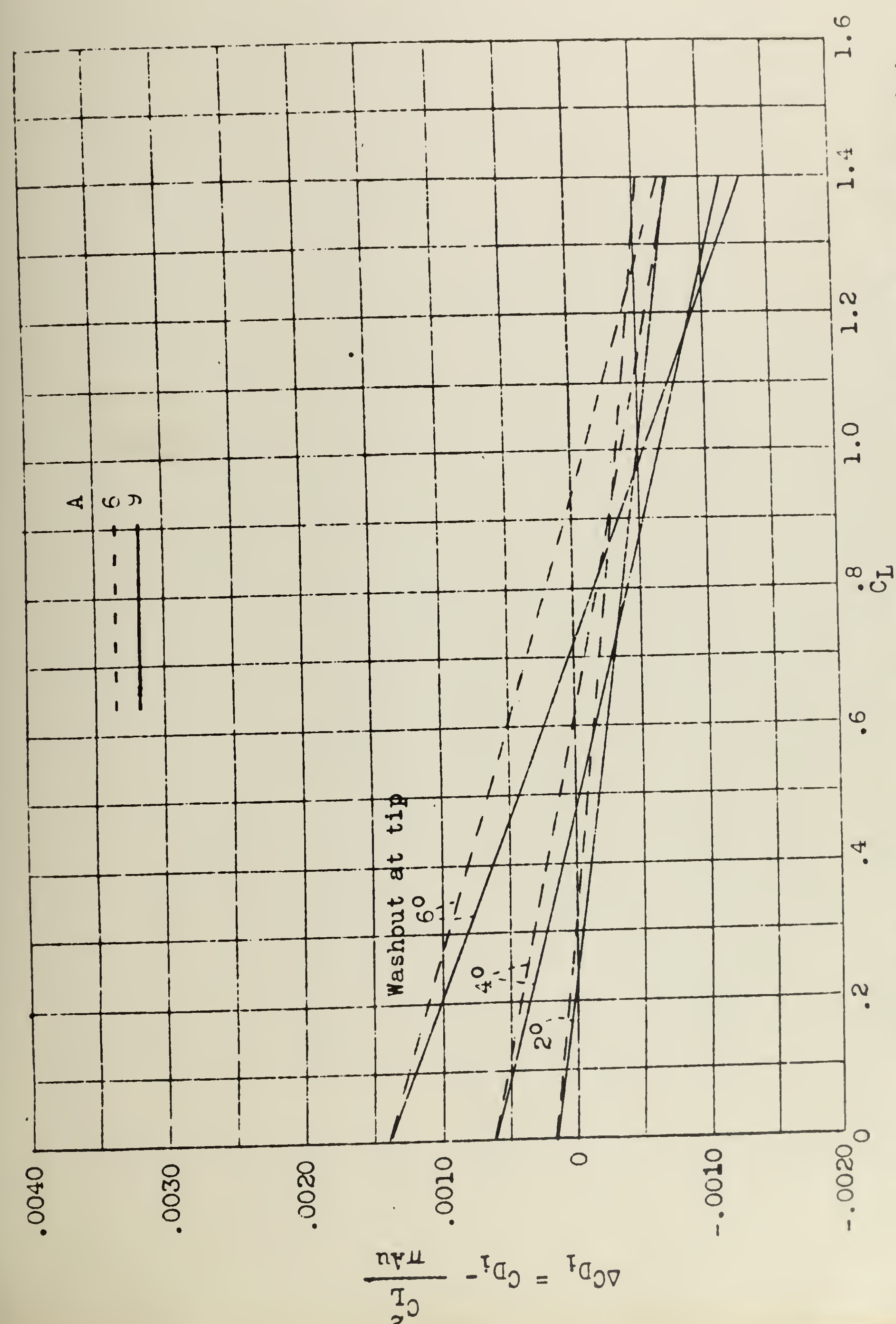

Figure 7.- Change in induced-drag coefficient due to linear washout; rounded-tip wings; taper ratio, 3/4.

892

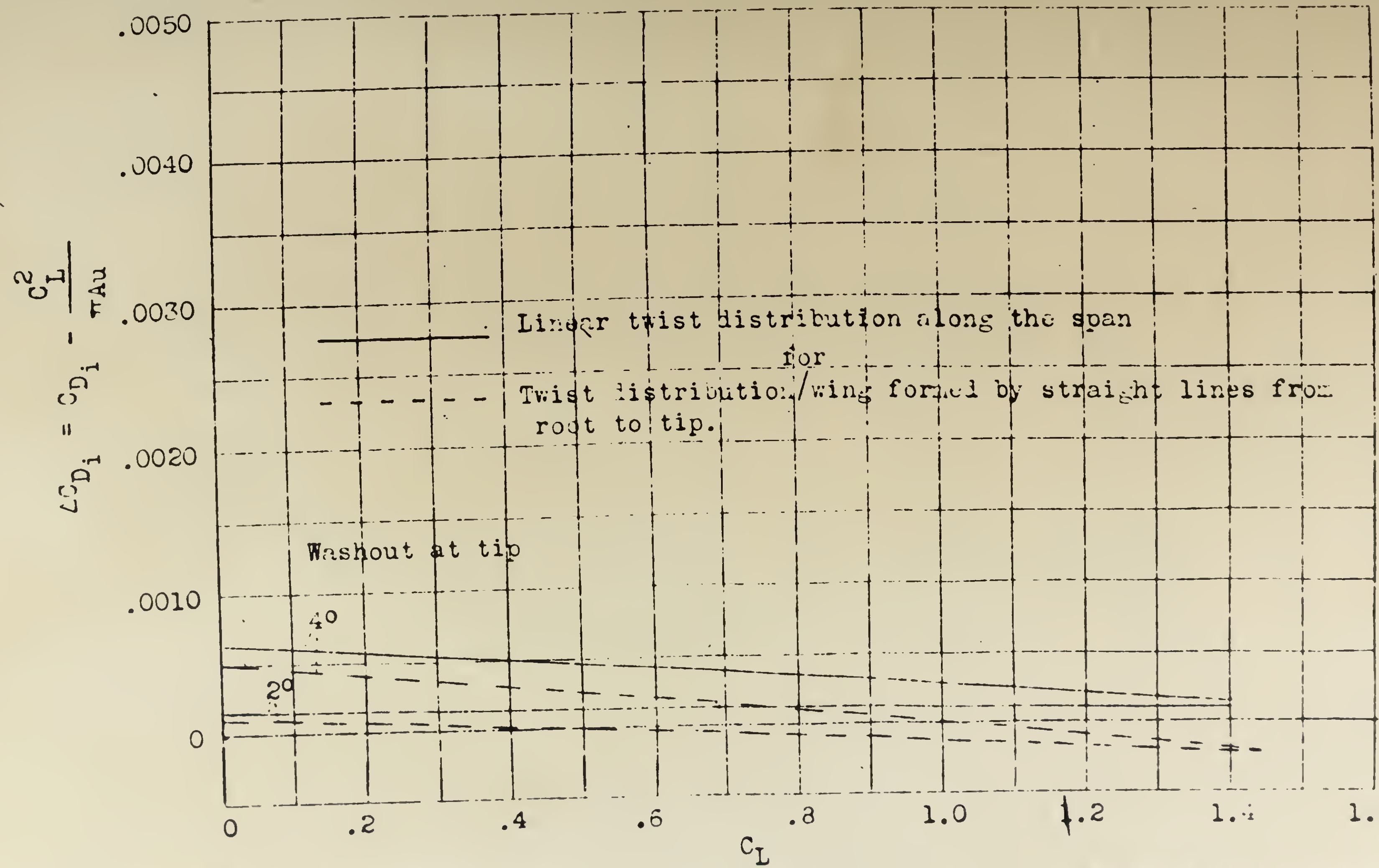

Figure 8.- Effect of type of twist distribution on ΔC_{D_i} ; wings with trapezoidal tips: aspect ratio, 6 ; taper ratio, 1/2 .

Admitted November 24, 1950.

DEFENDANTS' EXHIBIT VV

District Court of the United States, Southern
District of California, Central Division
Civil Action No. 10930-Y

MAURICE A. GARBELL, INC., a California Corporation, and GARBELL RESEARCH FOUNDATION, a California Corporation,

Plaintiffs,

vs.

CONSOLIDATED VULTEE AIRCRAFT CORPORATION, a Delaware Corporation, and AMERICAN AIR LINES, INC., a Delaware Corporation,

Defendants.

STIPULATION #2

It is hereby stipulated subject to proof of error that the appended "Exhibit 18" is a reproduction of pages 267-275, Vol. 3 No. 8 from a printed publication issued and published in the "Journal of the Aeronautical Sciences" about June, 1936, and that said copy may be used in evidence with the same force and effect as an original, subject to any objection which may be made thereto as irrelevant or immaterial when offered in evidence, viz.:

LYON & LYON,
/s/ FREDERICK W. LYON,
Attorneys for Plaintiffs.

/s/ FRED GERLACH,
/s/ ROBERT B. WATTS,
Attorneys for Defendants.

JOURNAL OF THE AERONAUTICAL SCIENCES

Volume 3 JUNE, 1936 Number 8

Technological Developments of the Curtiss-Wright "Coupe"

Presented by T. P. Wright at the Pacific Coast Meeting of the I. Ae. S., February 7, 1936

ALBERT E. LOMBARD, Jr., *Curtiss-Wright Airplane Company*

Summary

THIS paper presents the results of research which was carried out in the development of the Curtiss-Wright "Coupe," a two place, all-metal cantilever monoplane. Wind tunnel data of the effects of split flaps is reported, as is also that dealing with the drag of certain features of the airplane. Structural tests of a series of stiffened sheet metal panels in edge compression are reported which show good correlation with the "effective width" conception of the action of thin sheet in the buckled state. Comparison is made of fifteen types of stiffeners suitable for use on reinforced sheet structures subjected to compression. The results of flight tests and theoretical studies combined with wind tunnel tests of airfoils are discussed, which indicate that the stalling characteristics of tapered monoplane wings can be appreciably improved without the use of aerodynamic twist, by using a highly cambered airfoil at the tip having a high value of $C_{L\,max}$.

Aerodynamic Design

Wind tunnel tests were conducted on a 1/12 scale model of the preliminary design in the Buffalo wind tunnel of Curtiss Aeroplane and Motor Company, shown in Fig. 1. These tests included the effect on the lift and pitching moments of the installation of split flaps, 20% of the wing chord, 42% of the span, set at 60 degrees, (Fig. 2). It is seen that the flaps produced a positive pitching moment (tail heavy) on the complete model, which is desirable since thereby the airplane can be glided at a reduced airspeed after the flaps have

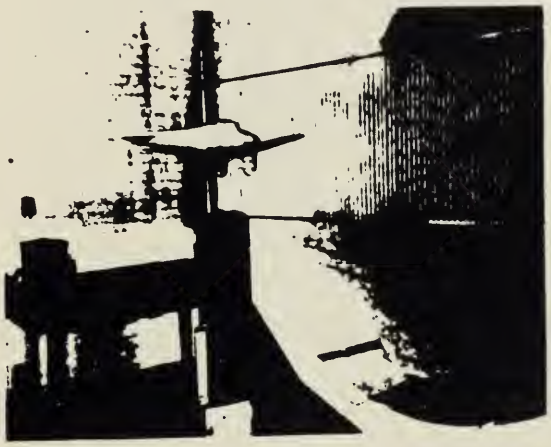

Fig. 1. Model in Buffalo wind tunnel of Curtiss Aeroplane and Motor Company.

been extended without retrimming the elevator. This effect has been checked in flight test and found to simplify controlling the glide to the field. With flaps down, the speed of trim is about 10 m.p.h. less than with the flaps neutral, so that a constant margin is maintained over the stalling speed which is also reduced 10 m.p.h. by the flaps. Fig. 2 further shows that the middle portion of the flap is more effective in producing this positive moment than in increasing the maximum lift coefficient.

The results of certain of the drag tests run at 60 m.p.h. are shown in Figs. 3 and 4. Interpreted in the terms of the two units, "percentage of total airplane drag," and "miles per hour," these items become:

EXHIBIT 18

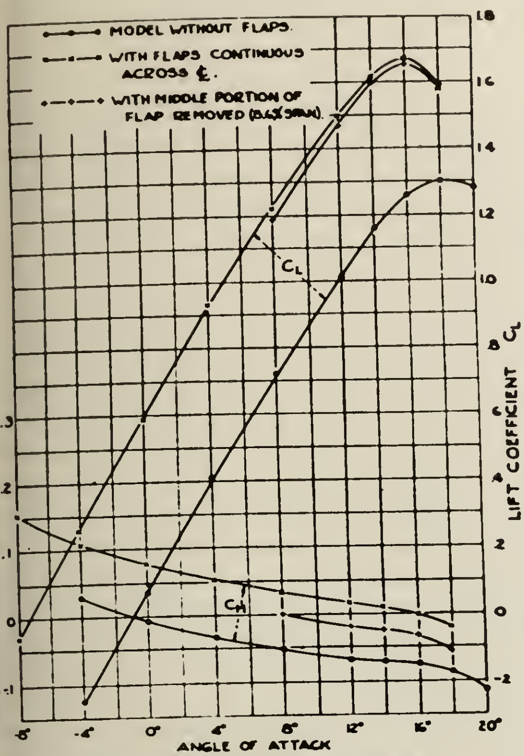

FIG. 2 EFFECTS OF FLAPS.

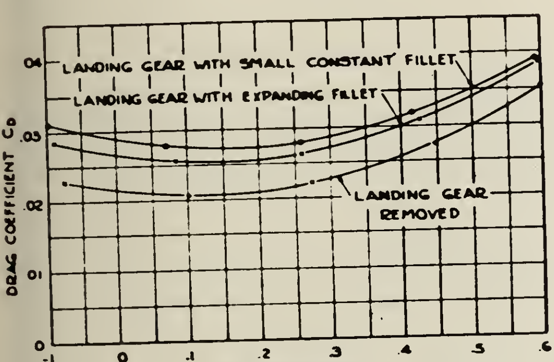

FIG. 3. DRAG OF LANDING GEAR.

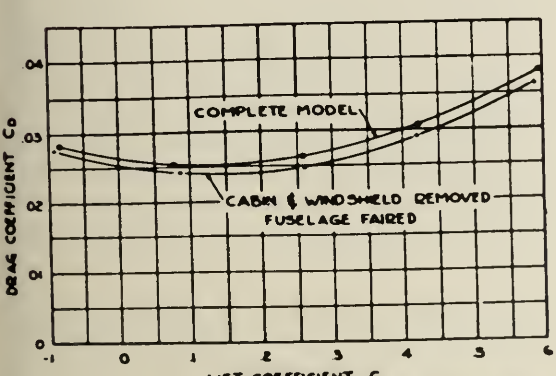

FIG. 4. DRAG OF CABIN & WINDSHIELD.

TABLE I TESTS OF STIFFENED 24ST ALCLAD PANELS

Stiffener Type	Material	Stiffener Area sq in	Panel Thickness in	No. of Stiffeners	Load Carried lbs	Total Effective Area sq in	Effective Stress lb/sq in	Average Effective Stress lb/sq in
1	24ST ALCLAD	.0617	.0315	2	5560	269	20 600	20 000
		.0606	.0317	2	5270	272	19 400	
2	24ST ALCLAD	.0753	.0321	2	7490	289	25 900	27 000
		.0755	.0313	2	7870	280	28 100	
3	24ST ALCLAD	.0794	.0320	2	7490	297	25 200	24 900
		.0817	.0318	2	7180	301	23 900	
4	24ST ALCLAD	.0777	.0099	2	9050	344	26 700	27 000
		.0771	.0318	2	7300	289	25 300	
5	24ST ALCLAD	.0944	.0317	2	8060	329	24 500	24 000
		.1034	.0320	2	8210	351	23 400	
6	24ST ALCLAD	.0773	.0318	2	9790	276	35 500	34 900
		.0774	.0320	2	9500	279	34 200	
7	24ST ALCLAD	.0764	.0317	2	8640	280	30 800	31 800
		.0757	.0317	2	8140	277	31 400	
		.0745	.0318	1	5650	179	31 600	
		.0752	.0320	1	6040	180	33 000	
8	24ST ALCLAD	.0764	.0326	2	8060	291	27 700	28 600
		.0765	.0318	2	8550	285	29 500	
9	17ST TUBE	.1009	.0319	2	9450	326	29 000	28 500
		.0961	.0315	2	9310	323	28 800	
10	17ST TUBE	.0785*	.0319	2	8830	287*	30 800*	30 400*
		.0785*	.0322	2	8490	291*	29 500*	
11	24ST EXTRUDED	.0882	.0323	1	6630	195	34 600	32 400
		.0888	.0324	1	6910	195	35 100	
		.0880	.0316	2	9400	306	30 700	
		.0880	.0315	2	10170	302	33 700	
		.0886	.0318	2	9790	309	32 100	
		.0882	.0322	2	10210	306	33 600	
		.0870	.0342	2	9140	298	33 400	
		.0810	.0306	2	9950	289	32 400	
		.0878	.0323	3	11590	420	27 600	
		.0886	.0320	3	12060	422	28 600	
		.0870	.0310	4	16090	501	32 100	
		.0870	.0306	4	16280	498	32 700	
		.0880	.0265	1	5560	167	33 300	
		.0888	.0272	1	5850	169	34 600	
		.0882	.0274	2	8750	271	31 700	
		.0880	.0275	2	9660	270	35 700	
		.0875	.0208	1	4440	144	32,400	
		.0890	.0207	1	4640	143	32 400	
12	24ST EXTRUDED	.104	.0313	2	11020	328	33 600	34 200
		.104	.0312	2	11300	326	34 100	
13	24ST EXTRUDED	.148	.0309	2	16280	448	36 400	36 800
		.148	.0306	2	16560	446	37 200	
14	24ST EXTRUDED	.0756*	.0316	2	8900	281*	32 000*	31 200*
		.0757*	.0324	2	8150	284*	30 300*	
15	24ST EXTRUDED	.172	.0305	2	15840	487	32 500	32 200
		.172	.0306	2	15980	489	32 700	

* AVERAGE AREA USED (= VOLUME/LENGTH).

	Percentage of Total Drag	Speed Effect
Landing gear drag:		
With constant fillet.........	18%	7 m.p.h.
With expanding fillet.......	13%	5 m.p.h.
Reduction due to expanding fillet	5%	2 m.p.h.
Cabin and windshield drag: (compared to smoothly faired fuselage, cabin removed)..	5%	2 m.p.h.

Structural Design

Edge compression tests of sheet metal panels of 24ST clad stiffened by various types of formed and extruded shapes were carried out to check the "effective width" method for computing the strength of stiffened sheet metal panels, and to select a suitable stiffener type.

The panel tests indicate that the "effective width" method, developed by von Karman, Sechler and Donnell,[1,2] and by Lundquist[3] (Method C), which assumes the stiffener and an effective width of adjacent sheet to act as a unit, all at the same stress, gives good coordination of the results. Referring to Table 1, it is seen that the "effective stresses" for stiffeners Type 7 and Type 11, which were tested on panels of various gauges with various numbers of stiffeners, lie within narrow bands which are no broader than the individual variations on supposedly identical panels. One exception to this close correlation occurred in the two tests of stiffener Type 11 with .032 sheet and three stiffeners per panel in which the sheet failed prematurely due, apparently, to a peculiarity of the rivet pattern on those panels, but this exception is not believed to invalidate the rule established. The "effective width" method of analysis is considered very satisfactory.

Stiffener Selection

In selecting a suitable stiffener type, certain restrictions were necessarily placed on the type of stiffener and its method of attachment to the sheet. These restrictions were:

(1) The stiffener should be of a type that attaches to the wing skin with one row of 1/8 inch dural modified brazier head rivets spaced 1 inch apart.

(2) The stiffener should be of a type suitable for use where the rib spacing would be approximately 20 inches.

(3) The stiffener should have sufficient area and strength such that, when used with .032 inch thick 24ST Alclad, the stiffener spacing at the root of the wings need be not less than 4 inches. This third requirement was only partially adhered to.

The tests are summarized in Table 1. It was endeavored to test representative sections of all types, some obviously designed for ease of fabrication, some for high structural efficiency. Inasmuch as any stiffener could be made somewhat larger or somewhat smaller if the area was not consistent with the load to be carried, the final selection of the stiffener type was based on the maximum effective stress which the stiffener was able to carry.

The eligible types for general use were Types 1 to 12. Types 13 to 15 were intended for use in special places and on other models involving higher loads. Of the "eligible" types, the formed-up stiffener, Type 6, was the strongest. This stiffener had several desirable characteristics in its shape and design which are worthy of comment:

(1) This stiffener had sufficient depth for the length tested to prevent failure by bowing as an Euler column.

(2) This stiffener was made of sufficiently thick material that it did not buckle locally. This characteristic was made possible by the fact that the stiffener had a small developed width. It can be generally concluded that the developed width of stiffeners should be as small as is consistent with the desired depth for Euler strength.

(3) The formed bulb of this stiffener was so shaped that the stiffener was well supported laterally without unduly stressing the free edge to cause it to roll out flat.

(4) The distance from the vertical leg of the stiffener to the line of rivets was small, thus enabling the vertical leg to give considerable support to the sheet panel.

(5) The upturned roll on the free edge of the riveted leg offered support to this leg and to the attached sheet.

The extruded stiffeners, Types 11 and 12, which were next best in order of merit, were selected for actual use because of:

(1) The high maximum stress which they developed,

(2) The manner in which they failed without sudden collapse so that after failure they were still able to carry a large percentage of their maximum load,

(3) The uniformity of manufacture of the extruded shapes, and

(4) The low fabricated cost of the extruded shapes.

It should be noted in passing that the extruded shapes were made of 24ST aluminum alloy, while the formed-up stiffeners, Type 6 specifically, were made of 24ST Alclad which is approximately 10% weaker than straight 24ST. Presumably, if the formed-up stiffener, Type 6, were made of pure 24ST it would be considerably stronger than the extruded shapes, but corrosion difficulties prevent the use of unprotected 24ST in thin sheets.

Test Equipment

All the sheet metal panels were supported in the framework, Fig. 5. The load was applied to each specimen by blocks which clamped on the ends of the sheet. The stiffeners, which butted against the steel face plates, were finished on the ends and accurately attached to the sheets to provide the correct

---

[1] Th. von Karman, E. E. Sechler, and Donnell, *The Strength of Thin Plates in Compression*, Applied Mechanics Transactions A.S.M.E., June, 1932.

[2] E. E. Sechler, *The Ultimate Compressive Strength of Thin Sheet Metal Panels*, Thesis at Calif. Inst. of Tech. 1934.

[3] Eugene E. Lundquist, *Comparison of Three Methods for Calculating the Compressive Strength of Flat and Slightly Curved Sheet and Stiffener Combinations*, NACA Tech. Note No. 455, 1933.

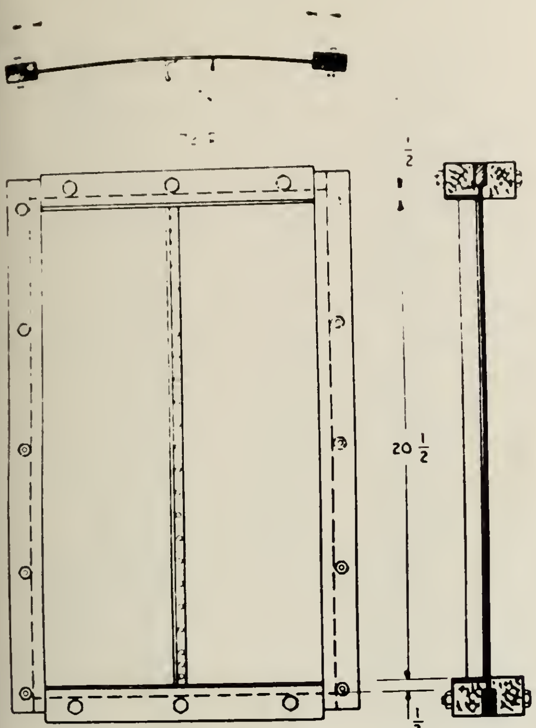

FIG. 5 TEST JIG FRAME

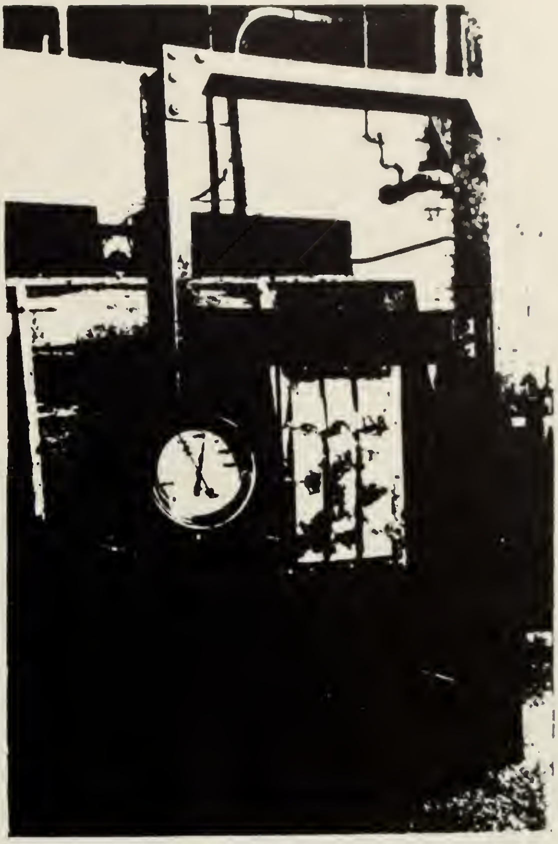

FIG. 6. Hydraulic test machine for sheet metal panels.

overhang of the sheet on the end to fit the depth of the clamping blocks. In order to take care of small variations in the ends of the stiffeners, small brass shims (.002 in. to .010 in. thick) were inserted until they were tight before the load was applied.

The vertical guides of this frame were made of steel and held to the 12 inch spacing by steel bars across the back. The thickness of the slot thru which the sheet could slide was accurately maintained by clamping shims between the bars slightly thicker than the sheet to be tested.

This method of supporting the edges of the sheet was found to be very satisfactory when testing panels with stiffeners. On such panels the buckling was always more severe in the middle of the panels, and the failures always occurred in the middle of the panels —never along the edges—at the instant when the stiffeners failed. The frictional load carried in the guides, up to the point of failure of the stiffeners, could be only a relatively small percentage of the total load in the sheet edges. Previous to the time of failure the guides would drop freely of their own weight whenever the load was removed. It is estimated that the frictional load in the guides increased the observed maximum load by possibly 50 pounds, which is considered negligible.

The testing machine shown in the photograph, Fig. 6, developed after the fashion of the one described, (see Reference 2), incorporates a hydraulic jack with a maximum load capacity of 20,000 pounds.

Method Used to Compute Stress in Stiffener and Sheet in Panel Tests

Reference 2 shows that the load carried by a simply supported, unstiffened sheet metal panel can be represented by the formula

$$P = C t^2 \sqrt{E \sigma},$$

and the "effective width" can be written

$$2w = C t \sqrt{E / \sigma},$$

in which

C is a function of η and λ as shown in Fig. 9.

$$\eta = (b / R) \sqrt{E / \sigma}$$

$$\lambda = (t / b) \sqrt{E / \sigma}$$

E is Young's modulus of elasticity.

σ is stress at the supported edge of a panel and also, in the case of stiffened panels, the stress in the stiffener and adjacent sheet (of effective width = 2 w).

t is thickness of the sheet.

b is width of sheet panels between supports.

R is radius of curvature of sheet.

The curves of C given in Fig. 9 for the range of η and λ encountered in the wings were derived from data

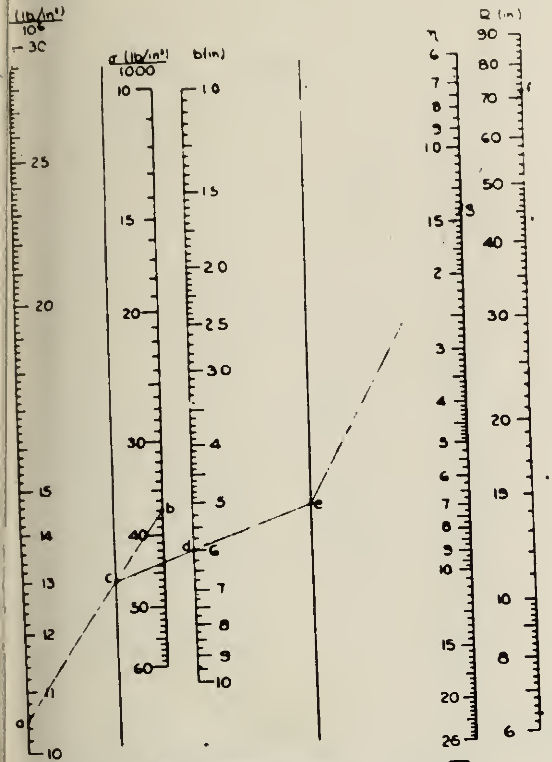

FIG. 7 SOLUTION OF $\eta = \frac{b}{R}\sqrt{\frac{E}{\sigma}}$

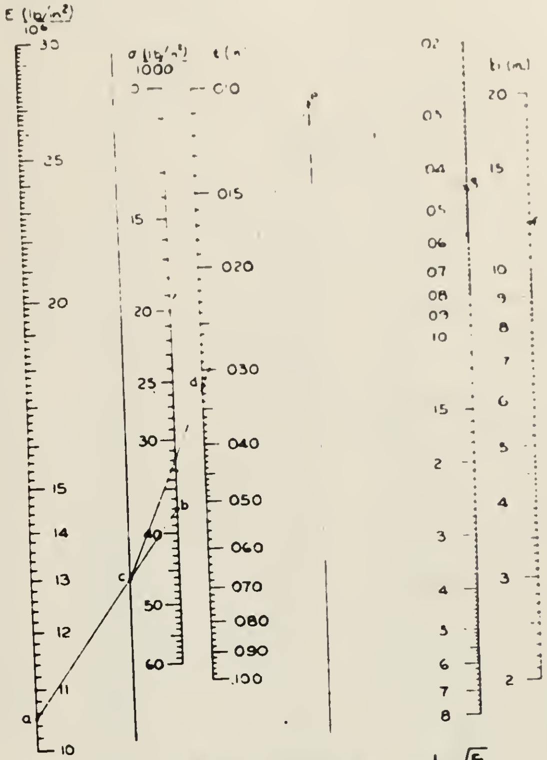

FIG. 8. SOLUTION OF $\lambda = \frac{t}{b}\sqrt{\frac{E}{\sigma}}$

of Reference 2. The nomograms, Figs. 7, 8, 10 and 11, were developed to simplify the computation of the parameters and the values of $2w$ and P.

The assumed stress distribution in the stiffeners and sheet of the panel tests is shown in Fig. 12, in which the stresses in the stiffeners and adjacent sheet elements and in the edges of the sheet are all the same inasmuch as the shortening of the panel under load is the same at all points. Because of the support offered the sheet by the side guides, it was assumed also that all the width of the sheet inside the guides would act effectively at the maximum stress. The justification of this assumed stress distribution is believed to lie in the close correlation of the tests of the stiffeners Types 7 and 11, Table 1.

Wing Static Test

A complete wing for one side was static tested to the full design loads for high angle of attack and inverted flight. This wing, designed to close margin in accordance with the method as developed in the panel tests, carried the design loads without failure. Clips and fittings, designed according to this assumed distribution of stress in the sheet and stiffener, were all found satisfactory. These facts speak for the practical applicability of the method of analysis to the design of all-metal aircraft.

Flight Tests

The most interesting part of the flight test program was that devoted to the stalling characteristics in which modifications were effected in the wing contour which enabled the airplane to be stalled in a smooth and controllable manner.

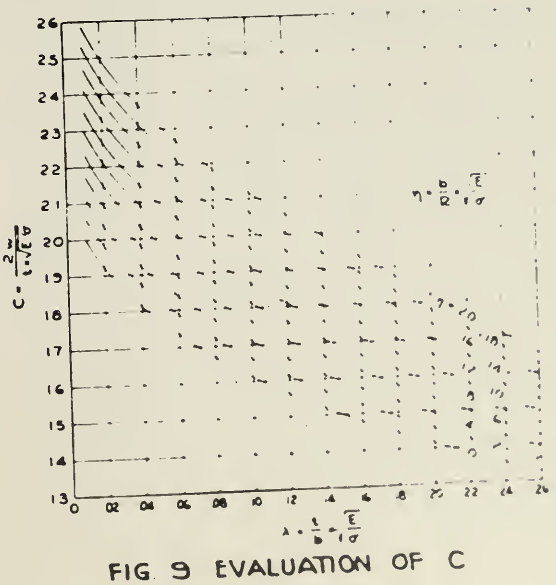

FIG. 9 EVALUATION OF C

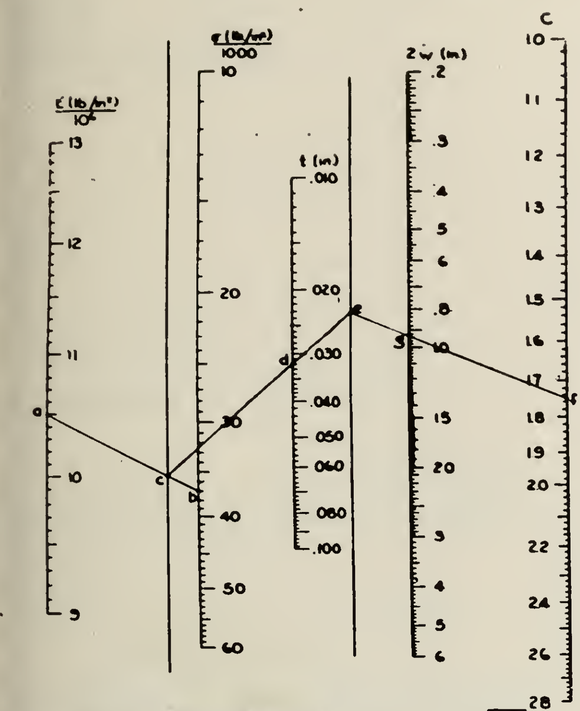

FIG. 10. SOLUTION OF $2w = Ct\sqrt{E/\sigma}$

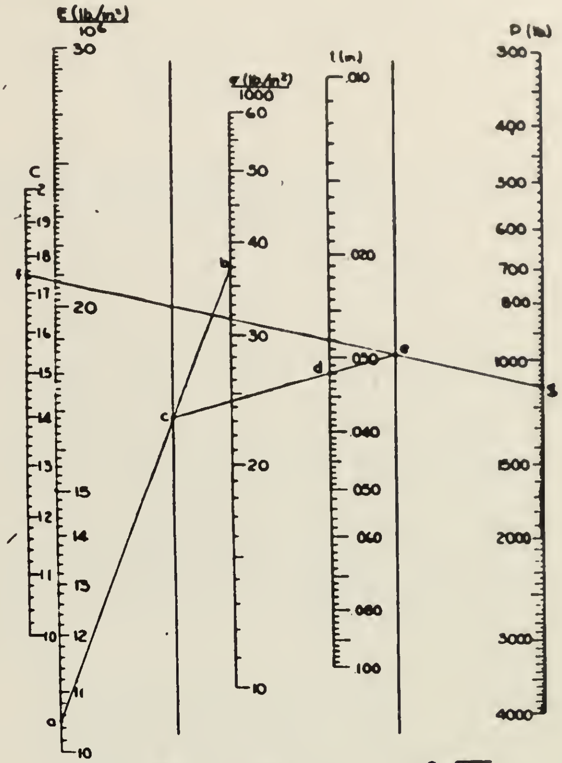

FIG. 11. SOLUTION OF $P = Ct^2\sqrt{E\sigma}$

As originally flown, the airplane had a straight tapered wing with an N.A.C.A. 2315 airfoil at the root and N.A.C.A. 2309 airfoil at the tip with no twist. The N.A.C.A. 2309–2312–2315 series was selected because, on the average, it showed the smoothest shaped lift curve peaks of all the low cambered, low drag airfoils tested in the N.A.C.A. Variable Density Tunnel.[4] The stall of this wing was observed in flight, by wool tufts, to start at the leading edge near the right wing tip and progress rapidly to cover the whole tip portion of that wing, whereupon it would drop uncontrollably. The conditions with the split flaps extended were essentially the same as with them retracted.

Flight tests were then carried out with fixed auxiliary airfoils, 14.5% chord, extending over the outer 50% of the span. Two types were investigated, one with a symmetrical N.A.C.A. 0012 section and the other with a highly cambered N.A.C.A. 22 section.[5]

It was found that, under certain combinations of angles, these fixed auxiliaries improved the stalling characteristics by reducing the autorotational tendencies and improving the aileron control. The effects of these auxiliaries were quite insensitive to their angular setting; i.e., a large change in angular setting was necessary to bring about an appreciable change in the stall.

The cambered auxiliaries appeared to be better than the symmetrical in their effects on the stall. However, the installation of either type of auxiliary was so detrimental to the take-off and climb characteristics, particularly with the auxiliaries at the angles necessary for the best stall characteristics, that the use of the fixed auxiliaries could not be considered satisfactory and was, therefore, abandoned.

The other course which was followed to improve the stalling characteristics was to modify the airfoil sections on the outer portions of the wing by fairing out the under side of the leading edge in successive steps, increasing the leading edge radius, and increasing the airfoil camber. This procedure was found definitely to improve the stalling characteristics. With the final configuration, the CW-19 airfoil (Fig. 13) at the tip tapered to the N.A.C.A. 2315 airfoil at the root, all autorotational tendencies below the stall were eliminated and the airplane could be positively controlled in the stalled condition. The wool tufts showed that the stall of this wing started along the trailing edge near the mid point of the semi-span and proceeded gradually in all directions. The leading edge at the tip remained unstalled throughout. It is interesting to note that when the nature of the stall was changed so that the separation started at the trailing edge, instead of at the leading edge, the whole character of the stall became smooth, more controllable.

It appeared that the change to the CW-19 airfoil at the tip was equal in effectiveness at the stall to the

---

[4] Jacobs, Ward and Pinkerton, *The Characteristics of 78 Related Airfoil Sections from Tests in the Variable Density Wind Tunnel, N.A.C.A. Tech. Report 460*, 1933.

[5] Fred E. Weick & Robert Sanders, *Wind Tunnel Tests on Combinations of a Wing with Fixed Auxiliary Surfaces Having Various Chords and Profiles, N.A.C.A. Tech. Report 472*, 1933.

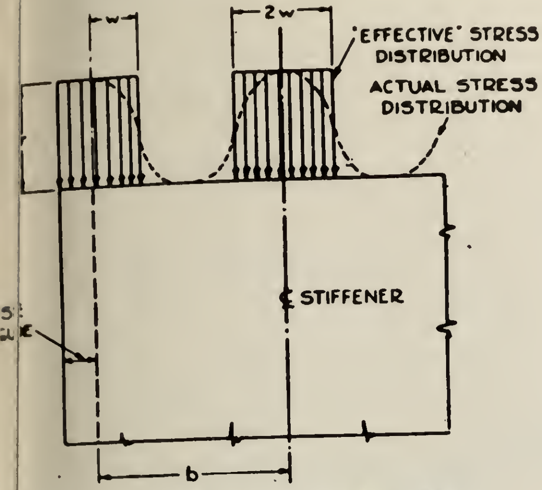

FIG. 12. STRESS DISTRIBUTION.

[illegible]stallation of either type of fixed auxiliary airfoil. [illegible] was no observable adverse effect on the stability [or pe]rformance due to this modification.

Theoretical Investigation of Tapered Twisted Wings

[On]e method of improving stalling characteristics of a [w]i[ng] is to use aerodynamic twist reducing the incidence [al]o[ng] the span so that the tip will stall at a higher [an]g[le] of attack than the root. The effects of this twist [can b]e determined analytically by the method developed [by G]lauert.[6] (Chapter XI.) The circulation about any [poi]nt on the wing span is expressed by the Fourier [seri]es

$$\Gamma = 2bV\Sigma A_n \sin n\theta \qquad (1)$$

[whe]re

Γ is circulation ($= C_L c V/2$)

b is wing span

c is wing chord at any point

V is velocity at infinite distance from wing.

θ represents point on wing span defined by the equation:

$y = (b/2)\cos\theta$

y is distance out from center line.

[T]he downwash velocity w at any point θ becomes

$$w = V\Sigma nA_n \sin n\theta / \sin\theta \qquad (2)$$

[B]y equating the circulation defined by the basic series [E]q. 1) to the circulation derived from the angle of [att]ack as affected by downwash (Eq. 2), and assuming [a s]traight line variation of lift coefficient with angle of

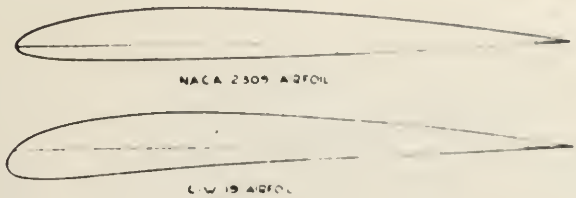

FIG 13

attack, the following equation is obtained for the tapered wing with constant twist along the span:

$$\Sigma A_n \sin n\theta[n/\sin\theta + 1/\mu] = \bar{\alpha}\ [illegible]\ (\cos\theta)\epsilon \qquad (3)$$

where

$\mu = (c/4b)(dC_L/d\alpha_0)$

$\bar{\alpha}$ is absolute angle of attack at the root measured from zero lift

ϵ is aerodynamic twist at tip (positive when the angle of attack is less at the tip than at root.)

The first four coefficients of the series A_1, A_3, A_5 and A_7 can be evaluated by satisfying Eq. (3) at the four points $\theta = 22\frac{1}{2}°, 45°, 67\frac{1}{2}°, 90°$. This evaluation has been made for a straight tapered wing as follows:

Aspect Ratio R [illegible] b^2/S 6.721

Tip Chord/Root Chord .461

$dC_L/d\alpha_0$ 5.84/radian

$$\begin{aligned} A_1 &= .21513\,\alpha\ [illegible]\ .08832\,\epsilon \\ A_3 &= .00471\,\alpha\ [illegible]\ .01585\,\epsilon \\ A_5 &= .00063\,\alpha + .00362\,\epsilon \\ A_7 &= .00087\,\alpha\ [illegible]\ .00613\,\epsilon \end{aligned} \qquad (4)$$

The total lift of an airfoil is (by page 136, Ref. 6)

$$L = \tfrac{1}{2}\pi b^2 \rho V^2 A_1$$

when the average lift coefficient is

$$C_{Lav.} = 2L/S\rho V^2 = \pi b^2 A_1/S = \pi R A_1 \qquad (5)$$

It is now convenient to evaluate the coefficients in terms of $C_{Lav.}$ and ϵ, which become

$$\begin{aligned} A_1 &= .04734\,C_{L} \\ A_3 &= .00104\,C_{L}\ [illegible]\ .01791\,\epsilon \\ A_5 &= .00212\,C_{L}\ [illegible]\ .00757\,\epsilon \\ A_7 &= .00040\,C_{La}\ [illegible]\ .00479\,\epsilon \end{aligned} \qquad (6)$$

The induced drag [illegible] (page 130, Ref. 6)

$$D_i = [illegible]\,\pi\,[illegible]\,\rho V^2\,\Sigma nA_n^2$$

[illegible]

$$C_{Di} = \pi R\,\Sigma nA_n^2 \qquad (7)$$

[illegible]

C_{Di} [illegible] .04788 C_L [illegible] [illegible]

[illegible]

[illegible]

[illegible]

[6] Glauert, *Airfoil and Airscrew Theory*, Cambridge Press, London.

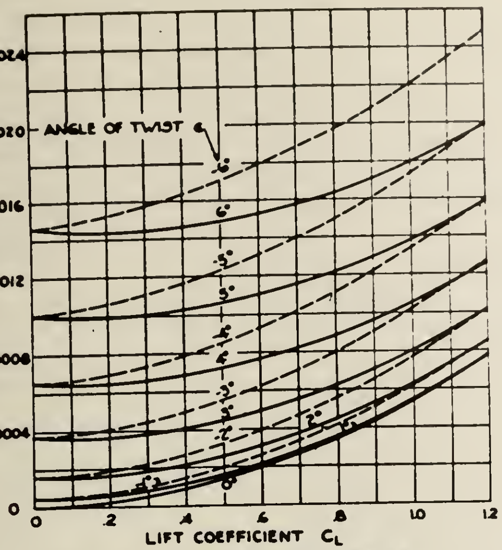

FIG. 14. ΔC_{Di} FOR TAPERED WING.
ASPECT RATIO = 6.724 $dC_L/d\alpha_0$ = 5.84/rad.
TIP CHORD = .461 ROOT CHORD

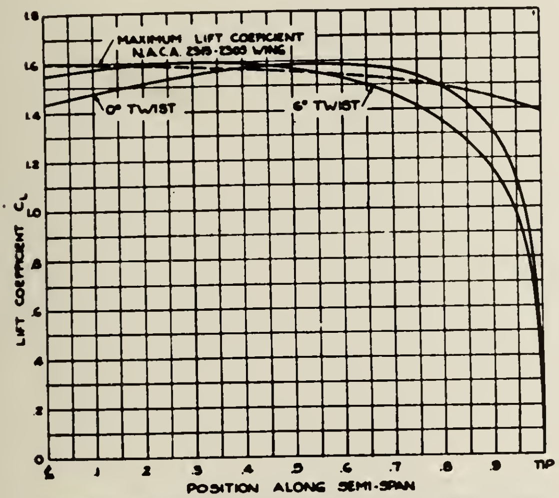

FIG. 15. LIFT COEFFICIENT ALONG TAPERED WING.
$C_{L_{av}}$ = 1.50
ASPECT RATIO = 6.724 TIP CHORD = .461 ROOT CHORD.

Curves are plotted in Fig. 14 giving the values of ΔC_{Di} for various angles of twist. For a twist up to 2° the induced drag is not serious, amounting to not over 1% of the drag of an average airplane, but as the twist is increased above 2° the drag becomes appreciable.

The lift coefficient at any one of the four points $\theta = 22\frac{1}{2}°$, 45°, $67\frac{1}{2}°$ and 90° is obtained from Eq. (1) to be:

$$C_L = 2\Gamma / c\,V = (4\,b/c)\,\Sigma A_n \sin n\,\theta \qquad (10)$$

In Fig. 15 are plotted the lift coefficients along the span of this wing with zero twist and a wing with a hypothetical 6° of twist, both at $C_{L_{av}} = 1.50$. In this figure is plotted also a curve for the maximum lift coefficient along the span which was developed taking into

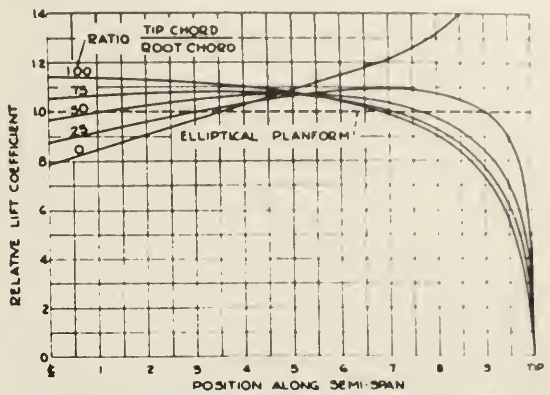

FIG. 16 LIFT COEFFICIENT GRADING CURVES
TAPERED WINGS A R = $dC_L/d\alpha_0$ = 5.8

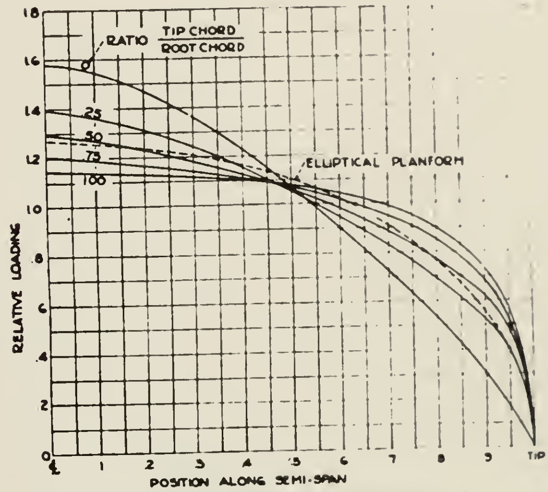

FIG. 17. LOAD GRADING CURVES
TAPERED WINGS A R = $dC_L/d\alpha_0$ = 5.8

account the variation in the maximum lift with airfoil thickness ratio and with Reynolds Number, which varies along the span due to the taper.

It is seen that the wing with 0° twist exceeds the maximum lift coefficient for the 2315 2309 series over a considerable portion of the outer wing, and it is therefore reasonable that there should be a pronounced tendency to stall at the tip first, bringing about uncontrollable autorotation. The curve with 6° twist represents a wing that should be satisfactory in the stall if the N.A.C.A. 2315 to 2309 wing were retained. However, referring again to Fig. 14 it is seen that such a wing would have an appreciably higher drag than the untwisted one. It is to be concluded, therefore, that to try to obtain good stalling characteristics merely by twisting the wing is decidedly inefficient. It is much better to use only 1°–2° of aerodynamic twist in combination with a tip airfoil having a high value of $C_{L_{max}}$ and having a lift curve with a round smooth top.

It is of interest to note that the benefits gained by substituting the CW-19 airfoil for the N.A.C.A. 230

2

tip were due entirely to the extension of to a high value of C_{Lmax} at a high angle There was only 0.2° shift of the zero lift the N.A.C.A. 2309 airfoil to the CW-19 ed to a common chord as determined by Buffalo wind tunnel of the Curtiss Aero-lotor Company. However, these tests on rfoils at 80 m.p.h. showed that the CW-19 oped a high uncorrected $C_{Lmax.} = 1.36$ with unded lift curve peak, comparable to $C_{Lmax.} = 1.00$ for the N.A.C.A. 2309 and $C_{Lmax} = 1.18$ for the Clark Y.

Figs. 16 and 17 have been prepared using coefficients from Reference 6 to show the load grading curves and lift coefficient grading curves for a series of airfoils with various taper ratios for an aspect ratio $R = d\,C_L/d\alpha_0 =$ approximately 5.8. It is important to recognize that while structural efficiency is gained with the high taper ratios, the problems of obtaining good stalling characteristics are increased.

Admitted November 24, 1950.

DEFENDANTS' EXHIBIT WW

District Court of the United States, Southern District of California, Central Division

Civil Action No. 10930-Y

MAURICE A. GARBELL, INC., a California Corporation, and GARBELL RESEARCH FOUNDATION, a California Corporation,

Plaintiffs,

vs.

CONSOLIDATED VULTEE AIRCRAFT CORPORATION, a Delaware Corporation, and AMERICAN AIR LINES, INC., a Delaware Corporation,

Defendants.

STIPULATION #3

It is hereby stipulated subject to proof of error that the appended are reproductions of the following printed publications and that the said copies may be used in evidence with the same force and effect as originals, subject to any objection which may be made thereto as irrelevant or immaterial, when offered in evidence, viz:

"Exhibit 19" is a reproduction from a printed publication, Vol. XLI, pages 175-180, entitled "Aerodynamic and Structural Features of Tapered Wings" issued and published during the year 1937; by the "Royal Aeronautical Society" of London, England.

"Exhibit 20" is a copy of a reproduction of a publication entitled "Correspondence," Vol. XLII, pages 754-755, issued and published during the year 1938 by the "Royal Aeronautical Society" of London, England.

"Exhibit 21" is a reproduction of pages 660, 661, 671, 672, 690, and 697, Vol. XXII, of an article entitled "Development of Sailplanes" issued and published during the year 1938 by the "Royal Aeronautical Society" of London, England.

LYON & LYON,
/s/ FREDERICK W. LYON,
Attorneys for Plaintiffs.

/s/ ROBERT B. WATTS,
/s/ FRED GERLACH,
Attorneys for Defendants.

905

The better response to ailerons and its resulting effect of manœuvrability which is afforded by wings of higher taper ratio can therefore only be utilised ...re is taken to maintain a sufficient degree of lateral control at and beyond ... stall.

The Stalling of Tapered Wings.

This subject has recently received a good deal of attention in this country and America in view of the unpleasant characteristic of tapered wings, especially ...se of high taper ratios, of dropping a wing when stalled in a more vicious way ...an rectangular wings. It has also been observed in flight and on models in the ...nd tunnel that for highly tapered wings there is a very definite tendency to stall ...t at the tips and not at the centre. The stalling characteristics of wings of ...w taper ratios are still very much disputed, and some designers of aircraft ...ing wings of relatively small taper ratio claim stalling characteristics comparable to those of rectangular wings.

When first faced with the phenomenon one is inclined to explain the behaviour ... the stall of tapered wings solely on the basis of the aerofoil theory. The ...rofoil theory indicates, as illustrated in Fig. 7, that an elliptical wing or a wing

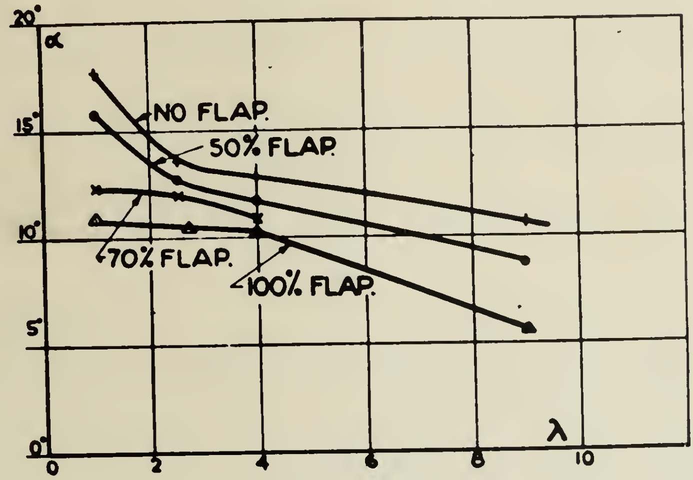

FIG. 10.

... taper ratio of about 2 : 1 which approaches the elliptical distribution should ...all simultaneously over the whole span. Wings of higher taper ratio should ...all first at a point somewhat inboard of the wing tips as there the local C_L or ... effective angle of incidence reaches a maximum value prior to other portions ... the wing. However, it has been found that the aerofoil theory alone does ... give a satisfactory explanation and that a number of other parameters have ... be considered. Tests carried out by Millikan (14) at the Pasadena Institute ... Technology, indicated that for a wing of a given taper ratio the characteristics ... stalling changed decisively as the aspect ratio of the wing was increased.

More recent tests by Irving at the N.P.L. and observations in flight by ...ray (15) have indicated the existence of a spanwise flow which depends on the ...ection of sweepback. On a tapered wing with no sweepback of the leading ...ge and a sweep forward of the trailing edge, Irving observed a transverse ...w near the trailing edge which was directed from the tips towards the centre ... the aerofoil. A similar type of flow was observed by Gray on wings which ... negative angle of yaw. *Vice-versa* an outward flow (towards the tips) ...s observed on a tapered wing having a swept back leading and correspondingly ... full-scale on a monoplane with positive angle of yaw. Corresponding to the ...ection of this secondary flow the stalling of the tips was either delayed when

the flow had an inward direction and accelerated when the flow had an o direction. The explanation for this phenomenon, as given by Gray (*I* July 16th, 1936), due to the transverse pressure gradient, is not conv C. N. H. Locke, of the N.P.L., has pointed out in a letter addressed to *Flig* (August 27th, 1936) that in the case of a yawed aerofoil the flow may be re into a two-dimensional flow in planes normal to the aerofoil together w uniform velocity along the span which will not affect the equilibrium of the verse flow. The spanwise component of the flow will affect the boundary especially when the aerofoil is stalled. In the case of a yawed aerofoil, the case of an aerofoil with swept forward trailing edge, dead air will be ported from the tips towards the centre thus delaying the stalling of the tips accelerating the stalling of the tips and accelerating the stalling of the cen comparison with the corresponding aerofoil with straight trailing edge.

This aspect of stalling still requires fuller research, and it seems a litt early to form a definite opinion, but it is most likely that the phenomenon o spanwise dead air transport will explain certain observations in regard t point where the breakaway of the flow first occurs on the wing which a contradiction to the ordinary aerofoil theory.

Apart from this phenomenon it is usually overlooked when applying the ge aerofoil theory that the wing section along the span is not constant on a monoplane wings as the thickness chord ratio varies usually from the c towards the tip, apart from the change in chord.

In predicting the point where stalling will first occur, it is necessary to r allowance for the actual stalling angle of a section at any point of the span. by varying the geometric angle and the characteristics of the section (thic chord ratio and camber) it should be possible to control to some exten commencement of burbling in relation to the wing plan form.

(a) *Influence of Twist.*

A mere twist, *i.e.*, an outwash towards the tips seems to be a very ob scheme to delay the stalling of the tips, but it is, in my opinion, a very ineffi way unless the twist becomes so excessively large that the drag and th distribution at small angles of incidence are substantially affected. J. Hueber published some theoretical investigations in 1933 on twisted tapered w The distribution of twist along the span was so chosen as to obtain an ellip C_L distribution. The following table contains the angle of twist and the in of induced drag compared with the minimum value for elliptical lift distrib at an overall $C_L = 1$.

Taper Ratio.	Angle of twist equals difference of geometric angle at root and tip for overall $C_L = 1$.	Di/Di ellip.
5	20	1.21
2.5	19	1.11
1.25	15	1.01
1	13.5	1.0

On a wing which was actually used on a glider consisting of a recta centre portion and tapered tips (taper ratio = 1.54) the twist required fo tapered portion was $-9.5°$.

Hueber's assumption of an elliptical C_L distribution, although rationa quite arbitrary and may appear too severe. In a more recent publication o influence of twist by Albert E. Lombard (18) in the *Journal of the Aerona Sciences* ("Technical Developments of the Curtiss Wright Coupé") the a comes to the conclusion that even a mild twist not exceeding $-6°$ is a v inefficient way of obtaining good stalling characteristics. The wing investig by Lombard had an aspect ratio of 6.724 and a taper ratio of 2.16. The in

induced drag for various angles of twist and the resulting C_L distribution are shown in Fig. 11.

For a twist up to 2° the increase in induced drag is not serious, amounting to not over 1 per cent. of the drag for an average aeroplane, but as the twist is increased above 2° the additional drag becomes appreciable.

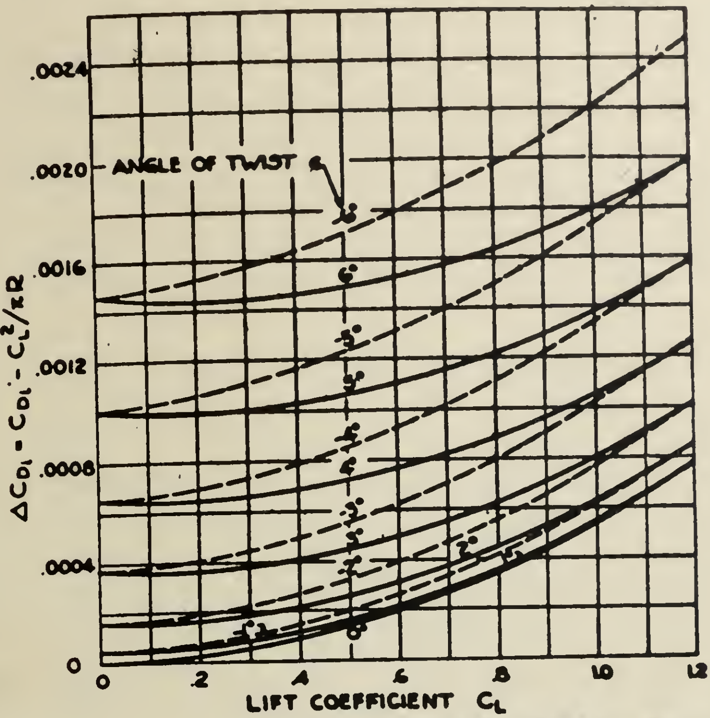

ΔC_{Di} FOR TAPERED WING.

ASPECT RATIO = 6.724 $dC_L/d\alpha_0$ = 3.84/rad.

TIP CHORD = .461 ROOT CHORD

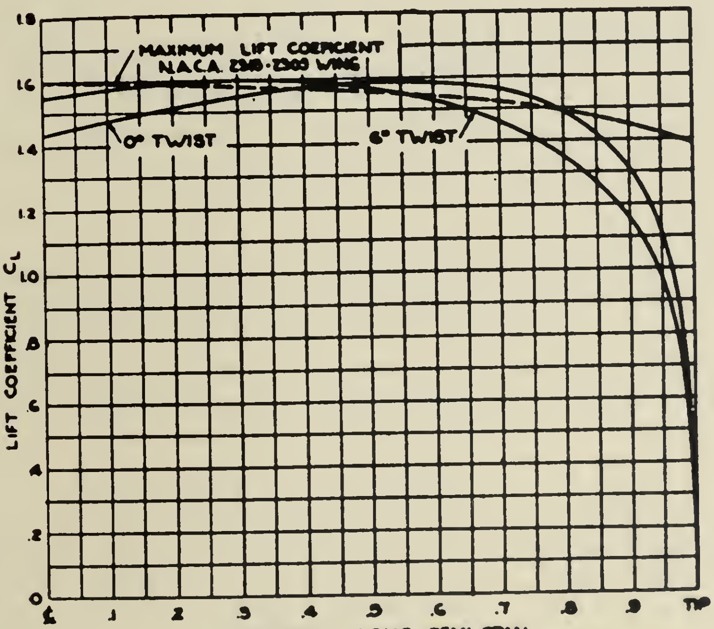

LIFT COEFFICIENT ALONG TAPERED WING.

$C_{L_{AV.}}$ = 1.50

ASPECT RATIO = 6.724 TIP CHORD = .461 ROOT CHORD

FIG. 11.

(b) Twist Combined with Change of Camber.

More efficient than a mere twist is the combination of twist and chan camber as follows from Fig. 12, where lift curves are plotted for a sec small and a section of higher camber. Provided that the difference in α smaller than the difference in zero lift angle, it is obvious that the total an range for the more highly cambered section is greater than for the section low camber. This increase of total effective angular range can be utilise delay stalling of the tips. If we consider first a section of a relatively low car near the root of the aerofoil, and if we base our consideration on a theoretical C_L distribution depending on the taper ratio of the wing, a cer local value of C_L is required. The margin against stalling of this section

$$\gamma = (\alpha_{max}) \text{ absolute} - \alpha_1 = C_{Lmax}/(dC_L/d\alpha) - C_L/(dC_L/d\alpha)$$

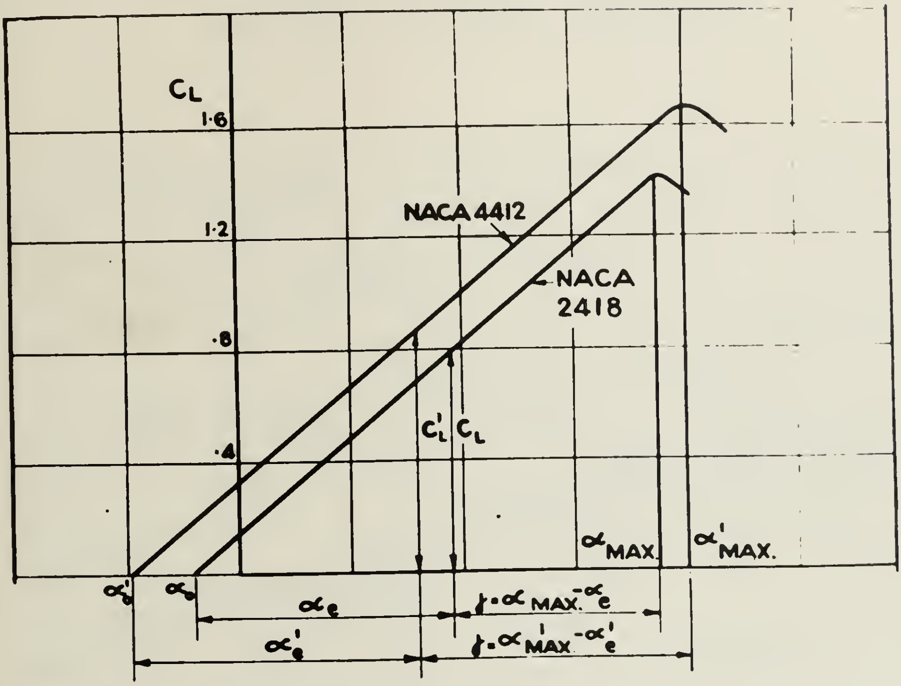

FIG. 12.

$dC_L/d\alpha = 2\pi$ (theoretical value), but this value is actually slightly influenced thickness chord ratio and camber; (α_{max}) absolute $= \alpha_0 + \alpha_{max}$ where α_0 zero angle and α_{max} is the angle at which C_{Lmax} is measured from $\alpha = 0$.

Let us now consider a section further outboard at which the local lift coeffic required may be C_L'. The local margin against stalling at this portion of wing is therefore :—

$$\gamma' = (\alpha'_{max})/\text{absolute} - C_L'/(dC_L/d\alpha).$$

It is obvious that if $\gamma' > \gamma$, the wing will stall first at the inner section the difference between γ' and γ will then represent the margin against stal of the outboard section compared with the inboard one. It can easily be veri that the required geometric angle and therefore the necessary amount of tw to produce the value of C_L' is equal to the difference of the respective zero angles of the two wing sections.

An investigation on these lines has been made for wings of various ta ratios, and the assumptions in regard to distribution of thickness chord ra

camber ratio along the span are plotted in Fig. 12*a*. This figure contains the amount of twist required in order to produce the theoretical ribution for a given overall C_L value. It seems advisable to choose an al C_L value corresponding to climbing flight. For this condition of flight will then be no increase of induced drag compared with an untwisted wing constant section. Fig. 13 shows the distribution of the margin against ng across the span for wings of various taper ratios and for wing sections ng the maximum camber at various positions of the chord. The charac- stics are taken from N.A.C.A. Report No. 460 (1). As the figure indicates ons with the camber at 0.4 and 0.5 of the chord give satisfactory results e sections with the camber at 0.3c are less suitable.

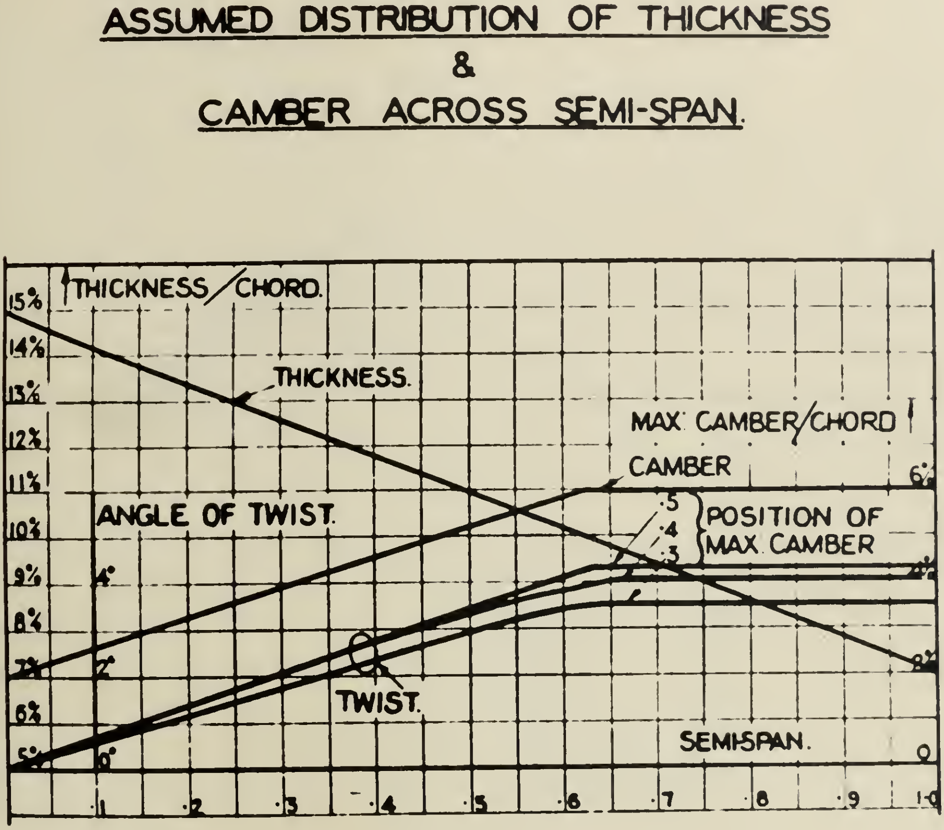

FIG. 12*a*.

Tapered Wings and Wing Tip Slots.

The method described above is based upon the increase of angular range mainly to the lower zero lift angle of higher cambered sections compared with those ow camber. The obvious disadvantage, of course, is the difficulty to fair sections of varying camber and also the concentration of high torque at the s where the resistance of the wing against torsional deflection is weakest. other method consists in utilising such sections where the angular range is eased at the high lift end of the angular range, for example, by using a ted section at the tips.

Sucking away the boundary layer is also a means to increase the high lift end the angular range, and one could conceive a method to prevent tip stalling this basis. Such a method would, however, suffer from the obvious practical advantage that the effect is bound up with the working of the power plant ch drives the pump.

5. Tapered Wings and Longitudinal Stability.

(a) *Analysis of Pitching Moments.*

Most designers who began to design monoplanes with tapered w... applied the knowledge and experience gained from biplane design ... faced with the difficulty to obtain satisfactory longitudinal stability ...

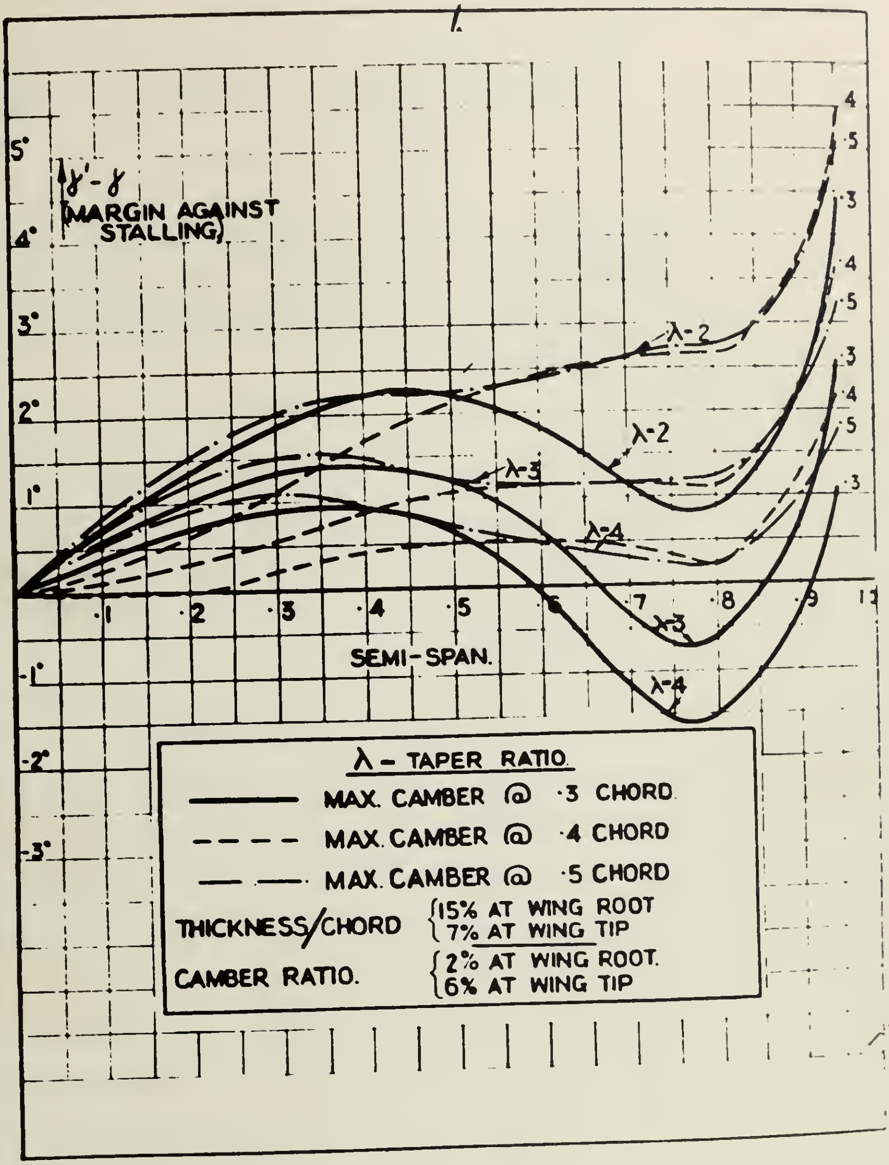

Fig. 13.

found it necessary either to shift the C.G. much more forward of the ... assumed position or to increase the tail volume considerably beyond ... which gave satisfactory stability on biplanes. There are various rea... account for this mysterious instability of the monoplane, and in th... I propose to deal with some of the major causes, but I am not claim... effects mentioned are the only ones. The conclusions drawn are ba... careful analysis of wind tunnel tests with a twin-engined monopla... taper ratio of about 4 : 1 and a tail volume of 0.55.

Fig. 14 shows a typical pitching moment diagram for a twin-en... plane. The resulting pitching moment has been resolved into mom...

Admitted November 24, 1950.

DEFENDANTS' EXHIBIT XX

District Court of the United States, Southern District of California, Central Division

Civil Action No. 10930-Y

MAURICE A. GARBELL, INC., a California Corporation, and GARBELL RESEARCH FOUNDATION, a California Corporation,

Plaintiffs,

vs.

CONSOLIDATED VULTEE AIRCRAFT CORPORATION, a Delaware Corporation, and AMERICAN AIR LINES, INC., a Delaware Corporation,

Defendants.

STIPULATION #4

It is hereby stipulated subject to proof of error that the appended "Exhibit 22" is a reproduction of pages 604 to 613 of a printed publication "Luftfahrforshung" containing an article entitled "Elliptische Autriebsverteiling durch Verwindung und Profilanderung" published and issued by Z.W.B. in Berlin, Germany, in the year 1937 and that "Exhibit 22a" is a translation of said article (subject to correction if any error is contained therein), and that said "Exhibit 22a" may be used in evidence with the same force and effect as an original, subject to any objection which may be made thereto as irrelevant or immaterial when offered in evidence, viz:

LYON & LYON,
/s/ FREDERICK W. LYON,
Attorneys for Plaintiffs.

/s/ ROBERT B. WATTS,
/s/ FRED GERLACH,
Attorneys for Defendants.

C+Ic exhibit 22a

(Translation from Luftfahrtforschung, [illegible] -615, 1938)

ELLIPTICAL LIFT DISTRIBUTION BY TWIST AND CHANGE IN PROFILE

by Shih Cheng Zien, Shanghai[1]

[1]. Thesis, Technical University, Berlin.)

Abstract

An examination is made of the methods by which elliptical lift distribution can be attained spanwise by twist and profile variation. By this means air flow separation (or burbling) occurs at the wing tips later than in the center of the wing.

Elliptical lift distribution gives the smallest induced drag [3].[2]

([2]. The numbers given in brackets refer to "References", Section IX.)

Lateral stability is guaranteed even at stall, by the delayed separation of the flow at the wing tips whereby the danger of spin [?] is reduced.

The trapezoidal wing has a simple planform. Highly tapered trapezoidal wings have especially greater depth at the root. Thereby, the stiffness is increased (singularly favorable for wing vibration) and the weight is reduced. This construction permits the useful load being placed in the center of the wing.

Contents

~~EXHIBIT 22a~~ C 21

I. Fundamentals of Airfoil Theory

he Lift of a portion of a wing of infinite span, having the
t dx, is given by Kutta-Joukowski's Circulation Theorem

$$dA = \rho v_\infty \Gamma(x)\, dx \tag{1}$$

:

ρ = the air density

v_∞ = the stream velocity at infinity.

$\Gamma(x)$ = the circulation at the point x.

Practically, the lift is calculated by the formula:

$$dA = C_a(x) \frac{\rho}{2} v_\infty^2\, t(x)\, dx \tag{2}$$

e:

C_a = the value of the lift (determined experimentally) at the point x.

$t(x)$ = the wing chord at the point x.

A comparison of equations (1) and (2) gives:

$$\Gamma(x) = \frac{1}{2} C_a(x)\, t(x)\, v_\infty \tag{3}$$

The circulation Γ is proportional to the product of C_a and t. C_a
roportional to the angle of attack, α, relative to the axis of
 lift.

$$c_a = \frac{dc_a}{d\alpha} \cdot \alpha$$

rculation distribution for a wing of infinite span is directly
tional to the angle of attack and the wing chord.

e lift distribution for airfoils of finite span is calculated by
l's Method [2]. The circulation is here no longer proportional
geometrical but to the effective angle of attack, α . The
ence between the geometrical angle of attack, α_g and the effective,
s the induced angle of attack, α_i

$$\alpha_i = \frac{v_i(x)}{v_\infty} = \frac{1}{4\pi v_\infty} \int_{-\frac{b}{2}}^{+\frac{b}{2}} \frac{d\Gamma}{d\xi} \cdot \frac{d\xi}{x-\xi} \qquad (5)$$

x is the point at which the induced angle of attack is calculated.
is the abscissa, variable over the span. The effective angle of
thus is then:

$$\alpha_e = \alpha_g - \alpha_i$$

ubstitution of α_e in equations (3) and (4) gives:

$$\Gamma(x) = \tfrac{1}{2} c'_{a\infty} (\alpha_g - \alpha_i)\, t(x) \cdot v_\infty \qquad (6)$$

ith reference to equation (5)

$$) = \tfrac{1}{2} t(x)\, v_\infty\, c'_{a\infty} \left[\alpha_g(x) - \frac{1}{4\pi v_\infty} \int_{-\frac{b}{2}}^{+\frac{b}{2}} \frac{d\Gamma}{d\xi} \cdot \frac{d\xi}{x-\xi}\right] \qquad (7)^3$$

See, Fuchs-Hopf-Seewald: Aerodynamics Vol. II, Chapter V, pp. 139-140)

irculation is determined spanwise by this integral equation when
ing contour and the distribution of the angle of attack are given.

II. Fuchs' Solution [1]

quation (7) was solved by Betz [4] by means of a power series, by
rt [6] and Lotz [5] by means of a Fourier Series, by Fuchs [1] by
of a trigonometrical polynomials and graphically by Lippisch [7].
n Fuchs' method the airfoil contour is approximated as well as
ble by the fewest possible members of a trigonometric polynomial
practical wing model, the approximate contour possesses thereby
h leading and trailing edges, as well as rounded wing tips. This
dvantageous compared to the zigzag sinusoidal wing edges for the

ximation of the contour by other methods.

quation (7) is simplified by the introduction of new variables:

$$x = -\frac{b}{2}\cos\varphi \quad , \quad \xi = -\frac{b}{2}\cos\psi$$

φ and ψ vary from 0 to π, when x and ξ vary from $(-\frac{b}{2})$ to

); furthermore $\Gamma(x) = 2bv_\infty G(x)$.

$$t = \frac{4b}{c'_{a\infty}}\mu(x)$$

e:

$$G(\varphi) = \mu(\varphi)\left[\alpha_g(\varphi) - \frac{1}{\pi}\int_0^\pi \frac{dG}{d\psi}\frac{d\psi}{\cos\psi - \cos\varphi}\right] \tag{8}$$

ontour function $\mu(\varphi)$ is an odd sine function with odd members, if irfoil is symmetrical about the center, $\varphi = \frac{\pi}{2}$., and decreases ds the wing tips.

$$\mu(\varphi) = \mu_1\sin\varphi + \mu_3\sin3\varphi + \mu_5\sin5\varphi + \dots\dots$$

arly for the circulation

$$G(\varphi) = G_1\sin\varphi + G_3\sin3\varphi + G_5\sin5\varphi + \dots\dots$$

relation transforms (8) into:

$$\varphi\sum_{n=1}^{\infty}G_{2n-1}\sin(2n-1)\varphi = \alpha_g\mu\sin\varphi - \mu\sum_{n=1}^{\infty}(2n-1)G_{2n-1}\sin(2n-1)\varphi \tag{9}$$

he geometrical angle of attack, α_g, is represented in the al case by:

$$\alpha_g(\varphi) = \alpha_0 + \alpha_2\cos2\varphi + \alpha_4\cos4\varphi + \dots\dots \tag{10}$$

is symmetrical about the wing center and decreases towards the wing

he evaluation of the coefficients $G_1, G_3 \dots$ according to equation (9) is:

$$\left.\begin{aligned} G_1 &= S_1 - \sum_{\lambda=1}^{\infty}(2\lambda-1)\mu_{2\lambda-1}G_{2\lambda-1} \\ G_{2k+1} - G_{2k-1} &= S_{2k+1} - S_{2k+1} \\ &\quad - \sum_{\lambda=1}^{\infty}(2\lambda-1)(\mu_{2\lambda+2k-1} \pm \mu_{2\lambda-2k-1})G_{2\lambda-1} \end{aligned}\right\} \tag{11}$$

the minus sign is valid as long as $\lambda \leqq k$ and plus if $\lambda > k$, so one takes: $\mu_{-1} = -\mu_1$, $\mu_{-3} = -\mu_3$.

his way:

$$S_{2i+1} = \alpha_0\mu_{2i+1} + \frac{\alpha_2}{2}(\mu_{2i+3} + \mu_{2i-1}) + \frac{\alpha_4}{2}(\mu_{2i+5} + \mu_{2i-3}) + \dots\dots$$

275

$k = 2$

$$\left.\begin{aligned} (1+\mu_1)G_1 + \quad 3\mu_3 G_3 + \quad 5\mu_5 G_5 &= S_1 \\ \mu_3 G_1 + [1 + 3(\mu_1 + \mu_3 + \mu_5)] G_3 + 5(\mu_3 + \mu_5) G_5 &= S_3 \\ \mu_5 G_1 + 3(\mu_3 + \mu_5) G_3 + [1 + 5(\mu_1 + \mu_3 + \mu_5) G_5 &= S_5 \end{aligned}\right\} \quad (1?)$$

r:

$$S_1 = \alpha_0 \mu_1 + \frac{\alpha_2}{2}(\mu_3 - \mu_1) + \frac{\alpha_4}{2}(\mu_5 - \mu_3)$$

$$S_3 = \alpha_0 \mu_3 + \frac{\alpha_2}{2}(\mu_5 + \mu_1) + \frac{\alpha_4}{2}(-\mu_1)$$

$$S_5 = \alpha_0 \mu_5 + \frac{\alpha_2}{2} \mu_3 \qquad + \frac{\alpha_4}{2}\mu_1$$

he approximation of the contour gives us $\mu_1, \mu_3, \ldots \mu_{k+1}$, the ximation of the twist $\alpha_0, \alpha_2 \ldots \alpha_{2\lambda}$; we have therewith $(k+1)$ ions for the calculation of the $(k+1)$ unknown of the lift function $_3 \ldots G_{2k+1}$. The series $\mu(\varphi), G(\varphi), \alpha_q(\varphi)$ are rapidly convergent [1]. he calculation of the lift, it is, in general sufficient to ximate three terms each for $\mu(\varphi)$ and $\alpha_q(\varphi)$ in order to solve for hree unknowns G_1, G_3, G_5 from the three linear equations.

onversely, for a given lift distribution $G(\varphi)$ and a given wing ur $\mu(\varphi)$ the twist $\alpha_q(\varphi)$ can easily be calculated. Fuchs treats roblem: How must the airfoil be twisted for an elliptical lift ibution?

n this work Fuchs' proposal is further developed and, indeed that low separates at the tips later than in the center is considered. or the solution of the proposed problem, a series of assumed zoidal airfoils is investigated, in which the wing contour is ximated by several members of a trigonometric polynomial and the calculated thereby compared with the desired condition.

n this work is given a method according to which all such ximations can easily be performed graphically.

III. Approximation of the Wing Contour

The contour function:

$$\mu(\varphi) = \mu_1 \sin\varphi + \mu_3 \sin 3\varphi + \mu_5 \sin 5\varphi \quad \text{or}$$
$$t(\varphi) = t_1 \sin\varphi + t_3 \sin 3\varphi + t_5 \sin 5\varphi$$

hereby wanted so that $t(\varphi)$ accurately defines the airfoil surface d represents as far as possible an experimental wing contour.

The first coefficient μ_1 or t_1 is given analytically by the condition the equality of the surfaces:

$$F = \int_{-\frac{b}{2}}^{+\frac{b}{2}} t(x)\,dx = \frac{b}{2}\int_0^{\pi} t(\varphi)\sin\varphi\, d\varphi \doteq \frac{b}{4}\cdot\pi\cdot t_1$$

$$t_1 = \frac{4F}{\pi b}$$

$$\mu_1 = \frac{c'_{a\infty}}{4b}\cdot t_1 = \frac{c'_{a\infty}}{\pi A} \qquad \left(A = \frac{b^2}{F}\right)$$

The members of higher order are without influence on the surface ea; they are a function only of the chord distribution. They are aphically determined.

The half span is obtained from the abscissa, the wing chord from e ordinate (See Appendix, Fig. 1).

e semi-span is subdivided in the cosine of the angle varying by its of 10°. The cosine division is obtained quickly and accurately a quarter-circle with radius $r = \frac{b}{2}$ is drawn below the figure, the arter circle is divided into nine equal parts and from the parts tained in this way, perpendiculars are dropped on-to the base. It recommended that the scale of the diagram be chosen so that $\frac{b}{2}$ approximately 20 to 30 cm.

The cosine division of the abscissa is plotted twice on transparent per. The ellipse

$$y_1 = t_1 \sin\varphi$$

s drawn over one of the cosine divisions. The function

$$y_3 = t_3 \sin 3\varphi$$

s superimposed in this ellipse for various t_3's. It is sufficient n most cases to put:

$$\frac{2t_3}{b} = \pm 0.05, \ \pm 0.10, \ \pm 0.15, \ \pm 0.20, \ \pm 0.25$$

e Appendix, Fig. 2)

The transparent paper is then laid on the figure on which the actual rd is plotted and one judges which curve y or which t_3 best rresponds to the actual airfoil contour. The first approximation of t_3 is determined sufficiently accurate by interpolation of the lividual curves:

$$\mu_3 = \frac{c'_{a\infty}}{4b} \cdot t_3$$

e curve

$$y = t_1 \sin\varphi + t_3 \sin 3\varphi$$

plotted on the other cosine division where t_3 corresponds to the lue just found by interpolation. The function

$$y_5 = t_5 \sin 5\varphi$$

plotted over this curve for different t_5's. It is sufficient to ot:

$$\frac{2t_5}{b} = \pm 0.025, \pm 0.050, \pm 0.075, \pm 0.100$$

e Appendix, Fig. 3)

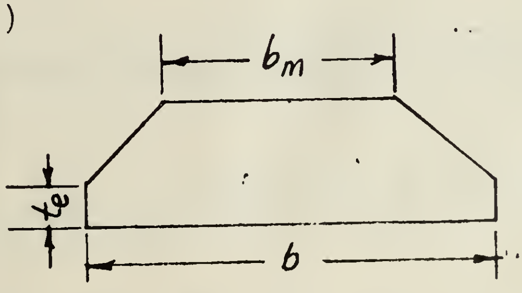

Fig. 1: On the Trapezoidal Ratio

This transparent paper is now laid over the figure on which the tual wing chord is plotted and one judges which curve y or t_3 orresponds best with the actual outline:

$$\mu_5 = \frac{c'_{a\infty}}{4b} \cdot t_5$$

The values of y_1, y_3, y_5 are obtained quickly and accurately in rawing circles about a point with radii t_1, t_3, t_5 and the

diculars at every 10°. Firstly, it can be established for the ination of t_5 if this first approximation for t_3 was well chosen. , the process must be repeated, i.e. t_3 and t_5 are again ined. As the actual wing contour can be scrutinized each time if the first approximation is as good as the former. It is sufficient practically if only the first three members of the ometric series are used.

the present work, 26 trapezoidal airfoils with the same area, the ratio of sides ($\Lambda = 5$) but different trapezoidal ratios were tigated. (See Appendix, Table 1 examples for that purpose, dix, Figs. 4 to 8)

rapezoidal ratio, Fig. 1.

$$\frac{b_m}{b} = 0;\ 0.2;\ 0.4;\ 0.6;\ 0.8;\ 1$$

$$\frac{t_e}{t_m} = 0;\ 0.2;\ 0.4;\ 0.6;\ 0.8$$

he dimensionless coefficients, μ_1, μ_3, μ_5 of the contour function nversely proportional to the ratio of the sides Λ. For other s of the sides, μ_1, μ_3 and μ_5 must change correspondingly.

IV. Calculation of Twist for an Elliptical Lift Distribution

The twist function

$$\alpha_q(\varphi) = \alpha_0 + \alpha_2 \cos 2\varphi + \alpha_4 \cos 4\varphi$$

o be found.

The contour functions

$$\mu(\varphi) = \mu_1 \sin\varphi + \mu_3 \sin 3\varphi + \mu_5 \sin 5\varphi$$

the condition, that the circulation distribution shall be elliptical,

$$G(\varphi) = G_1 \sin\varphi$$

$$C'_{a\infty} = \text{constant spanwise}$$

given.

Analytical Solution

If, in equation (12),

$$G_3 = G_5 = 0$$

bstituted, then

$$\left.\begin{aligned} \mu_1) G_1 &= \alpha_0 \mu_1 + \frac{\alpha_2}{2}(\mu_3 - \mu_1) + \frac{\alpha_4}{2}(\mu_5 - \mu_3) \\ \mu_3 G_1 &= \alpha_0 \mu_3 + \frac{\alpha_2}{2}(\mu_5 + \mu_1) + \frac{\alpha_4}{2}(-\mu_1) \\ \mu_5 G_1 &= \alpha_0 \mu_5 + \frac{\alpha_2}{2}\mu_3 + \frac{\alpha_4}{2}\mu_1 \end{aligned}\right\} \qquad (13)$$

ained. The solution of the equations gives:

$$\left.\begin{aligned} \alpha_0 &= \left(1 + \frac{1}{\mu_1}\,\frac{q}{ps - rq}\right) G_1 \\ \alpha_2 &= \frac{2}{\mu_1}\cdot\frac{p}{ps - rq}\, G_1 \\ \alpha_4 &= \frac{2}{\mu_1}\,\frac{1}{ps - rq}\left[\frac{\mu_5}{\mu_1} q - \frac{\mu_3}{\mu_1} p\right] G_1 \end{aligned}\right\} \qquad (14)$$

$$p = \frac{\mu_3}{\mu_1} + \frac{\mu_5}{\mu_1} \qquad r = \frac{\mu_3}{\mu_1}\left(\frac{\mu_5}{\mu_1} - \frac{\mu_3}{\mu_1}\right) + 1$$

$$q = 1 + \frac{\mu_3}{\mu_1} + \frac{\mu_5}{\mu_1} \qquad s = \frac{\mu_5}{\mu_1}\left(\frac{\mu_5}{\mu_1} - \frac{\mu_3}{\mu_1} + 1\right) - 1$$

the numerical values for μ_1, μ_3, μ_5 are introduced into these ons, it is shown that q is much larger than p, p is much larger than $\left[\frac{\mu_5}{\mu_1} q - \frac{\mu_3}{\mu_1} p\right]$ ries $\alpha_g(\varphi)$ converges very rapidly, so that $\alpha_g(\varphi)$ is determined iently accurately by three terms. The twist sought is then:

$$= \alpha_0 + \alpha_2 \cos 2\varphi + \alpha_4 \cos 4\varphi$$

$$G_1\left[1 + \frac{1}{\mu_1}\,\frac{q}{ps - rq} + \frac{2}{\mu_1}\,\frac{p}{ps - rq}\cos 2\varphi + \frac{2}{\mu_1}\,\frac{1}{ps - rq}\left\{\frac{\mu_5}{\mu_1} q - \frac{\mu_5}{\mu_1} p\right\}\cos 4\varphi\right]$$

$$= G_1 + \frac{G_1}{\mu_1}\left[\frac{q}{ps - rq} + \frac{2p}{ps - rq}\cos 2\varphi + \frac{2}{ps - rq}\left\{\frac{\mu_5}{\mu_1} q - \frac{\mu_3}{\mu_1} p\right\}\cos 4\varphi\right]$$

e geometrical angle of attack is composed of two parts, the d angle of attack

$$\alpha_i = \frac{C_a}{\pi \Lambda} = G_1,$$

is constant spanwise, and the effective angle of attack which is le spanwise but which is everywhere proportional to

$$\frac{G_1}{\mu_1} = \frac{C_a/\pi\Lambda}{C'_{a\infty}/\pi\Lambda} = \frac{C_a}{C'_{a\infty}} = \alpha_e \text{ ellipt. Fl.}$$

is, moreover, the constant lift coefficient, which corresponds with lliptical airfoil contour, $\alpha_{e \text{ ellipt. Fl.}}$ is the accompanying constant effective of attack, then

$$(\varphi) = \alpha_i + \alpha_{e \text{ ellipt. Fl.}} \left[\frac{q}{ps-rq} + \frac{2p}{ps-rq}\cos 2\varphi + \frac{2}{ps-rq}\left\{\frac{\mu_5}{\mu_1}q - \frac{\mu_3}{\mu_1}p\right\}\cos 4\varphi \right. \quad (15)$$

he twist function is calculated for the airfoils examined for $= 0.3 : C'_a = 2\pi\, 0.833$. The numerical values of the calculations are in Table 1 of the appendix; for that purpose, Fig. 4 to 8 of the dix are drawn as examples.

2. Graphical Solution

quation (9) is transformed into:

$$\alpha_q(\varphi) = \frac{G_1 \sin\varphi + G_3 \sin 3\varphi + G_5 \sin 5\varphi + \dots\dots}{\mu_1 \sin\varphi + \mu_3 \sin 3\varphi + \mu_5 \sin 5\varphi + \dots\dots} + \frac{G_1 \sin\varphi + 3G_3 \sin 3\varphi + 5G_5 \sin 5\varphi + \dots\dots}{\sin\varphi} \quad (16)$$

an elliptical distribution: $G_3 = G_5 = \dots\dots = 0$

$$\alpha_q(\varphi) = G_1 + \frac{G_1 \sin\varphi}{\mu_1 \sin\varphi + \mu_3 \sin 3\varphi + \mu_5 \sin 5\varphi}$$

elliptical wings, the effective angle of attack is

$$\alpha_{e \text{ ellipt. Fl.}} = \frac{G_1 \sin\varphi}{\mu_1 \sin\varphi} = \frac{G_1}{\mu_1}.$$

$$G_1 \sin\varphi = \alpha_{e \text{ ellipt. Fl.}} \cdot \mu_1 \sin\varphi$$

ce:

$$\alpha'_q(\varphi) = \alpha_i + \alpha_{e \text{ ellipt. Fl.}} \frac{\mu_1 \sin\varphi}{\mu_1 \sin\varphi + \mu_3 \sin 3\varphi + \mu_5 \sin 5\varphi} \quad (16a)$$

e

$\alpha_{e \text{ ellipt. Fl.}} = \frac{C_a}{C'_{a\infty}}$ = the constant effective angle of attack for elliptical wings.

$\alpha_i = \frac{C_a}{\pi\Lambda} = G_1$ = the constant induced angle of attack.

The distribution function of the effective angle of attack is obtained ivision of the wing chord of the elliptical airfoil by the roximated wing contour (See, appendix, as example, Fig. 4).

3. Comparison of the Analytical and Graphical Methods

Comparison of equations (15) and (16a) must yield agreement oth distribution functions:

$$\frac{\ }{q}+\frac{2p}{ps-rq}\cos 2\varphi+\frac{2\left(\frac{\mu_5}{\mu_1}q-\frac{\mu_3}{\mu_1}p\right)}{ps-rq}\cos 4\varphi=\frac{\mu_1\sin\varphi}{\mu_1\sin\varphi+\mu_3\sin 3\varphi+\mu_5\sin 5\varphi}$$

For a special case, namely, the elliptical airfoil, i.e. $\mu_3 = \mu_5 = 0$ s the equation to be correct: both sides are unity. The curves wist from the graphical process are somewhat smaller in the center, gradually become larger towards the wing tips than those from the ytical procedure. The greatest deviation between the analytical graphical methods amounts to approximately 2% for rectangular wings 16% for delta wings. It can, therefore, be concluded that the hical method is applicable only for rectangular and ellipsoidal oils.

4. Discussion of the Twist Results.

For elliptically contoured wings, the angle of attack is stant spanwise. For trapezoidal airfoils, with a taper ratio, $\frac{t_e}{t_m} = \frac{1}{3}$ e Appendix, Fig. 9), the angle of attack is the same in the center at the wing tips.

$$\alpha_m = \alpha_{end}$$

For all trapezoidal airfoils with a taper ratio $\frac{t_e}{t_m} < \frac{1}{3}$, the le of attack increases towards the tips. They are useless. The ference between the angle of attack at the center of the wing and that the wing tips attains its greatest value for delta wings $\Delta\alpha_g = 5.4°$

For all trapezoidal airfoils with a taper ratio $\frac{t_e}{t_m} > \frac{1}{3}$, the le of attack decreases towards the tips. They are useful. The ference between the angle of attack at the center and that at the s becomes a maximum for rectangular airfoils, $\Delta\alpha_q = 2.2°$

Comparison with an elliptical wing gives a good appraisal of the nwise distribution of twist. Wherever the chord of a trapezoidal

s greater than that of an elliptical (wing), the angle of attack
ller and conversely.

e mathematical condition therefor, that the angle of attack decreases
ically towards the wing tips is:

$$\frac{d\alpha_g}{dx} < 0$$

n our case,

$$\alpha_2 > 0 \text{ or } p > 0$$

I the aspect ratio Λ increases, the geometrical angle of attack, $\alpha_g = \alpha_e$, decreases for the induced angle of attack, $\alpha_i = \frac{C_a}{\pi\Lambda}$, distributed
nly spanwise, is inversely proportional to Λ, and the effective
of attack

$$\alpha_e = \frac{C_a}{C'_{a\infty}} f(\mu, \varphi)$$

ependent of Λ. The taper ratio $\frac{t_e}{t_m} = \frac{1}{3}$ at $\alpha_m = \alpha_{end}$, is thus
for all trapezoidal wings haveing equal wing area and different
s

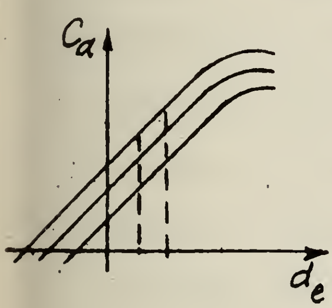

Fig. 2
the Influence of C_a

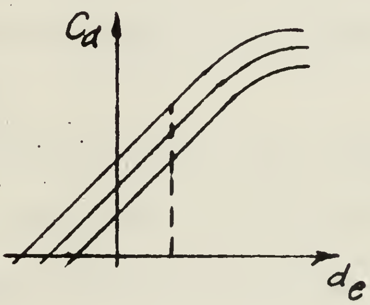

Fig. 3
On the Influence of C_a

I. Determination of the Angle of Attack which Corresponds to the Change in Profile for a Elliptical Lift Distribution

1. C_a Spanwise Distribution and the Influence of C_a.

From the condition that the lift $C_a \cdot t$ shall be elliptical
ise, a definite course of C'_a is given for each distribution of
hickness, t

$$C_a = C'_{a\infty}\alpha_e = C'_{a\infty}(\alpha + \beta)$$

β is the angle of zero lift C_a' is practically equal and constant
ll profiles.

may vary in three ways.

a. One and the same profile is retained over the whole span and the angle of attack is varied so that a definite angle of attack belongs to one value of C_a and conversely

$$\alpha_e = \alpha_{e\ ellipt. Fl.} \frac{G_1 \sin \varphi}{\mu_1 \sin \varphi + \mu_3 \sin 3\varphi + \mu_5 \sin 5\varphi}$$

This problem corresponds to the twist in Chapter V. For a given distribution of C_a, the distribution of the angle of attack is determined uniquely.

b. The same angle of attack is retained along the entire span and the profile varied, Fig. 2, so that a different value of C_a corresponds to the same angle of attack; i.e. profiles with different zero lift angles β are available in practice. Thereby, a spanwise distribution of the angle of attack is arbitrarily given, and the profile sought, in order to obtain a definite distribution of C_a.

c. The angle of attack and profile are both varied (Figure 3). Thereby, a distribution of C_a is given and the profile and angle of attack are to be found. The latter two belong to changes in profile [9].

2. Profile Systematics

A profile [11, 12] is characterized by the magnitude and ition of the camber and the thickness ratio $\frac{\delta}{t}$. The greater the ber $\frac{f}{t}$, the greater becomes the zero lift angle β and the maximum t coefficient, $C_{a\,max}$. The farther the maximum camber line lies rwards, the farther to the rear is the center of pressure.

The greater the thickness ratio, $\frac{\delta}{t}$, the smaller is $\frac{dc_a}{d\alpha}$.
he maximum value of the lift coefficient $C_{a\,max.}$ increases at first with he thickness ratio, reaches a maximum at approximately $\frac{\delta}{t} = 0.12$ and hen decreases again, where (Fig. 4)

β the angle of zero lift; α the angle of attack

α_1 the angle of attack referred to the axis of zero lift.

3. <u>Graphical Method for the Evaluation of the Distribution of the Angle of Attack</u>

Given the spanwise distribution of C_a and the condition that the angle of attack as well as the thickness ratio must decrease towards the wing tips.

The profiles and the geometrical angle of attack at each position are to be found.

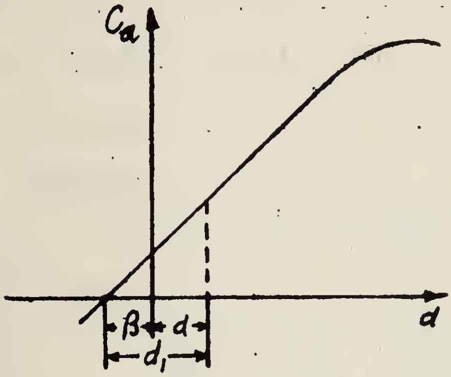

Fig. 4: On Profile Systematics

The greater the zero lift angle of a profile, the smaller is the angle of attack which is due to a definite value of C_a and the less is the danger of flow separation. It is recommendable that the angle of zero lift of the profile be as large as possible at the wing tips, i.e. in practice the camber of the profile shall be proportionally large at the wing tips.

It is sufficient here if the profiles and angles of attack are evaluated at five stations of the semi-wing. The value of C_a is calculated, the profile chosen, the effective angle of attack read off

$=f(\alpha)$ curve, the induced angle of attack, $\alpha_i = \frac{C_a}{\pi\Lambda}$ calculated and the geometrical angle of attack, $\alpha_g = \alpha_i + \alpha_e$, obtained. (See 10 to 12, Numerical Table 2).

r the determination of the range of the angle of attack up to flow ion for different locations of the wing, the profiles are plotted on n geometrical angle of attack by a point in Figure 12 Appendix, on he profiles are adjusted for fast flight. Up to $C_{a\,max}$ the NACA 0021 has a much smaller range of the angle of attack in the center of the an NACA 6409 profile has at the wing tips. In consequence the flow tes first in the center of the wing, then gradually outwards to the tips.

special case is where the profiles are to be found for a given bution of the angle of attack, e.g. for a distribution of the angle of decreasing linearly from the wing center to the tips. For a value and for an effective angle of attack, a definite point in the $C_a = f(\alpha)$ can be measured. By interpolation, the profile can be determined, Fig. 5. y this method, an elliptical lift distribution can be attained for apezoidal wings, for the difference in the angle of attack between ng center and the tips can be made.

Example

x =	0 (Wing Center)	$\frac{b}{8}$	$\frac{b}{4}$	$\frac{3b}{8}$	$\frac{b}{2}$ (Wing Tip)	Comparison Profile
ted NACA profile	0021	2418	4415	6412	6409	0015
r f/t in percent	0	2	4	6	6	0
of zero lift, β°	-0.1	-1.9	-3.8	-5.7	-5.9	0
ess Ratio, δ/t in %	21	18	15	12	09	15
$\frac{C_a}{\alpha}$, per degree	0.094	0.098	0.100	0.101	0.101	0.100
of maximum lift, $\alpha_{C_{a\,max}}$	17	15	15	15	15	17
ated effective angle attack, α_e degrees	2.92	0.92	-0.55	-2.19	-2.9	
lated Induced Angle Attack, α_i degrees	0.913	0.913	0.913	0.913	0.913	
trical Angle of ack, α_g degrees	3.833	1.833	0.363	-1.277	-1.987	
of Angle of Attack m the Angle of zero t to the Angle of $C_{a\,max}$ $^\circ = \alpha^\circ_{C_{a\,max}} - \alpha'_{C_a=0}$, degrees	17.1	16.9	18.8	20.7	20.9	

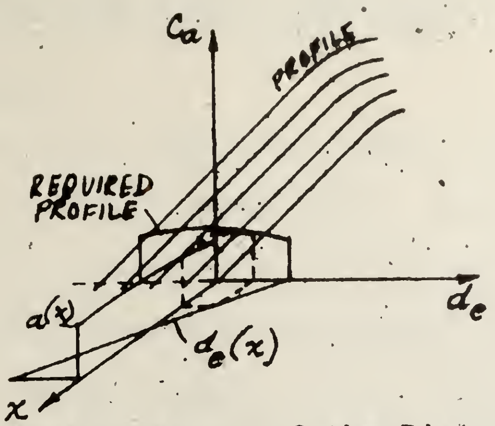

Fig. 5: On the determination of the Distribution of the Angle of Attack as great as the cambers of the profile permit.

4. Mathematical Examination of the Lift Distribution and of the Increase of Induced Drag

Two omissions are made in this method. The distribution of c_a is calculated from the approximate contour function. The coefficients of the contour function are determined by assuming that the mean value of the selected profiles $\frac{dc_a}{d\alpha}$ is constant spanwise. In reality, $\frac{dc_a}{d\alpha}$ vary somewhat for different profiles.

For the evaluation of the lift coefficient and of the angle of attack the flow around the wing has been considered as a plane problem. Actually the individual cross-sections mutually influence one another (space problem).

Whether these omissions are permissible will be verified by calculating the deviation of the lift distribution from the elliptical and the increase in the induced drag, which results from a profile with a mean $\frac{dc_a}{d\alpha}$ under the condition that the lift coefficient be invariable for the calculated five stations of the wing.

Example: Trapezoidal Wing: $\frac{t_e}{t_m} = 0.25$ $G_1 = 0.913$ $G_3 = -0.01404$

$G_3 = 0.00253$ $\frac{G_3}{G_1} = -0.01541$ $\frac{G_5}{G_1} = 0.00278$

$$\frac{\Delta c_{wi}}{c_{wi\,min}} = 3\left(\frac{G_3}{G_1}\right)^2 + 5\left(\frac{G_5}{G_1}\right)^2 = 0.00075 < 0.1\%$$

The increase in the induced drag compared to the smallest induced drag is very small.

VI. Comparison of an Untwisted Elliptical Wing and a Trapezoidal Wing with Twist and Profile Variation.

1. Induced Drag.

For elliptically contoured wings, the lift distribution lliptical under all flight conditions. For wings with any contour which an elliptical distribution is attained by twist or profile ation, the lift distribution is elliptical under one flight condition , generally under rapid flight. In the first case, the increase lft is proportional to t, in the second case, proportional to $t \cdot \frac{dc_a}{d\alpha}$. over, the Ca_{max} values (19) and the corresponding increase of the e of attack are ascertained. The lift distribution and the increase nduced drag are then calculated. It became evident that the ease in the induced drag is less than one percent (1%), in general, for Ca_{max}, on account of this deviation of the lift distribution the elliptical. The smaller the trapezoid ratio, the more vorable are the relations.

2. Flow Separation, Lateral Stability and Distribution Loss

For an elliptical wing with constant angle of attack nwise, the flow separates almost simultaneously at all points, i.e. profiles attain their maximum lift values simultaneously. Lateral bility at stall is poor.

A trapezoidal wing with an angle of attack decreasing from the wing ter to the tips has only one place in the center where the flow arates first and a Ca_{max} value appears. Not every profile attains maximum lift coefficient, because the total lift is smaller for a pezoidal wing than for an elliptical wing with the same wing area.

3. Comparison with Former Experimental Results.

C. B. Millikan [12] has experimentally established that w separation occurs for a rectangular wing first in the center of the g, for a trapezoidal wing first at the tips, moreover invariably the rear edge. Prandtl [16] previously found the same results.

the case of elliptical wings the flow has to separate everywhere ultaneously, but Prandtl showed in his experiments that the flow arates first at the tips. Irving [13] tested trapezoidal wings h straight leading and trailing edges. It was shown that the flow arates in the case of a trapezoidal wing, in the center of the g having a straight leading edge and in the rear third of the wing ing a straight trailing edge. Huebner [17] calculated theoretically t the loss in lift for a conventional trapezoidal wing with a constant file is approximately one percent (1%) compared to an elliptical wing equal area. A. E. Lombard [14] established, in wind tunnel tests t the flow for a strongly tapered trapezoidal wing, having a tip profile large $C_{a\,max}$ value, separates first in the center. Even in flight, observed that the stability is satisfactory. I. H Crowe [15] firmed that a twist of 8° is sufficient to prevent premature separation the flow at the wing tips. Large values improve the stability but reases the profile drag too much.

From the experimental results it appears:

1. That the flow separation at the wing tips is limited not only by the attitude of an individual cross-section but also by the wing form and the lift distribution altered simultaneously thereby (See Appendix, Table 3).
2. That for the prevention of premature flow separation at the wing tips of rectangular wings, no twist is needed compared to the greater twist of about 6° to 8° for strongly tapered trapezoidal wings.

According to the results of calculation for an elliptical lift tribution in Chapters IV and V, the twist for an approximately tangular wing amounts to about 2° (See Appendix, Figure 9 $\frac{t_e}{t_m} = 1$), a strongly tapered trapezoidal wing to about 6° (See Appendix, Figure 1.) The twist is according to the results of calculation, somewhat ater for a rectangular wing, somewhat smaller for a strongly tapered

ezoidal wing than that of experimental results hitherto obtained. The twisted rectangular wing is thus more advantageous than the isted and has therefore more lateral stability. The flow separation strongly tapered trapezoidal wings with a change in profile begins t in the center and proceeds then gradually outwards to the tips Chapter V, 3). It is influenced by the trapezoidal form, according hether it is provided with straight leading or trailing edges, as ng [13] established experimentally.

The results of calculation for an elliptical lift distribution and experimental results previously reported agree sufficiently well in e of small deviations.

The development of the JU-86 wing, reported by A. W. Quick [19] in 1936 Yearbook of the Lilienthal Company for Aeronautical Research n good agreement with my experimental results.

VII. Twist for an Arbitrary Lift Distribution

If the lift distribution is known and non-elliptical, the ficients G_1, G_3, and G_5 of the circulation distribution can ys be determined by the same graphical method as the coefficients he contour function, t_1, t_3, and t_5. An arbitrary lift ribution has been resolved into one elliptical, $G_1 \sin\varphi$ and two lift distributions, $G_3 \sin 3\varphi$ and $G_5 \sin 5\varphi$ while the integrals:

$$\int_{-\frac{b}{2}}^{+\frac{b}{2}} G_3 \sin 3\varphi \, dx = 0 \quad ; \quad \int_{-\frac{b}{2}}^{+\frac{b}{2}} G_5 \sin 5\varphi \, dx = 0$$

The values of G_1, G_3, and G_5 are substituted in equation (12) thereby three equations in three unknowns α_0, α_2, and α_4 are n obtained.

VIII. Summary

In the case of a trapezoidal wing with a taper ratio, $\frac{t_e}{t_m} > \frac{1}{3}$, elliptical distribution with good lateral stability at stall n be obtained by twist or profile change or both.

For a trapezoidal wing with a taper ratio, $\frac{t_e}{t_m} < \frac{1}{3}$ an elliptical stribution without endangering the lateral stability can be attained ly by variation in profile or by change in profile and twist. The teral stability is somewhat better for a weakly tapered trapezoidal ng than for a strongly tapered one.

IX. References

[1] Fuchs - Hopf - Seewald - Aerodynamics - Vol. II - 1935.

[2] L. Prandtl: Four Essays on Hydro - and Aero - Dynamics Wing Theory I and II.

[3] Max Munk: Isoperimetric Problems on the Theory of Flight. Inaug. Thesis, 1919.

[4] Betz: Contributions to Wing Theory with Special Consideration of a Simple Rectangular Wing. Gottingen. 1919.

[5] J. Lotz: Calculation of the Lift Distribution of an Arbitrarily Shaped Wing. Z. Flugtechn. Vol. 21 (1931).

[6] H. Glauert: Fundamentals of Wing and Air Screw Theory. Berlin, 1929.

[7] A. Lippisch: A Method for the Spanwise Lift Distribution. Luftf Forschg. Vol. 12 (1935) p. 89.

[8] A. V. Stephens: The Spin of Airplanes. Luftf Forschg. Vol. II, (1934) p. 140.

[9] Lachmann: Aerodynamic and Structural Features of Tapered Wings J. Roy. Aeron. Soc. (1937) III. pp. 176 - 179.

[10] Eastman, N. Jacobs, Kenneth E. Ward, and Robert M. Pinkerton: The Characteristics of 78 related Airfoil Sections from Tests in the variable-Density Wind Tunnel. NACA Rep. 460, 1933.

[11] Jacobs, N. Eastman and Robert Pinkerton: Tests on the Variable Density Wind Tunnel of Related Airfoils Having the Maximum Camber Unusually Far Forward. T.R. No. 537, NACA 1935.

[12] Clark B. Millikan: On the Stalling of Highly Tapered Wings. J. Aeronutical Sci. Bd. 3 (1936) Page 145.

[13] Irving, Some Notes on Tapered Wings, Aircr. Engng. Vol. 9 (1937) No. 96, II, 1937, p. 31.

[14] A. E. Lombard: Technological Development of the Curtiss-Wright Coupe. J. Aer. Sci. Vol. 3 (1936) p. 273.

[15] I. H. Crowe: An Examination of the Characteristics of a Popular Type of Wing: Aircr. Engng. Vol. 8 (1936) No. 91, XI, p. 290.

[16] L. Prandtl: Results of the Aerodynamic Experimental Station at Gottingen I, Lfg. (1921), p. 67.

[17] J. Hueber: The Aerodynamic Properties of Double Trapezoidal Wings Z. Flugtechn - Vol. 23 (1933), p. 271 · The Twisted Wing, Z. Flugtechn. Vol. 23 (1933), p. 307.

[18] Raymond F. Anderson: Determination of the Characteristics of Tapered Wings. NACA Rep. 572 (1936) p. 15.

[19] A. W. Quick: Lilienthal - Gesellschaft fur Luftfahrtforschung, (Lilienthal Co. for Aeronautical Research. Yr. 1936, p. 137, Printer R. Oldenbourg - Munchen-Berlin).

X Appendix

Fig. 2 On the approximation of the Contour

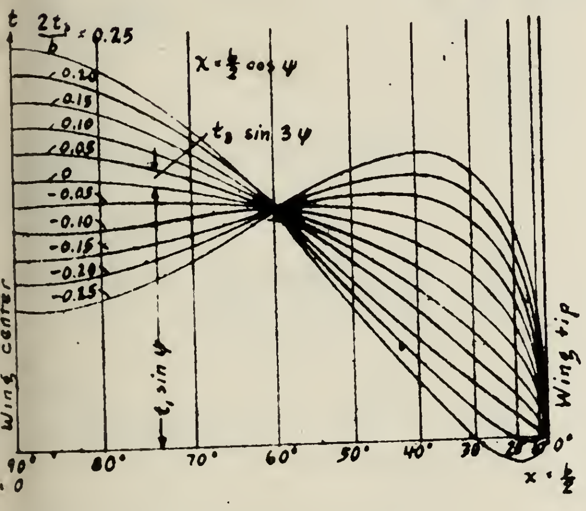

Fig. 1 On the approximation of the Contour

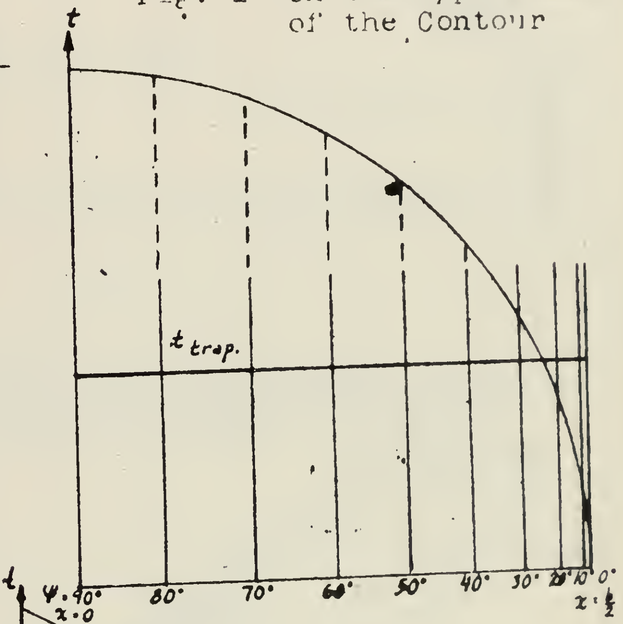

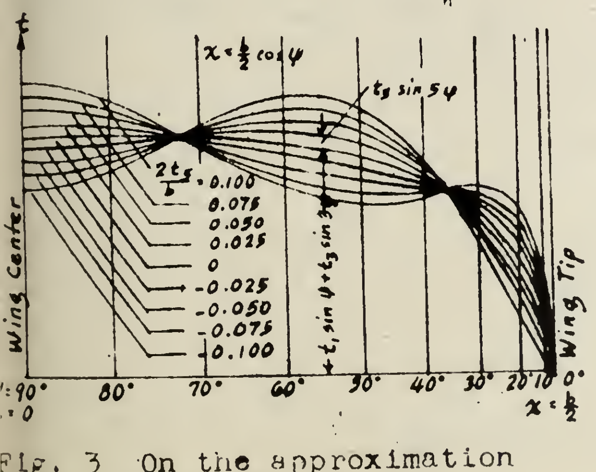

Fig. 3 On the approximation of the Contour

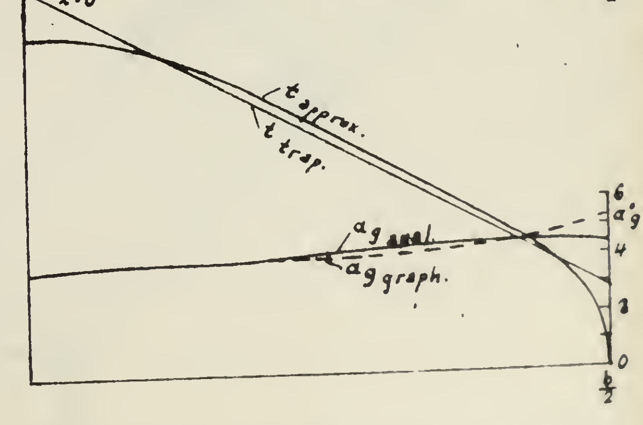

Fig. 4 Calculation of Twist Trapezoidal Ratio
$b_m/b = 0$, $t_e/t_m = 0.2$, $\lambda = 5$

Calculation of Twist:
Trapezoid Ratio

$\frac{b_m}{b} = 0.2, \frac{t_e}{t_m} = 0.4, \lambda = 5$

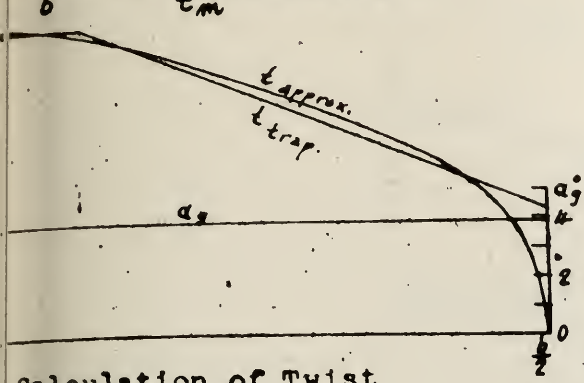

Fig. 6 Calculation of Twist
Trapezoid Ratio

$\frac{b_m}{b} = 0.4, \frac{t_e}{t_m} = 0.4, \lambda = 5$

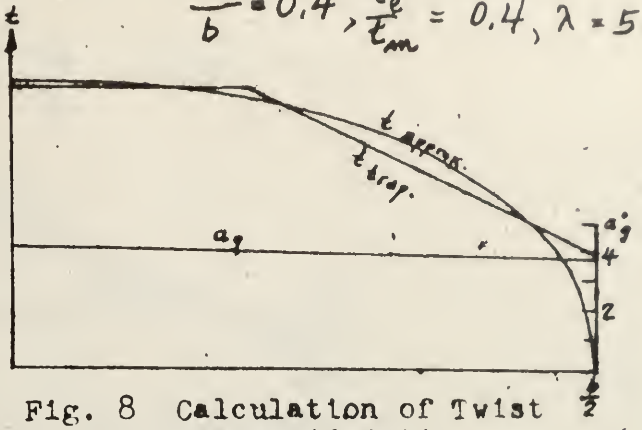

Calculation of Twist
Trapezoid Ratio

$\frac{b_m}{b} = 0.6, \frac{t_e}{t_m} = 0, \lambda = 5$

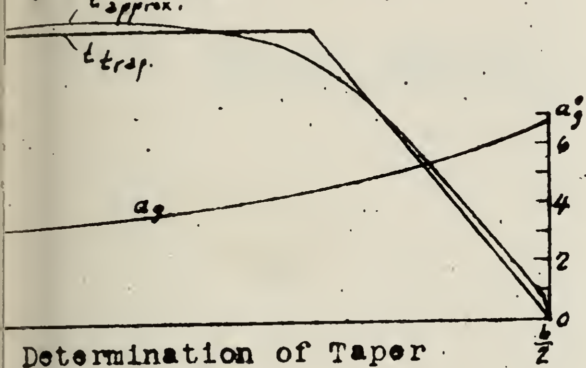

Fig. 8 Calculation of Twist
Trapezoid Ratio

$\frac{b_m}{b} = 0.8, \frac{t_e}{t_m} = 0.4, \lambda = 5$

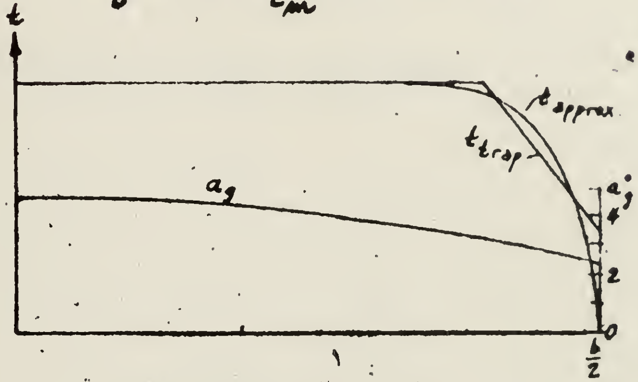

Determination of Taper
Ratio
For which

$a_m = a_{end}, \frac{t_a}{t_m} \approx \frac{1}{3}, \left(\frac{b_m}{b} = 0\right)$

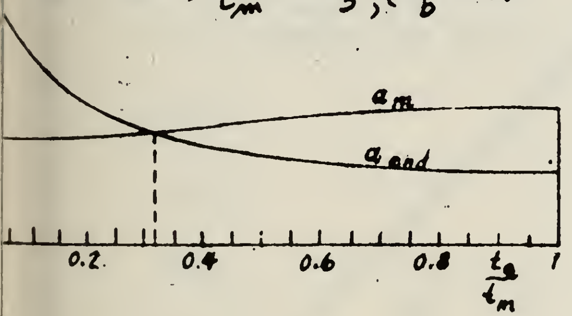

Fig. 10 Distribution of Angle of
Attack by Change in Profile

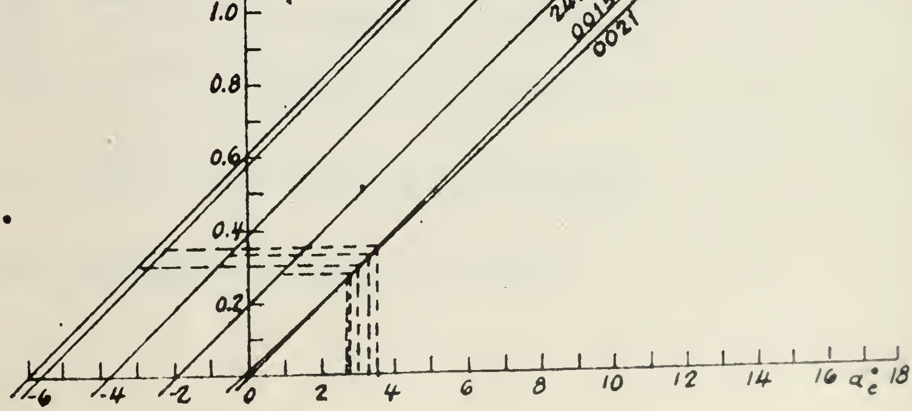

Fig. 11 Distribution of Angle of Attack by Change in Profile Trapezoid Ratio

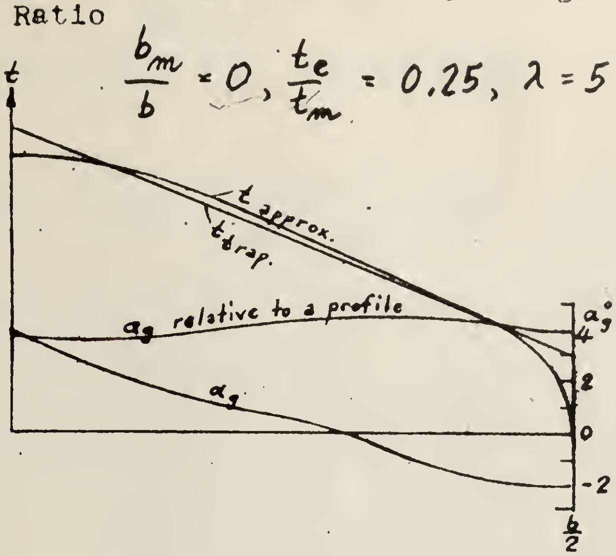

Fig. 12 Range of Angle of Attack to Flow Separation for Different Profiles

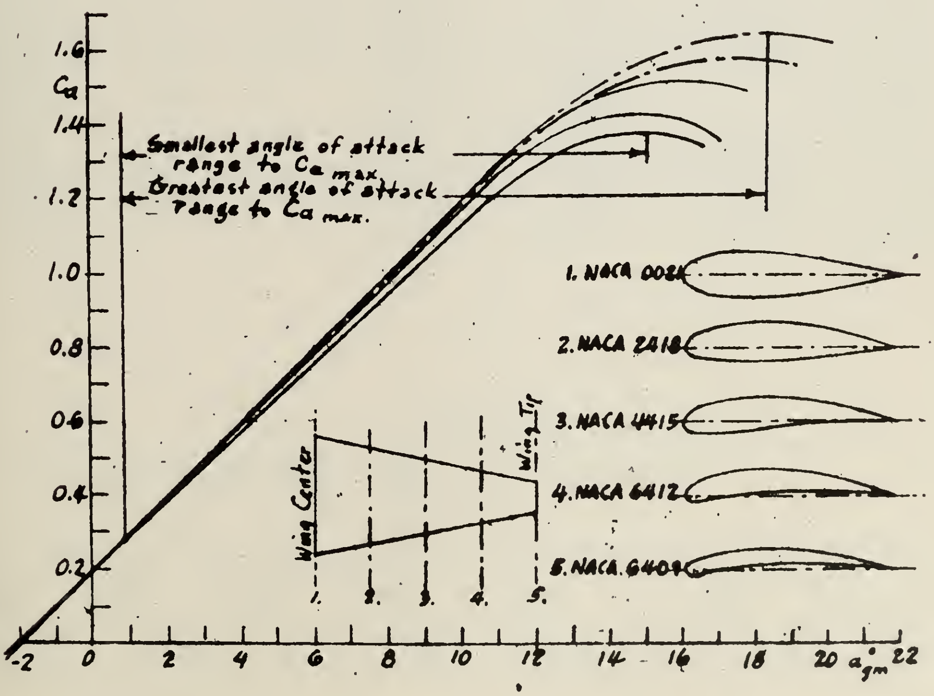

Mean Geometrical Angle of Attack

TABLE I

alculation of the Twist $(\Lambda = 5;\ c'_\alpha = 2\pi\,0.833)$.

d	t_1	t_3	t_5	μ_1	$\frac{\mu_3}{\mu_1}$	$\frac{\mu_5}{\mu_1}$	a_0	a_2	a_4
	cm	cm	cm				Deg.	Deg.	Deg.
	10.185	-1.308	0	0.333	-0.222	0	5.707	2.682	0.592
	10.185	-1.00	0.45	0.333	-0.0971	0.044	4.200	0.340	-0.234
	10.185	-0.33	0.40	0.333	-0.0324	0.039	3.950	-0.041	-0.234
	10.185	1.54	0.45	0.333	0.1512	0.0471	3.640	-0.863	-0.104
	10.185	1.80	0.50	0.333	0.177	0.0491	3.620	-0.967	-0.064
	10.185	2.12	0.50	0.333	0.208	0.0491	3.580	-1.055	-0.033
	10.185	-2.55	0	0.333	-0.25	0	5.960	3.310	0.795
	10.185	-1.45	0.50	0.333	-0.142	0.0491	4.410	0.750	-0.247
	10.185	0.50	0	0.333	0.0491	0	3.870	-0.282	-0.013
	10.185	1.00	0.50	0.333	0.0981	0.0491	3.680	-0.679	-0.067
	10.185	1.45	0.45	0.333	0.1424	0.0442	3.640	-0.830	-0.196
	10.185	-2.00	-0.50	0.333	-0.1965	-0.0491	5.710	3.050	1.061
	10.185	-0.80	0.25	0.333	0.0786	0.0245	4.210	0.365	-0.127
	10.185	0.31	0	0.333	0.0304	0	3.930	0.176	0.052
	10.185	1.00	0.20	0.333	0.0982	0.0196	3.739	-0.576	-0.050
	10.185	1.70	0.28	0.333	0.1670	0.0275	3.640	-0.858	-0.002
	10.185	-0.65	-1.00	0.333	0.0835	0.0982	4.941	1.752	0.121
	10.185	-0.35	0.30	0.333	-0.0344	0.0293	4.020	0.031	-0.176
	10.185	0.75	-0.25	0.333	0.0736	0.0245	3.760	-0.495	-0.099
	10.185	1.75	0.25	0.333	0.1720	0.0245	3.650	-0.572	0.019
	10.185	2.00	0.30	0.333	0.1965	0.0295	3.596	-1.012	0.042
	10.185	1.30	0	0.333	0.1275	0	3.740	-0.620	0.078
	10.185	1.75	0.25	0.333	0.1720	0.0245	3.650	0.870	0.019
	10.185	2.10	0.40	0.333	0.2061	0.0393	3.595	-1.021	0.010
	10.185	2.40	0.60	0.333	0.2360	0.0589	3.550	-1.162	-0.030
	10.185	2.15	0.50	0.333	0.2101	0.0491	3.580	-1.061	-0.026

TABLE II

hange in Profile: $\Lambda = 6;\ c'_{a\infty} = 2\pi\,0.91$

	t_1 cm	t_3 cm	t_5 cm	μ_1	μ_3	μ_5	0 Deg.	2 Deg.	4 Deg.
5	9.3	-0.8	0.6	0.303	-0.026	0.0195	3.95	0	-0.37

TABLE III

ison of Traction Surfaces With and Without Twist

	Wing with Twist	Wing Without Twist
bution	Elliptical only for a definite value of C_a	Elliptical only for wings with Elliptical Contour. For all other Forms of Wings, the Lift Distribution is not Elliptical. Rectangular Wing (Appendix Fig. 13) Trapezoidal Wing (Appendix Fig. 14) (strongly tapered)
ion of ration	Always in the wing center, because the range of the angle of attack to $C_{a\,max.}$ is less in the center than at the tips	Contour for Rectangular Wings (Appendix Fig. 15) — Position of Separation in the Center For elliptical wings (Appendix Fig. 16) at the wing tips. For Trapezoidal wings with straight leading edges (Appendix Fig. 17) — In the Center (rear) For Trapezoidal wings with straight trailing edges. (Appendix Fig. 18 — In the rear third of the outer wings.
ange max.	Not Simultaneous first in the center Small mean C_a	Theoretically, $C_{a\,max.}$ must be everywhere simultaneous. Experiments not simultaneous. Rectangular wings in the center. Trapezoidal wings and Elliptical Wings at the Tips. Larger mean C_a

Admitted November 24, 1950.

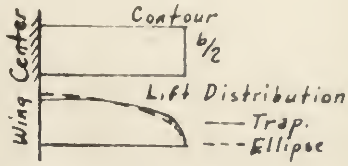

Fig. 13

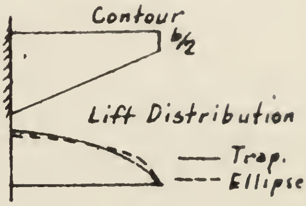

Fig. 14


Fig. 15


Fig. 16

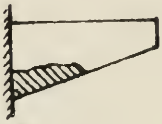
Fig. 17

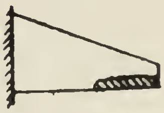
Fig. 18

DEFENDANTS' EXHIBIT AAA

District Court of the United States, Southern District of California, Central Division

Civil Action No. 10930-Y

MAURICE A. GARBELL, INC., a California Corporation, and GARBELL RESEARCH FOUNDATION, a California Corporation,

Plaintiffs,

vs.

CONSOLIDATED VULTEE AIRCRAFT CORPORATION, a Delaware Corporation, and AMERICAN AIR LINES, INC., a Delaware Corporation,

Defendants.

STIPULATION #7

It is hereby stipulated subject to proof of error that the appended are reproductions of printed publications and that said copies may be used in evidence with the same force and effect as an original, subject to any objection which may be made thereto as irrelevant or immaterial, when offered in evidence, viz:

"Exhibit 31" is a reproduction of page 140 No. 6 issued in the year 1937; "Exhibit 32" is a reproduction of page 419 No. 6 issued in the year 1937; "Exhibit 33" is a reproduction of page 609 No. 22 issued in the year 1937; "Exhibit 34" is a reproduction of page 421 No. 16 issued in the year 1938;

"Exhibit 35" is a reproduction of pages 144 and 145 No. 6 issued in the year 1939.

All are included in a periodical entitled "Flugsport" published and issued by "Flugsport" in Frankfurt, Germany, on said dates, respectively.

Exhibits 31a, 32a, 33a, 34a, 35a are translations of said articles respectively, subject to correction if any errors are found.

........................,
Attorneys for Plaintiffs.

/s/ ROBERT B. WATTS,
/s/ FRED GERLACH,
Attorneys for Defendants.

Exhibit 35a

Translation of page 144, No. 6—"Flugsport" (1939)

Performances and wing design of the DFS Reiher and DFS Weihe gliders were used in the construction of DFS Meise; for the root wing profile, Go 549 was thickened 16%; in the outboard wing Go 676 was used.

Illustration #1 shows that this profile is most suitable for the requirements of a compromise plane. The Ca region so important for this purpose is located between 0.6 and 1.4. Profile 549 is referred to twice in the series of experiments at Goettingen. As the coefficients disagree considerably, a third measurement has been undertaken by the DFS in a new larger tunnel at Goettingen—in illustration #1 marked III. A fourth comparative measurement should be based on the coefficients of profile Go 426.

This profile is identical with 549 with a slight change in thickness. For the purpose of comparison Profiles Go 532 and Go 535, well known in the construction of gliders as well as NACA 23012 are noted in the illustration; it was considered desirable to mathematically reduce the "Profile Resistance" of all these profiles to the thickness of Profile 549, Illustration I indicates that even if the most unfavorable units of measurement are used, the highest Ca is 0.6, Goettingen 549 is the best. Whether NACA 23012 is better for speed cannot be decided because of discrepancies in the measurements undertaken by DVL, compared to the measurements undertaken in the 7x10 tunnel and those in the American super-pressure tunnel. We shall have to wait for further measurements, possibly some taken in flight. On the other hand, it is a well-known fact, that Go 535 is the most favorable solution for slow flight.

In the outer panel of the wing from 0.6 of the semi-span Profile Go 676 has been used instead of 549; significant for Go 676 is the wide Ca range.

Admitted November 24, 1950.

DEFENDANTS' EXHIBIT BBB

District Court of the United States, Southern District of California, Central Division
Civil Action No. 10930-Y

MAURICE A. GARBELL, INC., a California Corporation, and GARBELL RESEARCH FOUNDATION, a California, Corporation,

Plaintiffs,

vs.

CONSOLIDATED VULTEE AIRCRAFT CORPORATION, A DELAWARE CORPORATION, AND AMERICAN AIR LINES, INC., a Delaware Corporation,

Defendants.

STIPULATION #8

It is hereby stipulated subject to proof of error that the appended "Exhibit 36" is a reproduction of pages 355 to 356 Vol. XVIII fasc. 3 of a periodical entitled "L'Aerotecnica" issued and published by the Institute Poligrafico Dello Stato in Rome, Italy, during the year 1938, and that "Exhibit 36a" is a translation of said article (subject to correction if any error is contained therein) and that the said copy and translation may be used in evidence with the same force and effect as originals, subject to any objection which may be made thereto as irrelevant or immaterial, when offered in evidence.

LYON & LYON,
/s/ FREDERICK W. LYON,
Attorneys for Plaintiffs.

/s/ ROBERT B. WATTS,
/s/ FRED GERLACH,
Attorneys for Defendants.

Exhibit 36a

Translation L'Aerotecnica Vol. XDIII fasc. 3, 1938,
Pages 335 and 336
Figure 8

The "Asiago"
High Performance Glider (Italian)

Description:

Wing:

The "Asiago" has a high wing, of monospar construction, with one streamlined steel strut on each side. The wing spar is of the box type and made of laminated fir. The leading edge acts as a second spar to prevent wing torsion. Airfoils used are: G535 for the rectangular part of the wing, M6 for the tapering extremities. Transition from one airfoil to the other is linear.

The ailerons are rather big. The differential control has a ratio of 1:2.5. Ball bearings are used everywhere in the aileron controls. This makes for an extremely smooth lateral control of the airplane.

Almost all metallic parts are of national duraluminum.

To facilitate landings and flight in clouds, two slotted spoilers are mounted above the wings. With these open, rate of descent can be increased by more than 200 ft./min.

Fuselage:

The front part of the fuselage has a hexagonal section, rounded at the top, while the rear part is conical. The fuselage is of the hull type. The cockpit is very comfortable, having been designed for minimum pilot fatigue in flights of a long duration. The towing mechanism, which can be used for either winch launching or actual air towing, can be released through a small lever. The barograph is installed close to the pilot's head. The landing skid is robust and well suspended.

A tennis ball is used to absorb tail skid shocks.

The control stick is mounted on ball bearings.

Empennage:

Horizontal surfaces are cantilever. The stabilizer is attached to the fuselage by only four bolts. Controls are all inside the hull.

* * *

The "Asiago" has been built for maximum maneuverability, keeping in mind low cost and ease of construction. Imported materials represent a negligible portion of the total, as wide use has been made of fir, poplar, and dural, all available in Italy.

The "Asiago" has passed the tests of the "Acrobatic gliders" category.

Glider "Penguin G.P. 1"

The Penguin G.P. 1 is a glider of high efficiency built as a project of the Application Center of the Politechnic Institute, financed by the Institute. Vittorio Bonomi, well known glider pilot, and Angelo Ambrosini, Engineer, have collaborated in its construction.

General characteristics:

Wing Span	50 ft.
Length	21 ft. 4 in.

Wing Surface	164 sq. ft.
Aspect ratio	15
Weight Empty	375 lbs.
Useful Load	175 lbs.
Total Weight	550 lbs.
Wing Loading	3.1 lbs./sq. ft.
Strength Coefficient	9
Minimum Sinking Speed	136 ft./min.
Angle of Descent	1:25.3

Description:

Cantilever wing, with diehedral in the center section. This insures good stability and unobstructed visibility in all directions. Monospar wing—Airfoils G535 for the rectangular part of the wing, NACA 23012 for the tapered extremities. Transition between the two airfoils is linear. In the immediate vicinity of the fuselage, airfoil section G535 progressively becomes an NACA 0015. The transition is parabolic. The ailerons have a big surface, and there are two pairs, the outboard ailerons having a bigger displacement angle. This gives an excellent lateral control. Aileron control is through double differentials, ratio 1:2.5.

Admitted November 24, 1950.

DEFENDANTS' EXHIBIT CCC

District Court of the United States, Southern
District of California, Central Division

Civil Action No. 10930-Y

MAURICE A. GARBELL, INC., a California Corporation, and GARBELL RESEARCH FOUNDATION, a California, Corporation,

Plaintiffs,

vs.

CONSOLIDATED VULTEE AIRCRAFT CORPORATION, a Delaware Corporation, and AMERICAN AIR LINES, INC., a Delaware Corporation,

Defendants.

STIPULATION #9

It is hereby stipulated subject to proof of error that the appended are reproductions of printed publications and that said copies may be used in evidence with the same force and effect as originals, subject to any objection which may be made thereto as irrelevant or immaterial, when offered in evidence, viz;

"Exhibit 37" is a reproduction of page 116 of a printed text book entitled "Sailplanes" issued and published by Chapman Hall, Ltd., in London, England, during the year 1937; "Exhibit 38" is a reproduction of pages 80-81 from a printed text book entitled "Flight Without Power" issued and published by Pittman Publishing Corporation in New York, N. Y., during the year 1940; "Exhibit 39" is a reproduction of pages 128-129 from a printed text book entitled "First Flight Principles" issued and published by the American Technical Society in Chicago, Illinois, during the year 1941; "Exhibit 40" is a reproduction of page 69 from the printed text book entitled "Aircraft Design" Vol. 1, issued and published by Chapman and Hall in London, England, in the year 1938; "Exhibit 41" is a reproduction of pages 68, 69, 74, 75, 78, 79 and 92 of a publication of the "Flugtechnische Fachgruppe" issued and published by Technischen Hochchule of Aachen, Germany.

LYON & LYON,
/s/ FREDERICK W. LYON,
Attorneys for Plaintiffs.

/s/ ROBERT B. WATTS,
/s/ FRED GERLACH,
Attorneys for Defendants.

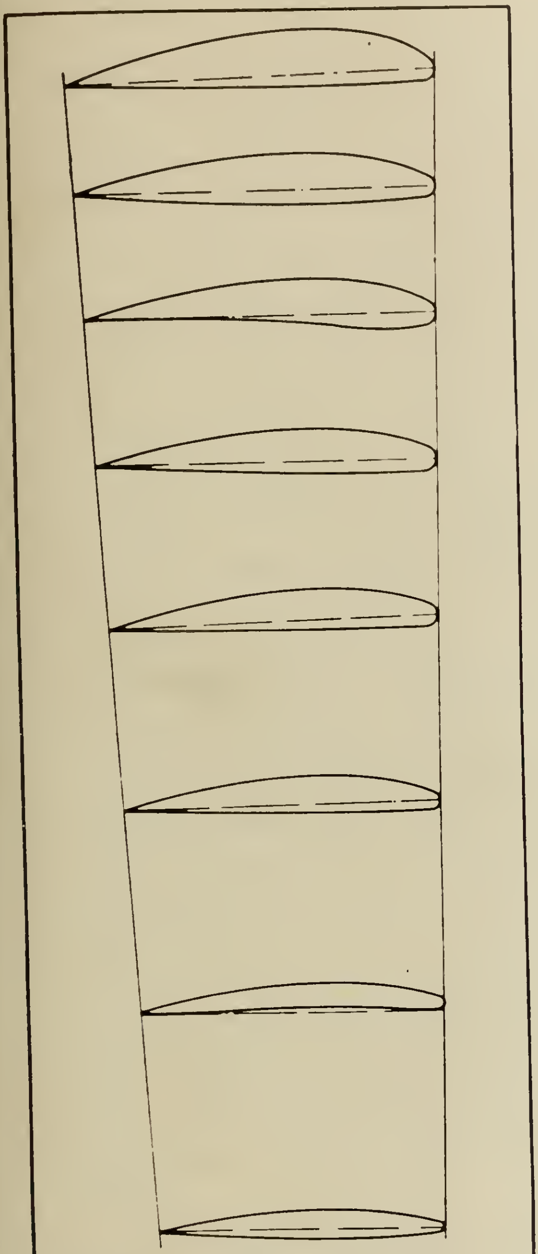

FIG 19

the L/D ratio at high angles of attack. This is in addition to its structural advantages which are great. Another may be mentioned. Satisfactory controlling effect may be obtained with smaller ailerons when the thicker sections are used in the wing.

Made possible by the development of the thick sections, the tapered wing has lately become very popular with designers. There are numerous reasons for this popularity. Some of these are structural and some are aerodynamic.

There are four ways in which the tapered wing may be constructed The first and simplest of these is the tapered planform. Fig. 16. In such a wing, the greatest chord is the root chord. This lies nearest the fuselage As the tip is approached, the chord decreases in length and with it all of the other dimensions of the section decrease in like ratio. If, for example, the chord at the tip is one-half of the chord at the root, the maximum upper ordinate at the tip is one-half of the maximum upper ordinate at the root and so on.

Fig. 17 shows another manner in which a tapered wing may be constructed. Here the planform is left rectangular and the thickness of the section is decreased as the tip is approached. The latter method is the same as multiplying all of the ordinates by some multiplier to obtain the ordinates for the section at each point To show what is meant by this we choose another example. Suppose t[illegible] we have already decided the length the chord. This will remain const[illegible] throughout the span of the wing. [illegible] the tip we desire to have our wing only one-half as thick as it is at the root. We multiply all of the ordinates of the root section by .5 and the results will be the ordinates of the tip section To obtain the ordinates of a section midway between the two, we multiply the ordinates of the root section by .75. There is thus established a relation between the location of a section and its ordinates. If we desire the ordinates of a section that lies midway between the

m: section already determined and the root, we seek a number which lies midway between .75 and 1. Obviously such a number is .875 and we obtain the ordinates of the desired section by multiplying the ordinates of the root section by .875. This will give the ordinates of the desired section. Similarly, to find the ordinates of a section that lies midway between the mid-section and the tip, we multiply the root ordinates by a number midway between .75 and .5 and this is, of course, .625. In this way we are able to construct a tapered wing having a variable section throughout its length. The section at any point, however, bears a simple relation to the section at the root.

There is a third way of tapering a wing that is a combination of t two mentioned. Fig. 18. Here the wing is tapered both in planform and in thickness. Certain advantages may be claimed for each of these types of tapered wings. A discussion of them does not properly come within the scope of this text. The individual prejudices of the designer are in many cases the determining factor in the selection of the type of taper used. Taper in thickness only is seldom used. Taper in planform is probably the most popular among designers.

There is another form of tapered wing in which the section at any point bears no simple relation to the root section. Fig. 19. According to this method, a section is selected which gives a satisfactory spar depth and satisfactory aerodynamic characteristics for each point of the wing.

All of the advantages that are possessed by the thick wing sections are possessed by the tapered wing. In addition, there is a great decrease in the weight of the structure. This follows, because the bending moments and shearing stresses are greatest near the root of the wing, and the tapered construction allows the wing to be strongest at the points of greatest stress. It is an ideal construction for a monoplane because of the general cleanness of design that it permits. The entire wing structure is internal No external braces are required and the parasite drag is diminished by the amount of the drag of the eliminated external parts. Some disadvantage attends, however. The use of such a construction usually means an increase in structural weight. The addition of any weight to the structure diminishes by the same amount the useful load that the airplane will carry. This increase in weight, it must be remembered, applies as compared to airplanes that are constructed with wings of moderate thickness. As was mentioned earlier, the tapered wing, cantilever construction, allows a decrease in structural weight over that of the thick wing constant section construction. Hence, the thick sections are suitable only for root sections and are commonly so used.

Aspect Ratio

See Fig. 20. There is a dimension of the airfoil that is of considerable importance in performance. It is not a dimension of the section but is a dimension of the wing itself. We are interested in the effect that the shape of the wing has upon its characteristics. We are interested for the same reason that we were interested in the shape of the section. We desire to find a shape which will give us the maximum amount of lift with a minimum amount of drag.

come, to a large extent at least, by giving a twist to the wing, though theoretically the geometric twist necessary to produce an elliptical C_L distribution across the span is considerable, varying from about $-13°$ for a taper ratio of 2, to $-20°$ for a ratio of 5 (the twist should not be uniform, but should increase progressively towards the tip), and this in turn causes increased induced drag, the increase for a 20° twist being roughly 10 per cent. for a ratio of 2·5, and 20 per cent. when the taper ratio is 5. On account of this it is doubtful whether a twist greater than 3° or 4° should be used, and 2° might be regarded as a preferable limiting figure.

In practice a lesser amount of wash-out than the theoretical figures given above has been found necessary due to the presence of a fuselage, or engine nacelles, which have the effect of accelerating the advent of unstable, or stalled, air-flow over the inner part of a wing.

A better method of preventing tip-stalling, or one which may be profitably employed in conjunction with a small degree of twist, is to increase the camber from root to tip, or at least over the outer sections of the wing. Alternatively, the aerofoil section may be graded along the span so that the tip section has a greater angle of maximum lift, sufficient wash-out being employed to keep the angle of zero lift constant along the span. Increase of camber results in a greater angular range of lift,* i.e., from the no-lift angle to the angle for $C_{L\ max}$, the greater angle of the latter being made use of for delaying stalling towards the wing-tips. For taper ratios up to 4, a camber grading of from, say, 2 per cent. at the root to 5 or 6 per cent. at the tip is generally sufficient for satisfactory results.

Aerofoil sections with rearward position of maximum camber,† i.e., behind the one-third chord position, give better results than forward camber locations. Rearward shift of the point of maximum camber over the tip portion of a wing is likewise beneficial in this respect.

Another solution to the tip-stalling problem, and again one that may be used in conjunction with camber variation, is provided by suitable grading of the wing thickness over the outer portion of the span, but avoiding, if possible, the rather critical region of 12 per cent.‡

* See p. 58 (Chap. V).
† See pp. 59 and 60 (Chap. V).
‡ See p. 60 (Chap. V).

DEFENDANTS' EXHIBIT GGG

District Court of the United States, Southern District of California, Central Division

Civil Action No. 10930-Y

MAURICE A. GARBELL, INC., a California Corporation, and GARBELL RESEARCH FOUNDATION, a California, Corporation,

Plaintiffs,

vs.

CONSOLIDATED VULTEE AIRCRAFT CORPORATION, a Delaware Corporation, and AMERICAN AIR LINES, INC., a Delaware Corporation,

Defendants.

STIPULATION #14

It is hereby stipulated subject to proof of error that the appended "Exhibit 128" is a reproduction of page 5 of the issue of February 5, 1938, of the printed publication "Le Vie Dell'Aria" containing an article entitled "Tre nuovi veleggiatori italiani" published and issued by Editorial Aeronautica in Milan, Italy, in the year 1938, and that "Exhibit 128a" is a translation of said article (subject to correction if any error is contained therein), and that said "Exhibit 128" may be used in evidence with the same force and effect as an original, subject to any objection which may be made thereto as

Defendants' Exhibit GGG—(Continued)

irrelevant or immaterial when offered in evidence, viz;

LYON & LYON,
/s/ FREDERICK W. LYON,
Attorneys for Plaintiffs.

/s/ FRED GERLACH,
/s/ ROBERT B. WATTS,
Attorneys for Defendants.

Exhibit 128a

Translation from Italian AJM:MS
Three New Italian Gliders

At the Arcore (Monza) Airport, where there took place the first flights of the one who is today the first aviator of Italy, there took place a few days ago the testing of three new gliders constructed during the last six months. The collaboration of the Center of Studies and Experiments for gliding of the Royal Polytechnical and of the GUF of Milan, on the one hand, and of the Aeronautica Lombarda, on the other hand, have resulted, with characteristic Fascistic rapidity, in a range of gliders which places Italy at the height of the most progressive countries, even with respect to gliding. There are not concerned planes constructed under license with foreign designs or copies like some planes which were made last year, but new models constructed on basis of the latest inventions and the latest Italian and foreign experience.

Each one of the three planes represents a stage in

Defendants' Exhibit GGG—(Continued)

the training of glider pilots of high class and in the sport development of future sport groups.

These are:

1. The "ASIAGO G.P. 2" designed by Garbell and Preti of the CVV, a glider for thermal soaring (C and D license).

2. The "ALCIONE B.S. 28" of Bonomi and Silva (Aeronautica Lombarda), an intermediate glider for high altitude gliding.

3. The "PINGUINO G.P. 1" of the CVV, a glider of the highest quality with which the college students of Milan will participate in the contests during the next season.

As we already announced last October in "Le Vie dell'Aria," the manufacturing program of the CVV is greatly assisted by the aeronautical fans Vittorio Bonomi and Eng. A. Ambrosini. The prototype of the CVV have been built by the shop-workers of the "Aeronautica Lombarda" and partly in the Cantu shop which up to the present time has supplied almost all the Italian elementary training gliders. At the same time the "Aeronautica Lombarda" has started the construction on a mass production basis of the models of the CVV, which has awakened general interest not only among the Italian glider pilots but also among the foreign pilots and organizations. Thus the collaboration between the CVV, a technical, scientific and sporting organization par excellence which must not and cannot attend to the mass production of its models, and the "Aeronautica Lombarda," a manufacturing plant of vast experi-

Defendants' Exhibit GGG—(Continued)

ence, was able to create in a short time these gliders for which the Italian pilots had been waiting.

The "Asiago G.P. 2" was born at the Aeronautical Exhibition of Milan. Thousands of visitors stopped in front of the stand of the RUNA and were present during the first stage of the assembling of this glider.

Here are its principal characteristic features:

Wing span 13.70 m.; length 6.50 m.; surface of the wings 12.70 m2; aspect ratio 14.8; weight without load 120 kg; useful load 90 kg; total weight 210 kg; wing loading 16.5 kg/m2 strength coefficient 9; minimum velocity of descent 0.80 m. per second; gliding angle 1:20.

The wing, of the mono-spar type with torsion-resisting leading edge, has a single profiled strut. For the purpose of good aero-dynamic efficiency and of low sucking speed of descent, there has been selected a comparatively large aspect ratio (14.8). The ailerons are very large (2.55 m2) and have a differential motion of a ratio of 1:2.5. On the upper side of the wing there is applied the well-known CVV flap which serves to increase, as may be desired by the pilot, the speed of descent of the apparatus, which is very necessary when landing outside of the aviation field and for flying into clouds. The CVV spoilers constitutes a simplified variant of the Jacobs spoiler (DFS).

The ample fuselage follows in general lines that of the "Anfibio Varese" of Rovesti-Mori. It is hexagonal (rounded) at the front part, and of rhombus

Defendants' Exhibit GGG—(Continued)

sections towards the tail. The pilot's seat is ample and commodious; it fits the shape of the body thus reducing to a maximum the fatigue of long flights. The cables of the pedal pass through the space between the double wall leaving the pilot's seat entirely free. The control stick is of duraluminum tubing so as not to affect the compass. All the controls move on ball bearings. Behind the head of the pilot between the fourth and fifth frames of the fuselage, there is a box for the recording barometer. Its cover serves at the same time as hand support. On the Asiago, the troublesome problem for the rest for the left hand has been solved. A simple but comfortable duraluminum rest finally assures the pilot the desired rest for his left hand. Near this rest are located the levers for the operation of the flaps and for the releases. The two releases—the open one for winch launching and the closed one for the air drag —are simultaneously opened with a single handle.

The horizontal empennage is of the cantilever type and is attached to the fuselage by means of three bolts, in addition to the inside control bolt. The rudder is low and of modern lines.

The greatest attention has been given to obtaining ease of operation in the controls, in connection with which up to the present time, many gliders used to leave a great deal to be desired. As is universally known, the sensitivity of the elevator of a glider is equal to, if not superior than, than that of a motor airplane; the ailerons are already more inert, but worst of all is the rudder which generally

Defendants' Exhibit GGG—(Continued)

has very little effect. In the Asiago, the ailerons are very efficient, this being due to selected profiles (G 535 and NACA M6) and also due to the aerodynamic wing warp. The rudder on the other hand has been placed behind the elevator in order to increase the arm and therefore the momentum. The apparatus responds very well to the controls. Someone who perhaps exaggerates states that "it is just like a CR." This arrangement has the advantage of also avoiding interference between the horizontal and vertical empennages during spinning, as was discovered a few months ago by the Zurich scientist Haller.

The landing members are the following: a standard front skid and a small tail skid made resilient by means of a tennis ball.

In the construction of the "Asiago," considerable use was made of material produced in Italy (fir, poplar, duraluminum).

The "Aeronautica Lombarda" is now manufacturing the "Asiago" on a large production basis—which plane, due to its simplicity, can be sold at comparatively low price—which, in addition to the surprising flight qualities which are superior to all the Italian and foreign planes manufactured up to the present time, will greatly favor its diffusion.

The "Alcione B.S. 28" of Engineer Camilla Silva is endeavoring to meet the need felt by the schools for high altitude gliding, which desired a comparatively economical plane which still had flying qualities like those of the large gliders in order to im-

Defendants' Exhibit GGG—(Continued)

prove the training of pilots who have already completed their training in the gliding school.

Here are the technical specifications of this glider: wing span 14.50 meters; length 6.55 meters; area of the wings 14 square meters; aspect ratio 15; weight without load 160 kgs; useful load 85 kgs; total weight 245 kgs; wing loading 17.5 kg/m2; strength coefficient 9; minimum velocity of descent 0.75 m/sec.; gliding angle 1:22.

The "Alcione" is provided with a middle wing, full cantilever, straight, and of a fully tapered plan.

The profiles used are G449, G693, NACA 23012, NACA 0012.

The entire trailing edge is occupied by movable surfaces. The inside third forms the camber flaps controlled by a lever located on the left side of the pilot. The other 2/3, the "ailerons," are divided into halves and are controlled with double differential. In addition to the differential motion between the right-hand aileron and the left-hand aileron, the outer aileron has a greater amplitude than the inside one and this motion approximates the warp of the wings of birds, thus improving the transverse maneuverability.

On the upper side of the wing, there is located the CVV flap.

The fuselage is of hexagonal section with rounded upper part. The tail surfaces correspond to those of the Asiago.

In addition to the main skid, there is a small cen-

Defendants' Exhibit GGG—(Continued)

tral wheel which facilitates the landing and the take-off.

* * *

Finally, the "Pinguino G.P. 1" has all the characteristic features of a large glider: middle M wing, rounded fuselage, very accurate connections. Its construction was made possible by the generosity of the Royal Polytechnical and of the well-known glider pioneer, Vittorio Bonnomi. Here are its characteristic features:

Wing span 15.30 meters; length 6.50 meters; wing surface 15.20 square meters; aspect ratio 15; weight without load 170 kgs.; useful load 80 kgs. total weight 250 kgs.; wing loading 15.2 kg/m2; strength coefficient 9; minimum descending velocity 0.69 m/sec.; gliding angle 1:25.3.

The wing is a full cantilever and has a dihedral angle of 6° at the central part. The profiles used are the G 535 and the NACA 23012, with aerodynamic warping of about 3°. The wing is of the single spar type. The ailerons are very large and have a strongly differential control. Also here, the CVV flaps are not missing.

The fuselage is of ovoid section. Special care was given to the connection between the wing and the fuselage.

* * *

The excellent flying qualities of these three new gliders have been shown by tests carried out on January 29th and 30th last, at the Arcore Airdrome by the Engineer, Colonel Nannini and by the In-

Defendants' Exhibit GGG—(Continued)

structor Aldo Tavazza, who, with the gliders, carried out some stunts, after having been released from the tugging plane at a height of 1,000 meters. There were present at the tests of the new gliders: Prof. Cassinis, President of the E. De Amicis Study Center; Engineer Silva of the Aeronautica Lombarda for gliding; Instructor Plinio Rovesti of Varese, and Engineer Bracale of the Aeronautic Registry.

The flight tests have fully confirmed the maneuverability and stability of the new gliders and will soon be followed by soaring tests. It must be noted that in the afternoon of the 30th, the Pilot Venturini effected, with the "Asiago G.P. 2," a series of stunts which were perfectly successful in view of the trim compensation of the glider. The pilot, who is a holder of a "C" flying license and of a first-grade airplane license, had not up to that time done any stunt-flying.

MAURIZIO GARBELL.

Caption Under Illustration:

Top: The "Alcione B.S. 28" taking off under the pull of the winch. There can be noticed the low camber flaps.

Bottom: The "Pinguino G.P." in full flight.

Admitted November 24, 1950.

DEFENDANTS' EXHIBIT HHH

District Court of the United States, Southern District of California, Central Division

Civil Action No. 10930-Y

MAURICE A. GARBELL, INC., a California Corporation, and GARBELL RESEARCH FOUNDATION, a California, Corporation,

Plaintiffs,

vs.

CONSOLIDATED VULTEE AIRCRAFT CORPORATION, a Delaware Corporation, and AMERICAN AIR LINES, INC., a Delaware Corporation,

Defendants.

STIPULATION #15

It is hereby stipulated subject to proof of error that the appended "Exhibit 129" is a reproduction of pages 58 and 59 of Issue No. 3, February 2, 1938, of the printed publication "Flugsport" containing an article entitled "Leistungssegler 'Pinguino G.P. 1'" published and issued by Flugsport in Frankfurt, Germany, in 1938, and that "Exhibit 129a" is a translation of said article (subject to correction if any error is contained therein), and that said "Exhibit 129" may be used in evidence with the same force and effect as an original, subject to any objection which may be made thereto as irrelevant or immaterial when offered in evidence, viz;

LYON & LYON,
/s/ FREDERICK W. LYON,
Attorneys for Plaintiffs.

/s/ FRED GERLACH,
/s/ ROBERT B. WATTS,
Attorneys for Defendants.

Exhibit 129a

Translation from "Flugsport" Feb. 2, 1938
No. 3, p. 58-59

High-Performance Glider "Pinguino G.P. 1"

The glider was built in the second half of the year 1937 by students of the Milan Technical College, with financial aid from the College, from the noted advocate for gliding flight in Italy: Vittorio Bonomi, and from the aircraft industrialist Angelo Ambrosini. The design for the machine came from Garbell and Preti, of the CVV (Centro Studi ed Esperienze per il Volo a Vela).

The "Pinguino" is constructed as a mid-wing cantilever with a gull wing. Single-spar construction; with plywood nose. Profile to the bend, Gottingen 535; from here outward it merges linearly into the NACA 23012 section. At the transition from the wing to the fuselage the G 535 wing section runs into the NACA 0015 fuselage profile. Big ailerons; double differential control, with an angular deflection ratio of 1:25. The outer halves of the divided ailerons are more deflected, whereby a considerable improvement of their action is obtained. A further advantage consists in that, during bending of the wing, no binding of the ailerons occurs. (An old and typical example of this arrangement is the Russian long-distance craft "Ant. 25," whose ailerons are subdivided into four single flaps). For the purpose of increasing the rate of descent at will, two CVV spoiler flaps are installed on the suction side, which, in the manner of the braker flaps developed by DFS (see "Flugsport" of 1937, page 350), may be deflected forward on a circular arc, and thereby leave a gap open between the lower edge of the flap and the suction side of the wing.

Fuselage of oval cross section, coming to an edge underneath. Comfortable pilot's seat. Instruments fastened to the fuselage itself, not to the cowling, in order that the cowling may not become too heavy, and possibly hinder rapid emergence when there is danger. The cowling is held in place by a DFS speed catch. The release lever simultaneously operates the open winch hook and DFS tow coupling, which are prescribed in Italy.

Wing span, 15.3 m; length, 6.5 m; area 15.2 m2; aspect ratio, 1.15; empty weight, 170 kg; load, 80 kg; flying weight, 250 kg; wing loading, 15.2 kg/m2; breaking load factor in case A, 9; minimum rate of descent, 0.69 m/sec.; maximum drag/lift ratio 1:25.3.

Translated by W. G. Weekley.

Admitted November 24, 1950.

DEFENDANTS' EXHIBIT III

District Court of the United States, Southern District of California, Central Division

Civil Action No. 10930-Y

MAURICE A. GARBELL, INC., a California Corporation, and GARBELL RESEARCH FOUNDATION, a California, Corporation,

Plaintiffs,

vs.

CONSOLIDATED VULTEE AIRCRAFT CORPORATION, a Delaware Corporation, and AMERICAN AIR LINES, INC., a Delaware Corporation,

Defendants.

STIPULATION #16

It is hereby stipulated subject to proof of error that the appended "Exhibit 130" is a reproduction of pages 538 and 539 of Issue No. 20 of September 29, 1937, of the printed publication "Flugsport" published and issued by "Flugsport" in Frankfurt, Germany, in the year 1937, and that "Exhibit 130a" is a translation of a part of said article (subject to correction if any error is contained therein), and that said "Exhibit 130" may be used in evidence with the same force and effect as an original, subject to any objection which may be made thereto as irrelevant or immaterial when offered in evidence, viz;

LYON & LYON,
/s/ FREDERICK W. LYON,
Attorneys for Plaintiffs.

/s/ FRED GERLACH,
/s/ ROBERT B. WATTS,
Attorneys for Defendants.

Exhibit 130a

Translation from "Flugsport" No. 20
Sept. 29, 1937, p. 538-9

The "Centro Studi ed Esperience per il Volo a Vela" (Testing Station for Gliding Flight) of the Milan Royal Technical College exhibits the construction of the training glider "Asiago G.P. 2" on the stand of the National Royal Aeronautical Club.

The machine is the result of experience in the Asiago Glider School, and is intended for training in thermal current and cloud flying. The designers Garbell and Preti also made use of their experience with the "Grunau-Baby" of the Polish Komar, and with the "H 17." As respects cloud flight, the machine has a load factor of 9, and air brakes on the upper side of the wing.

Profiles G 535 and M 6, with gradual transition. Most of the covering is pure Italian dural. In addition, all weak points that may be stressed use popular plywood instead of northern birch plywood. The fuselage is hexagonal in front, with a rounded cowling, and merges behind into a rectangular section.

Wing span, 13.7 m; length, 6.5 m; area, 12.7 m2; aspect ratio, 1:14.8; empty weight, 120 kg; flying weight, 210 kg; wing loading 16.5 kg/m2; drag/lift ratio, 1:20; rate of descent, 80 cm/sec.

The "Pinguino G.P. 1" machine built last summer by the same designers, and which belongs to the Sperber class, could not be exhibited for lack of space. This machine was built merely for study, and will therefore not go into production. Directly after the exhibition, this machine, which has an interesting choice of profiles (NACA 0015, G 535, NACA 23012), will be subjected to thorough tests at the Sezze-Littoria (Agro Pontino) fields.

In our next number, we shall report in detail about the Aeronautica Lombardia, the successor to Aeronautica Bonomi, company's mid-wing "Alcione B.S. 28" designed by Silva.

Translated by W. G. Weekley.

Admitted November 24, 1950.

DEFENDANTS' EXHIBIT JJJ

District Court of the United States, Southern District of California, Central Division

Civil Action No. 10930-Y

MAURICE A. GARBELL, INC., a California Corporation, and GARBELL RESEARCH FOUNDATION, a California, Corporation,

Plaintiffs,

vs.

CONSOLIDATED VULTEE AIRCRAFT CORPORATION, a Delaware Corporation, and AMERICAN AIR LINES, INC., a Delaware Corporation,

Defendants.

STIPULATION #17

It is hereby stipulated subject to proof of error that the appended "Exhibit 131" is a reproduction of page 5 of the Issue of October 16, 1937, of the printed publication "Le Vie Dell'Aria" published and issued by Editorial Aeronautica in Milan, Italy, and that "Exhibit 131a" is a translation of the article "Il Volo A Vela" (subject to correction if any error is contained therein), and that said "Exhibit 131" may be used in evidence with same force and effect as an original, subject to any objection which may be made thereto as irrelevant or immaterial when offered in evidence, viz;

LYON & LYON,
/s/ FREDERICK W. LYON,
Attorneys for Plaintiffs.

Defendants' Exhibit JJJ—(Continued)

/s/ FRED GERLACH,

/s/ ROBERT B. WATTS,

Attorneys for Defendants.

Exhibit 131a

Translation from Italian WB:FG

At the Milan Salon

Gliding

While at the first Aeronautical Salon of Milan gliding occupied a very modest position, at the recent Salon it has assumed the position and importance due it.

In accordance with the very great value attributed to gliding by the Germans, the German representative made a large contribution to this exhibition. The Minister of Aeronautics of Berlin presented at different stands, the technical and sporting results of his organizations. The N.S.F.K. (National Socialist Flying Corps) showed by various graphs, models, etc., their work in the field of gliding and aeronautical craftsmanship: about 20 regular gliding schools, about 200 gliding groups and a large number of schools in aeronautical construction are preparing future pilots and skilled workers for the Air Force and civilian aviation.

Among the gliding schools, there are some which give excellent instruction in blind flying, instrument navigation and aerobatics. The records attained by German gliding are: 41 hours flight, 4650 meters altitude and 504 kilometers distance. These figures confirm, even numerically, the great stage of development obtained by this branch of aeronautics.

Defendants' Exhibit JJJ—(Continued)

The DUL Institute for aeronautical research is exhibiting a vertical wind tunnel for spinning tests constructed by the DFS (German Glider Research Institute).

The DFS is exhibiting, in its own stands, extremely interesting scientific material. In addition to the diagrams and photographs on weather study, which have been of such vital importance in the history of gliding, the DFS is exhibiting its own two aerodynamic smoke tunnels. By introducing into the current of air, thin smoke filaments, an attempt is made to study the very minute aerodynamic problems which ordinary aerodynamics cannot solve. In particular, the action due to the moving parts of the wing, such as flaps, flip increasors, air brakes, etc., can be evaluated with clearer precision. The DFS has developed, under the supervision of Alessandro Lippisch, two types of smoke tunnels, one economical, low priced type for elementary demonstration purposes for glider schools and a more involved type for scientific investigation. Particularly the second type has found great appreciation on the part of the representatives of the leading Italian scientific institutions.

The same Institute is also exhibiting a series of models of the main planes created by Engineers Lippisch and Jacobs.

The German glider industry has sent two of its best representatives, Hirth and Schweper. Hirth has brought to the exhibit his new two-seater Minimoa 2, a real masterpiece of precision and design. The Minimoa Goppingen 3, the Goppingen 4, a two-

Defendants' Exhibit JJJ—(Continued)

seater with the seats arranged alongside each other for instruction purposes, and finally the Wolf, one of which is being tested at present at the glider school established at Sezze by the R.U.N.A., are also extremely interesting.

Schweyer however is exhibiting one of its most characteristic constructions, the "Habicht" plane for aerobatics, designed by Jacobs of the DFS. Of a structure similar to the Rhonsperber, which plane is designed for a speed officially measured at 400 kilometers per hour; however, piloted by the "Commander of Glider Pilots," Hanna Reitsch, it has already repeatedly obtained speeds of more than 450 km. per hour. Its amazing ease of handling makes it possible to effect practically any stunt maneuver. The Italian Olympic squadron had an opportunity to see, in Berlin, the stunts of Hannah, among them front loops with two barrels while ascending, etc. The glider which was finally acquired also by the French champion, Marcel Thoret, is of beautiful mechanical and structural design. Also the flap mechanism, the ailerons, rudders and elevators are of a perfection rarely found in aeronautical construction, but rather found in optical and electrical apparatus.

The Habicht, together with the famous "slow" airplane Storch, had already the very high honor of being thoroughly inspected by the Duce during his stay in Germany at the Rechlin Camp.

Schweyer also exhibits the usual models of planes constructed by it, such as the two-seater Kranich,

Defendants' Exhibit JJJ—(Continued)

the Rhonsperber and a few other types of lesser importance.

To this group of German exhibitors, rich in more than 15 years of experience, there is added a small but courageous Italian representation.

The Aeronautica Lombarda (formerly the Aeronautica Vittorio Bonomi) presents the BS 28 designed by Engineer Silva. There is concerned a glider with middle wing of 14.50 meters wing spar and an aspect ratio of 15 meters. Through a special selection of the profiles (G. 449, G. 693, NACA 23012 and NACA 0012) there has been obtained a very fine wing and at the same time a wing sufficiently rigid and light in weight. Along the trailing edges of the wing, camber flaps and the four ailerons follow each other. The ailerons are actuated by means of a special differential control so as to assure a greater amplitude of motion the outer ailerons than of the inner ailerons, thus obtaining a greater ease of handling. Also, the differential ratio between the two pairs of ailerons is rather high and reaches a value of 1:2.5. The plane is provided with flaps. The cabin is designed with special regard to visibility in all directions. As landing members there have been installed a skid and a single wheel undercarriage. The cowling covers not only the cockpit but also the junction of the wings. Upon removing same, everything is uncovered, which greatly facilitates the assembling of the plane. The wings are connected with each other by means of connections of duraluminum, while the fuselage is connected by means of only four bolts inasmuch

Defendants' Exhibit JJJ—(Continued)

as it does not have to support any bending force. In general, practically all the metal parts are of duraluminum. In all the points where the stresses are less, use is made of poplar plywood instead of birch plywood, and poplar and fir are used instead of spruce.

The Center for Gliding Studies and Experiments of the Royal Polytechnical is exhibiting at the stand kindly placed at its disposal by the R.U.N.A., a model shop, which, constructed during the period of the exhibition, the model of the "Asiago" glider the design for which had been made by the Milanese students, Preti and Garbell.

This Center organized in 1934 by the late Liberato De Amici was able, with the assistance of the Royal Polytechnical, to gradually develop during the last two years. The interest taken in same by Knight Commander Bonomi and by Engineer Amorosini and also the assistance of the aeronautical authorities have made it possible to continuously increase the work. Thus the meteorological section was able to organize, in agreement with the Ministry of Aeronautics, a weather study department, and lately also the model section has started a promising activity. Already this summer there has been built the "Pinguino G.P. 1" which is now being perfected. There has now been created the G.P. 2 "Asiago" which was actually constructed at the exhibition. There is concerned a training plane for students who wish to qualify for a C and D license for thermal gliding and gliding in the clouds. The entire project was carried out with the intention

Defendants' Exhibit JJJ—(Continued)

of reducing as much as possible the moments of inertia around the vertical and longitudinal axes in order to obtain a maneuverability of the aileron and foot (base?) harmonized with the always somewhat excessive maneuverability of the elevator. The experience obtained from the Asiago glider contest has brought about the development of the CVV (Gliding Center) flap which is not to be used for landing, which is already very easy with a glider of the Asiago kind, but is to permit students to avoid entering the clouds. While today a student who is drawn in by a thick cloud tries vainly to avoid zooming up into the cloud, the CVV flap has for its purpose increasing, without any strain on the plain, the speed of descent by at least 1 meter per second. Thus there is obtained a further safety device which will be appreciated both by the students and their instructors.

What we have already stated in connection with the BS 28 also applies to the use of independent equipment. The Asiago plane will be reproduced by the Aeronautica Lombarda, which has taken a special interest in the development of the model and of the future mass production of same. The plane, as also the BS 28 and the Pinguino, will pass the official gliding tests at the experimental field of Agro Pontino.

The Italian gliding exhibition finally includes a beautiful collection of the GUF of Rome which shows some fine projects of gliders and sailplanes in addition to an engine plane of Fidia Piatelli.

Gliding is obtaining the position it deserves also

Defendants' Exhibit JJJ—(Continued)

among us, as was the case in other countries. As His Excellency Valle stated at the Asiago contest, we have made great progress also in gliding in achieving the standing to which Italian aviation has arisen.

MAURIZIO GARBELL.

Admitted November 24, 1950.

Case No. 10930-Y
CARBELL vs. CONSOLIDATED
DFT EXHIBIT LLL
Date ______ No. ______ IDENTIFICATION
Date NOV 24 1950 No. LLL IN EVIDENCE
Clerk, U. S. District Court, Sou. Dist. of Calif.
John A. Childress Deputy Clerk

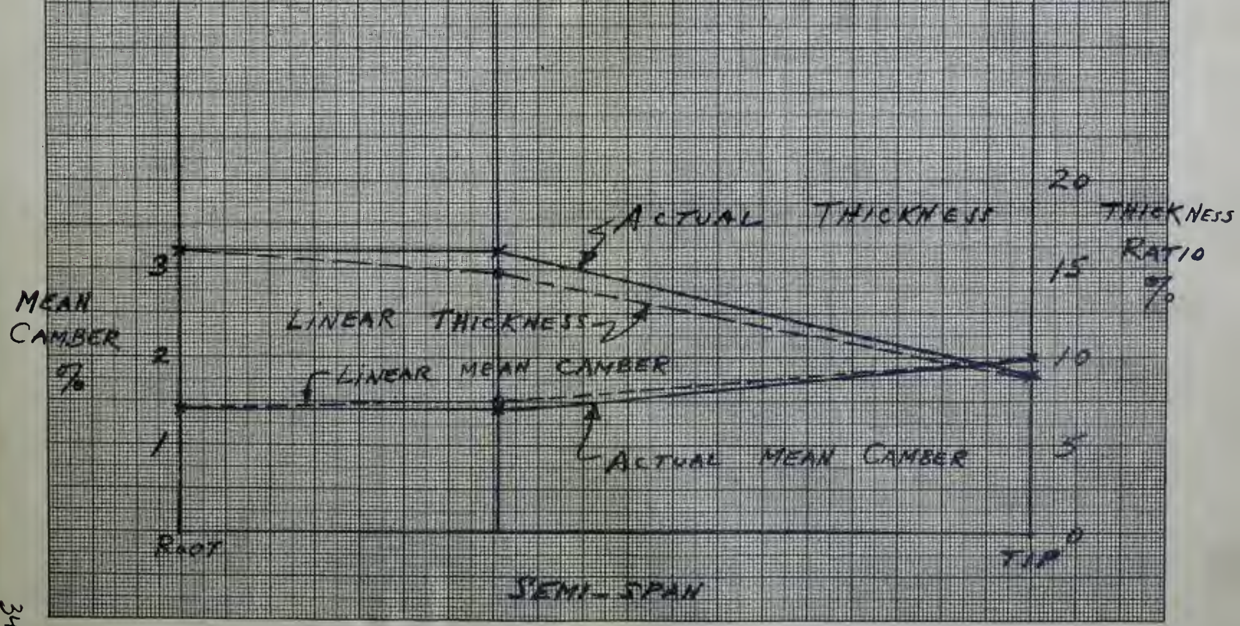

DEFENDANTS' EXHIBIT MMM

REPORT NUMBER [illegible]

MODEL NUMBER [illegible]

ENGINEERING REPORT

CURTISS-WRIGHT CORPORATION

SAINT LOUIS AIRPLANE DIVISION

ROBERTSON, MISSOURI

TITLE: AERODYNAMICS REPORT

AUTHOR: W.A.Sangster & W.T.Butterworth

Two-Place Basic Combat, Model 23
Engine - P & W Wasp, S3H1
Circular Proposal No. 39-100
U.S.Army Type Specification No. C-901

Approval [illegible] Ch.Engr.

DATE: February 20, 1939 APPROVALS: [illegible] Proj.Engr

REVISIONS

CHANGE LETTER	DATE	DESCRIPTION	AUTHOR	APPROVAL	NO. OF PAGES
					109

DEFENDANTS'

EXHIBIT 136

Physical Characteristics

a. Design gross weight 4600 lbs. (Ref. 5)

b. Fuel: Normal 104 gals. 624 lbs. (Ref. 5)
Maximum 140 gals. 840 lbs. (Ref. 5)

c. Wing Dimensions

I - Airfoil section designation:
Root: CW-23 (at centerline)
Wing Splice: NACA 2314 (55.6 ins. outboard)
Tip: CW-19 (15 ins. from tip)

II Total supporting surface area: 174.3 sq.ft.

III Incidence: + 1° (Chord plane relative to Thrust Line)

IV Dihedral: 5.50° on Chord plane.

V Sweepback: Trailing edge normal to centerline of Airplane

d. Horizontal Tail Surfaces:

I	Total Area	25.56 sq.ft.
	(Including Blanketed Area	28.14 sq.ft.
II	Span	11.0 ft.
III	Maximum Chord	3.76 ft.

IV Distance from Normal c.g. to 1/3 Maximum Chord point 184.65 in.

V Stabilizer Area 16.98 sq.ft.
Normal position relative to Thrust line 30°

VI Elevator Area (including tab) 8.58 sq.ft.

2 Trim tabs, area each .35 sq.ft.

e. Flaps

I The wing is equipped with split flaps over the central portion of the span. The flap extends over the rear 15% of the wing chord and is hinged along its forward edge.

II The dimensions and location of the flap are shown on the wing drawing, page 19 fig. 3.

Ratio (flap chord)/(wing chord) = .15
Ratio (flap span)/(wing span) = .544
Total flap area = 17.[illegible] sq.ft.

Fig. 4

AIRPLANE BALANCE

b_1 = span of center panel = 55.6"
b_2 = span of outer panel = 149.4"
A_{tot} = Total wing area = 174.3 sq.ft.

The mean slope of the lift curve, moment coefficient about the aerodynamic center, and location of the aerodynamic center are determined in the following calculations. Tables 3 and 4 present the average values of drag coefficient and angle of attack for the complete range of lift coefficients.

<u>Aerodynamic Section Properties</u> (Ref. Fig. 6)

Item	C.W.-23	NACA 2314	C-W-19
m = Slope of lift curve for aspect ratio 7.03	.0801	.0805	.0856
C_m = Moment Coefficient about aerodynamic center	-.002	-.035	-.055
a.c. = Aerodynamic center in fractions of chord	.232	.245	.236

$$m_{av} = \frac{\left[(.0801)(84.00) + (.0805)(71.45)\right]55.6 + \left[(.0805)(71.45) + (.0856)(38.76)\right] \times (149.4)}{144(174.3)}$$

m_{av} = <u>.0816/deg.</u>

$$C_{m_{av}} = -\frac{\left[(.002)(84.00)+(.035)(71.45)\right]55.6+\left[(.035)(71.45)+(.055)(38.76)\right]149.4}{(144)(174.3)}$$

$C_{m_{av}}$ = <u>-.0335</u>

$$(a.c.)_{av} = \frac{\left[(.232)(84.00)+(.245)(71.45)\right]55.6+\left[(.245)(71.45)+(.236)(38.76)\right]149.4}{(144)(174.3)}$$

$(a.c.)_{av}$ = <u>.241</u>

The wing normal and chord force coefficients for the complete range of lift coefficients of the mean wing alone are computed in Table 5. The accompanying pitching moment, tail, and airplane force coefficients are computed in succeeding Tables for various specific loading and flight conditions of the airplane.

The airfoil section at the centerline (rib 1) is a symmetrical section, generated in the following manner: The upper contour of an N.A.C.A. 2315 airfoil section was reflected about the geometric chord line to form a symmetrical airfoil of 19% thickness lying in a plane normal to the plane of the chords. This resulting contour is designated as the CW-23 airfoil section, and to obtain the aerodynamic characteristics of that section, it was assumed to be equivalent to an N.A.C.A. 0019 airfoil section. The contours of the CW-23 airfoil section at rib 1, and of the N.A.C.A. 2314 airfoil section at rib 4 are obtainable from published N.A.C.A. airfoil data. The contour and table of ordinates of the CW-19 airfoil section is given on page 28a. All sections are taken in a plane normal to the plane of the chords.

W.A.Sang[illegible] CURTISS-WRIGHT CORPO[illegible]TION
ST. LOUIS AIRPLANE DIVISI[illegible]
ROBERTSON, MO.

1/20/3[illegible]

Page 1[illegible]
Model 2[illegible]
Report 2[illegible]

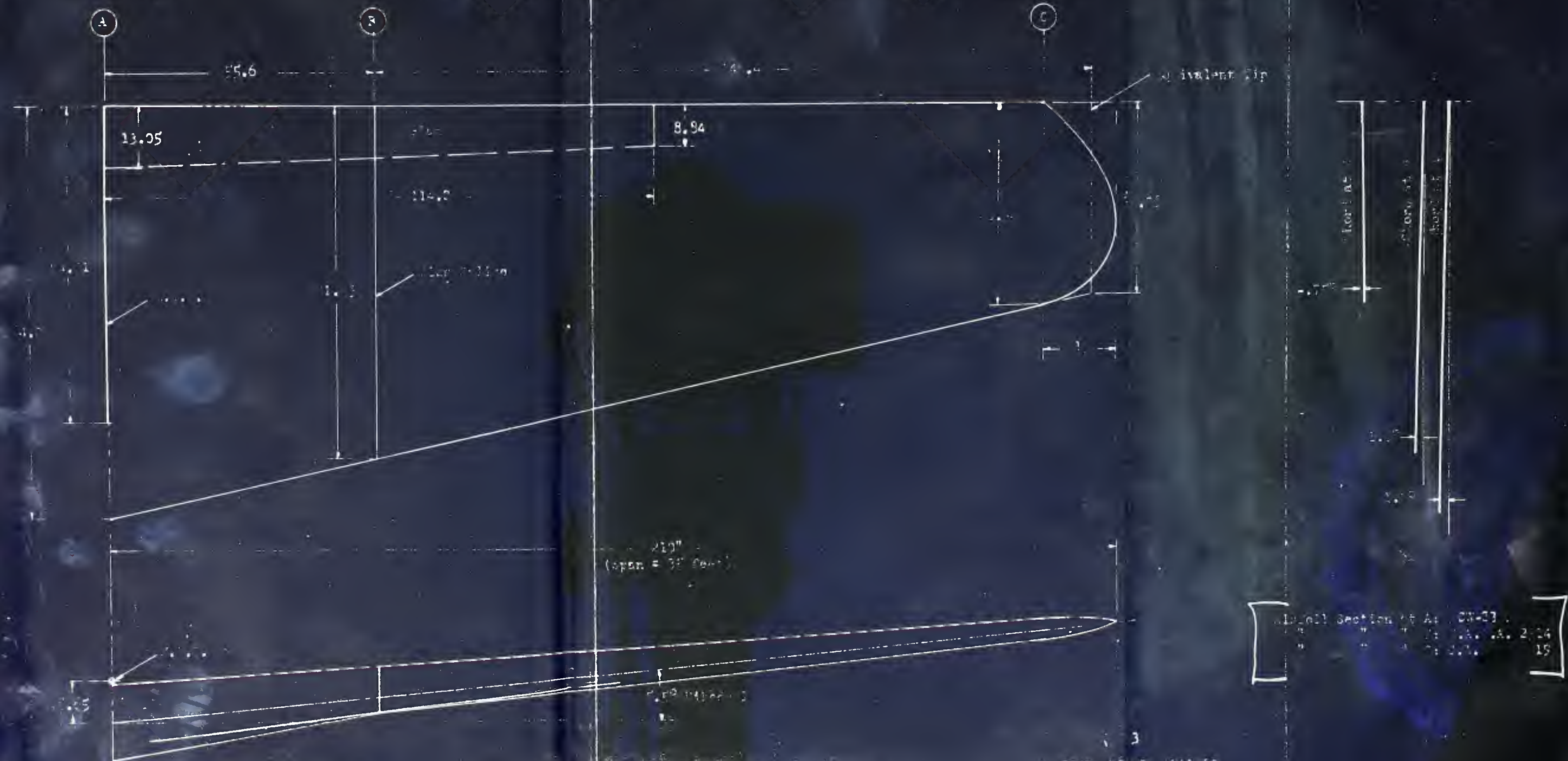

Scale 1/20

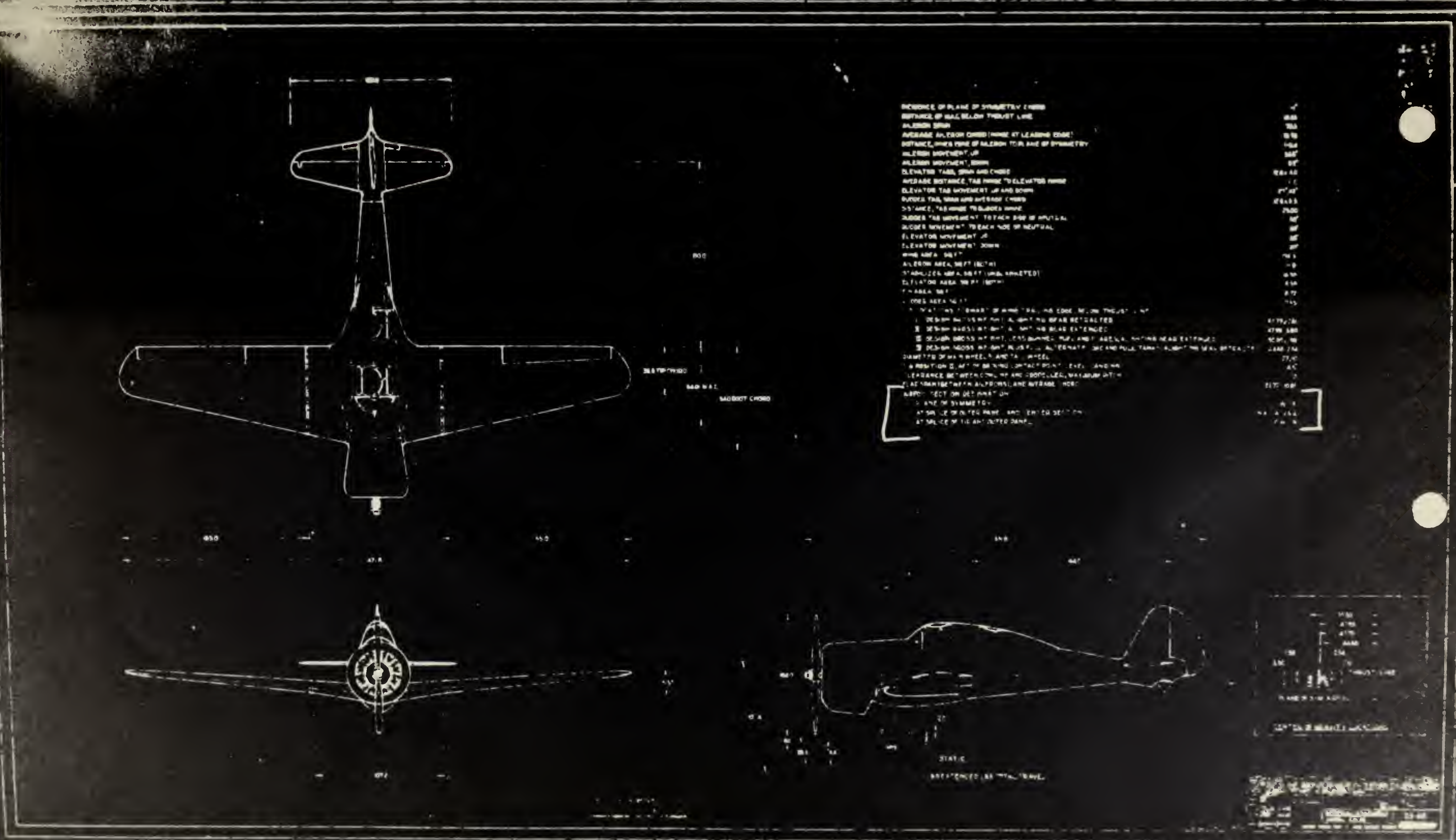

Admitted November 24, 1950.

Marbell Inc vs. Consol Vultee et al
Dfts EXHIBIT NNN
Date NOV 24 1950 No. NNN IDENTIFICATION
Date NOV 24 1950 No. NNN IN EVIDENCE
Clerk, U. S. District Court, Sou. Dist. of Calif.
Deputy Clerk

CURTISS-WRIGHT MODELS 21B AND 23
(REFER: DEF. EXH. 136)

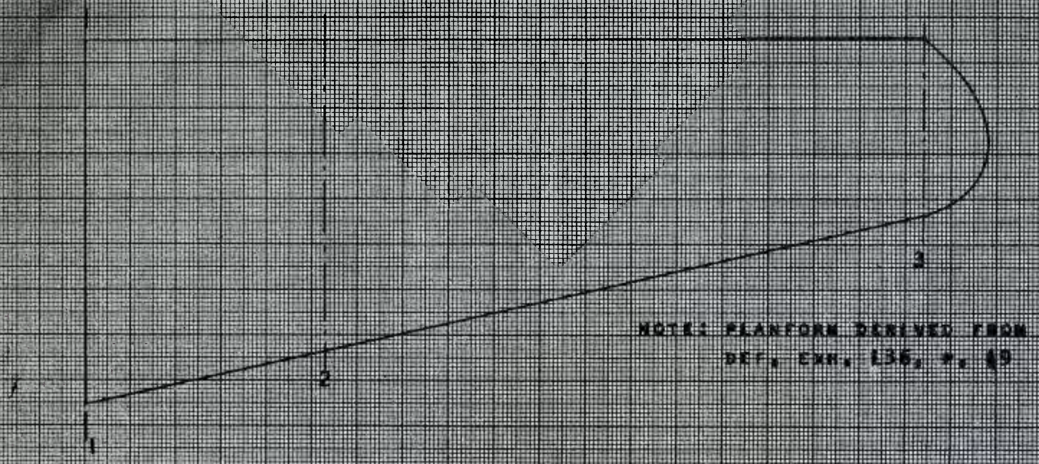

SECTION	1	2	3
PROFILE	CW 23	NACA 2314	CW 19
LOCATION % OF SEMI-SPAN	0	26.8	92.9
MEAN CAMBER % OF CHORD	0	2.0	3.4
THICKNESS RATIO % OF CHORD	19.0	14.0	10.0

LINEAR DISTRIBUTION

MEAN CAMBER % OF CHORD	0	.56	3.4
THICKNESS RATIO % OF CHORD	19.0	17.5	10.0

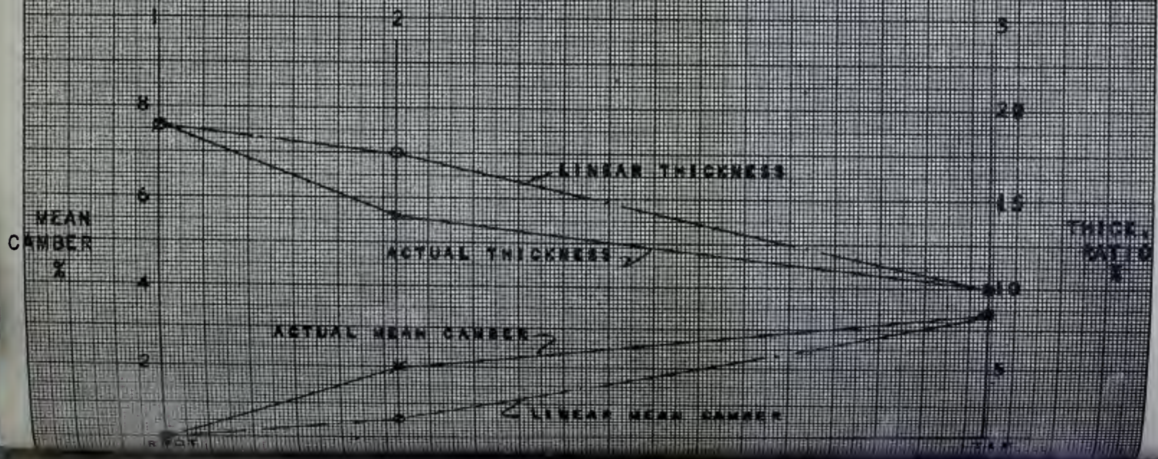

DEFENDANTS' EXHIBIT OOO

Report No. 19-C4

Curtiss-Wright Airplane Co.

Robertson, Mo.

Engineering Department

Curtiss-Wright Sparrow, Model 19L
(2PCLM)

1 Lambert R-266, 90 H. P. Engine

Modification of Wing
Structural Considerations

Submitted By
/s/ LLOYD F. ENGELHARDT

Section....Structures.

No. of Pages: 11. Date: Oct. 3, 1935.

Revisions ....

Pages...........
Date Affected Remarks

....

....

Modification of Wing

Introduction:

In order to meet the especially rigid requirements of a particular customer relative to stalling and spinning it was found necessary to modify the contour of the airfoil section in the outer portion

Defendants' Exhibit OOO—(Continued)

of the wing and at the same time to give the wing tip a certain amount of "wash-out."

To accomplish these changes an outer shell is added which extends below and slightly forward of the original lines. The plan form on Page 2 shows the change in area. The airfoil section on Page 3 shows the modification of the airfoil at the station 15 inches inboard of the tip (designated as A on page 2). On page 4 is a foreshortened plot of the mean camber lines of the modified airfoil and several of the N.A.C.A. series.

Drawing No. 19-03-13 gives all details of construction of the outer shell addition.

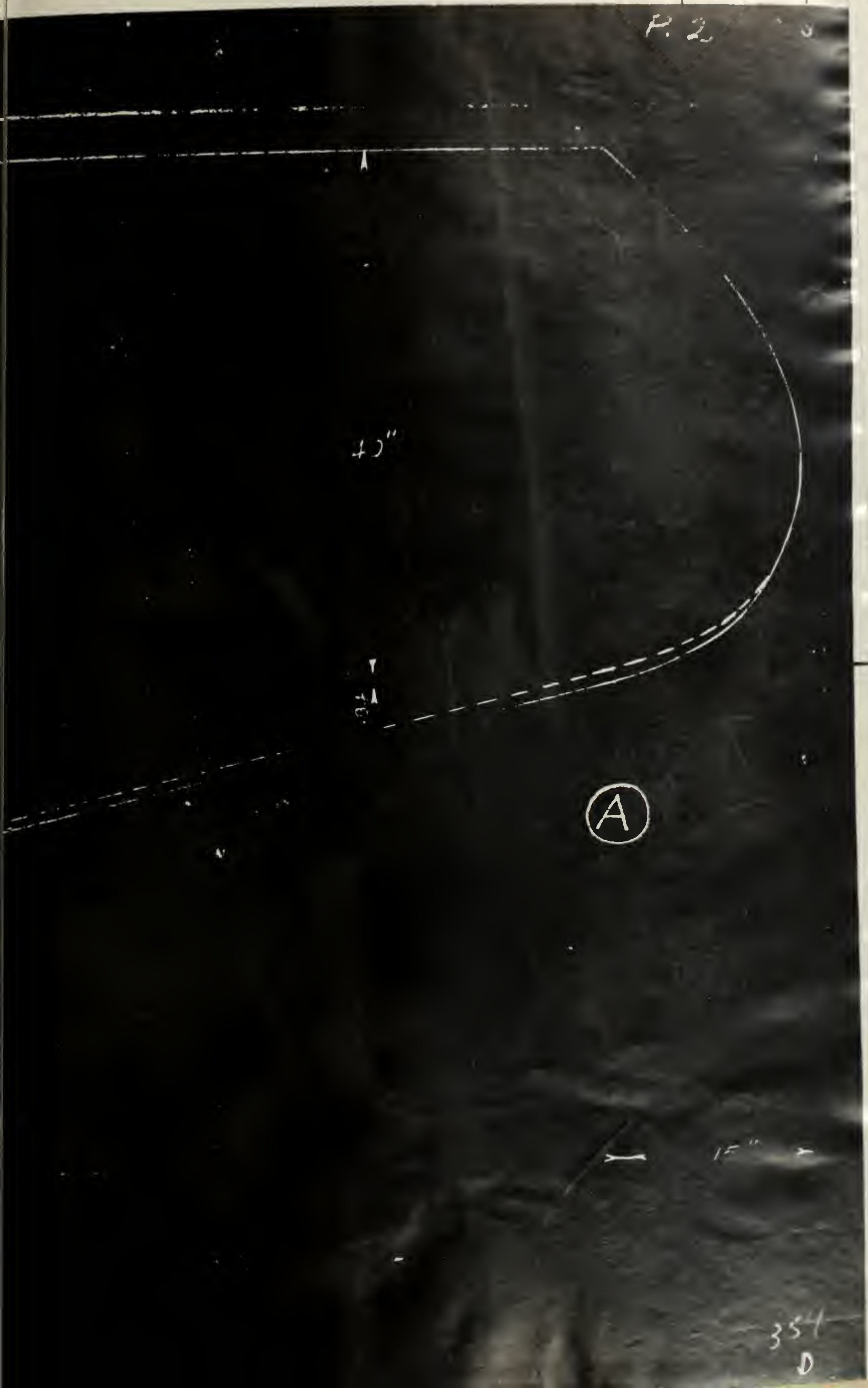
P. 2
A
354
D

gelhardt
3-35

CURTISS-WRIGHT AIRPLANE CO.
ROBERTSON, MO.

Page 2
Model 191
Report 19-C4

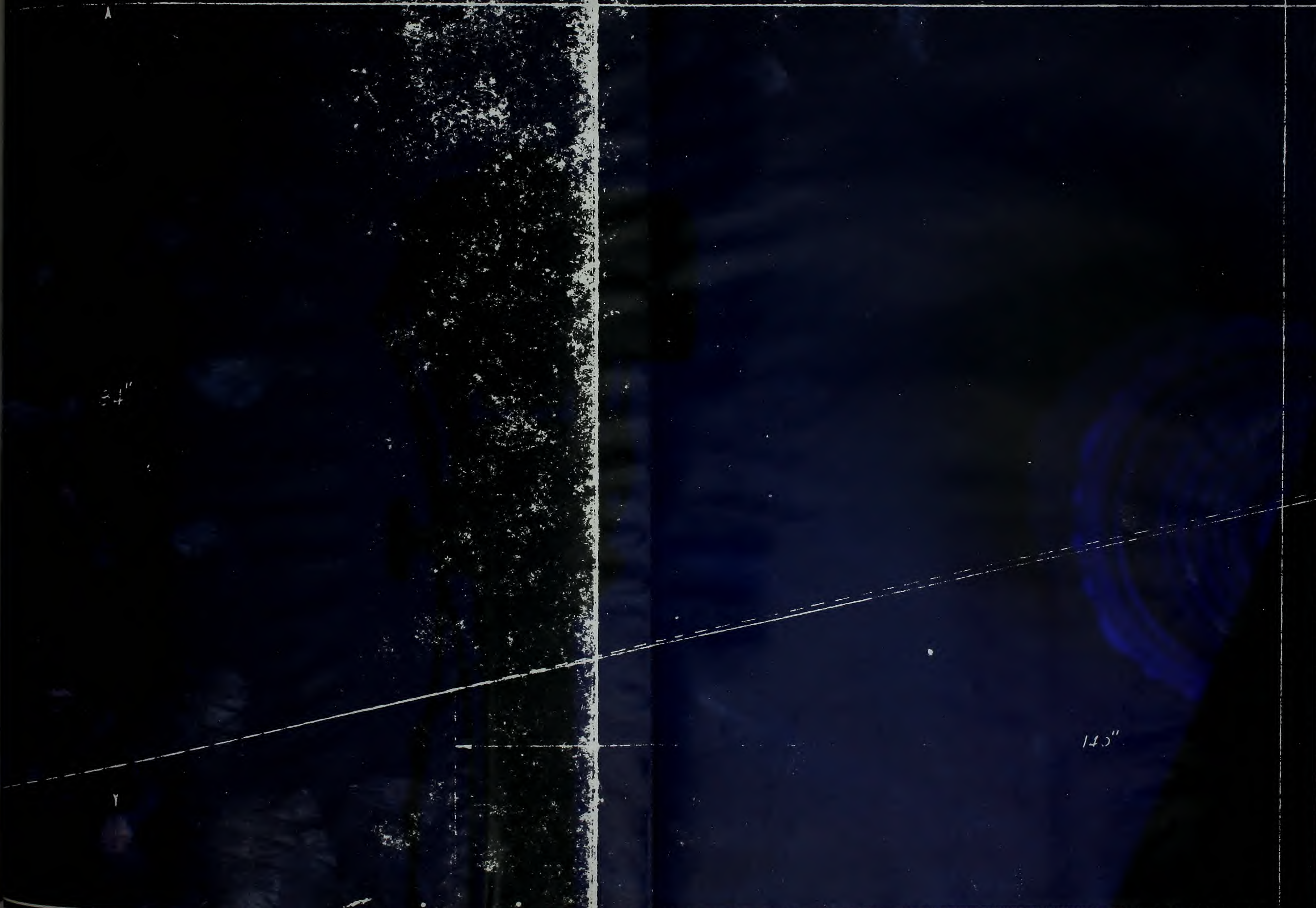

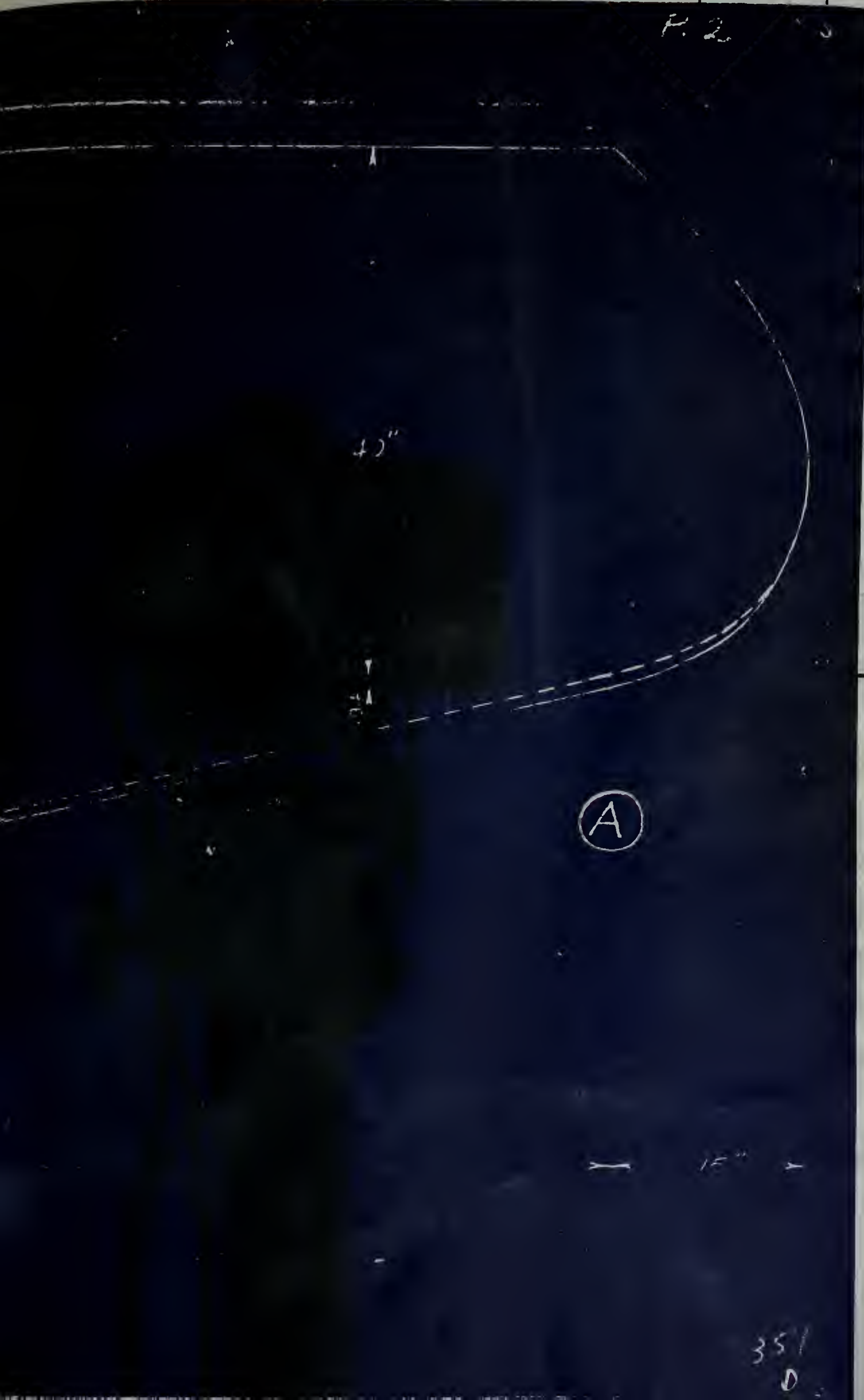
A

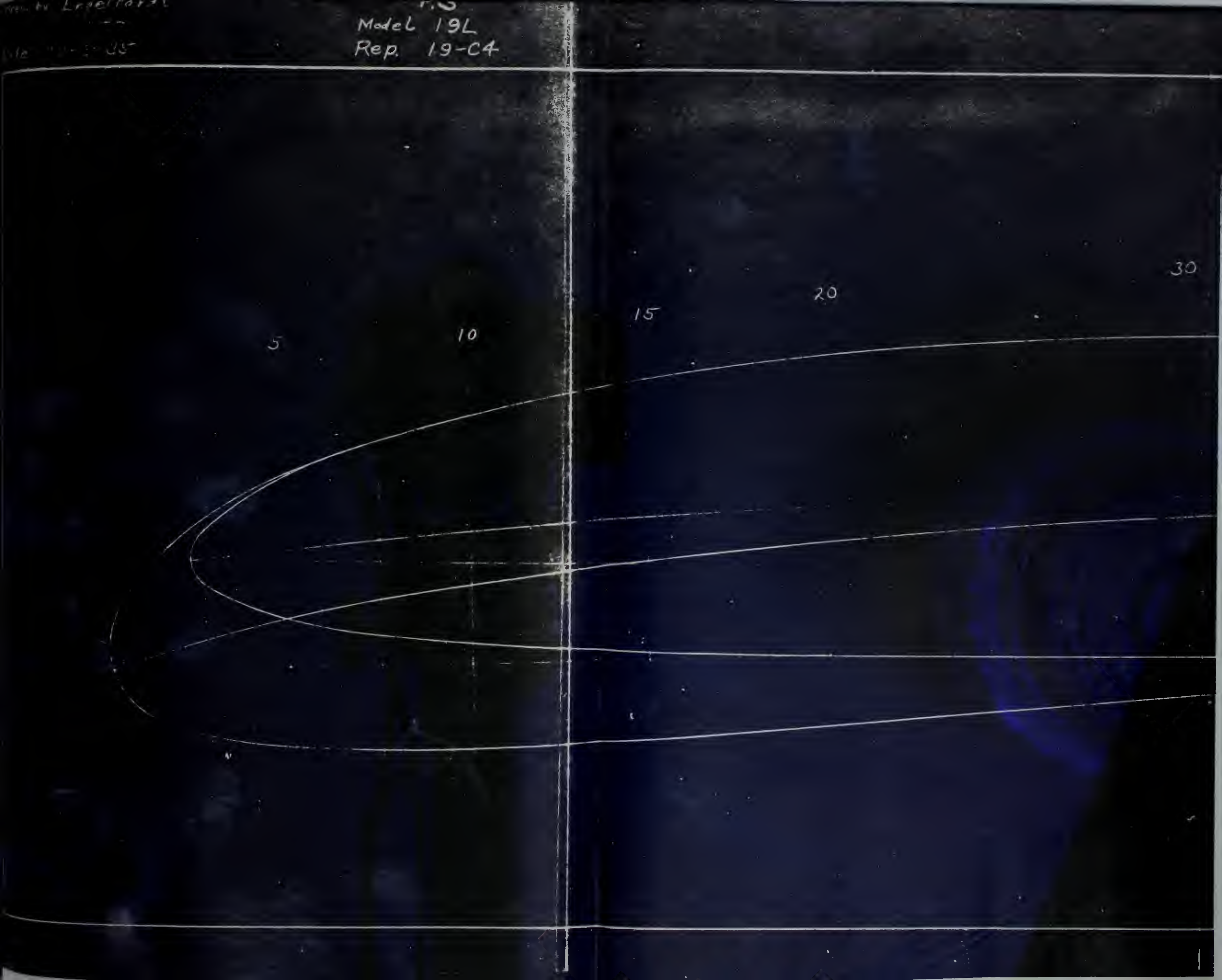
Model 19L
Rep. 19-C4
5
10
15
20
30

86

40

53

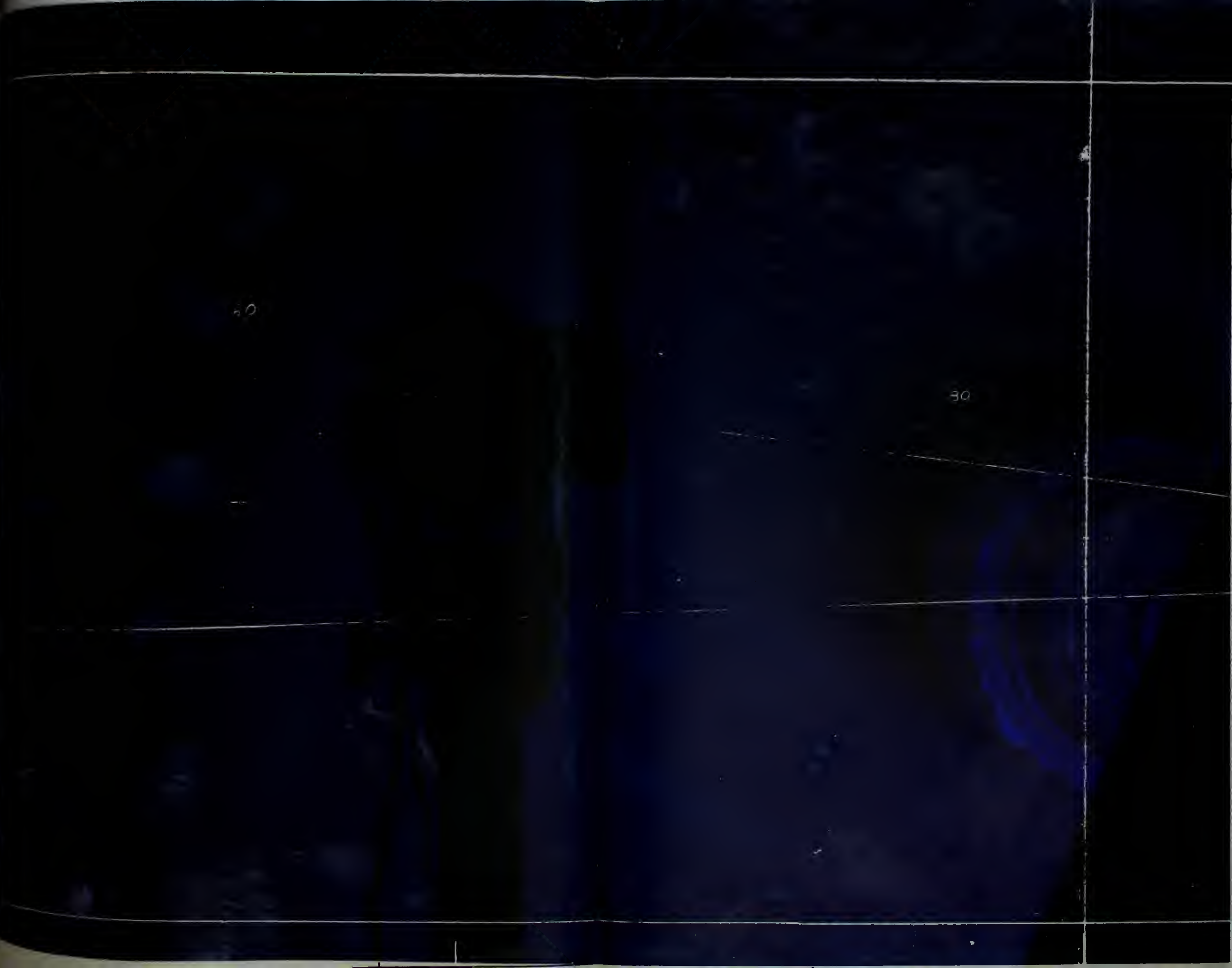

30

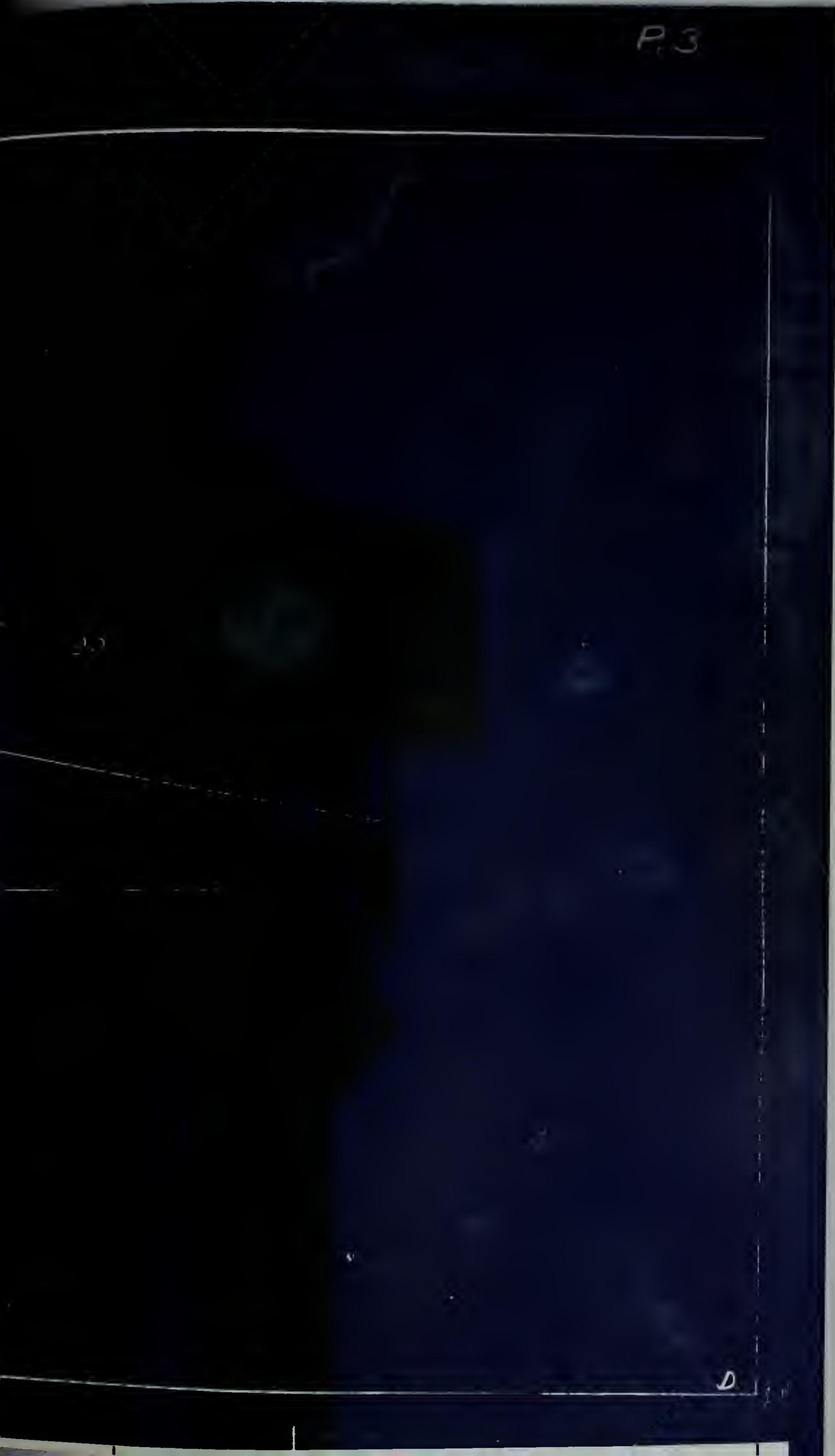
P.3
D

Defendants' Exhibit OOO—(Continued)

Report No. 19-Y3

Curtiss-Wright Airplane Co.

Robertson, Mo.

Engineering Department

Curtiss-Wright Sparrow, Model 19L
(2PCLM)
1 Lambert R-266, 90 H.P. Engine

Flight Tests
Sparrow No. 1

Submitted By

C. W. Scott. Section..........
No. of Pages...... Date 9/19/35
Revisions ....

Pages........
Date Affected Remarks

....

....

Flight No. 2

Date, 7/29/35 Pilot, E. K. Campbell
Take-Off, 6:30 A.M. Observer, C. W. Scott
Land, 7:15 A.M.
Place, Lambert Field
Sta. Temp. 92.
Sta. Wind, E. 5
Sta. Bar., 29.98
Gross Weight, 1,668
C. G. 22.65
Propeller Diameter, 6.5′
Propeller Pitch, 16 Deg.

Defendants' Exhibit OOO—(Continued)

Alt.	Temp.	I.A.S.	RPM	Oil
2000	83	94	2060	154
True C.A.S.		97	Speed	103

Eng. Compt.	Thermocouples					Man. Rdgs	("$H^2 0$)
	#1	#2	#3	#4	#5		
159	530	530	390	380	460	Ex. #1	8½
						Ex. #2	4
						Nose	7.2
						Eng.	6.5
						Ram	10.0

Fuel Pressure, 2.5
Oil Pressure, 65.

Full Throttle.				CAS.	TAS
2000	80	105	2270	109	115.3

Power Stall, Flaps Up, 54 I.A.S.,
Power Off, Flaps Down, 52 "

47 C.A.S. Vicious Stall—Fell to right.

44 C.A.S. Vicious Stall—Fell to right.

On landing, it was found the L.H. landing gear did not stay up.

After this flight the following work was done on the ship:

1. Repair safety catch, left hand gear.
2. Install strings on right hand wing.

The takeoff characteristics were poor, no doubt due in part to the fact that the fixed slot was stalled thruout take-off. The time to accelerate to flying speed seems too much. The take-off speed was approximately 50 mph indicated air speed. Landing speed, 45 mph.

None of these speeds are calibrated.

Defendants' Exhibit OOO—(Continued)

On this flight considerable back pressure was observed on #1 and #2 cylinders. These two cylinders were also running at the highest head temperature. A new manifold will be tried with larger tubing on these two cylinders to correct this trouble.

Previous to this flight the ship was weighed and the C.G. located at 22.65% of the M.A.C.

Results of this flight:

1. Ailerons good but too much lag.
2. Elevators very sensitive.
3. Rudder light and mushy at stall.
4. Stalls vicious and sudden with no warning.

The following work was done for flight #3:

1. Remove and inspect safety catch on L.H. landing gear.
2. Install silk threads on R.H. wing.

Report No. 19-Y4

Curtiss-Wright Airplane Co.

Robertson, Mo.

Engineering Department

Curtiss-Wright Coupe, Model 19L
1 Lambert R-266, 90 H.P. Engine

Summary of Flight Tests
Coupe No. 1

Submitted By

C. W. Scott — Section

No. of Pages 15 — Date Nov. 22, 1935.

Defendants' Exhibit OOO—(Continued)

Revisions

Pages———

Date Affected

Remarks

. . . .

. . . .

Introduction

The Model 19L has been run through a long series of very special flight tests. The purpose of this report is to draw conclusions from the results obtained rather than to go in to the detail of all of the different phases of the flight tests conducted. Briefly, the purpose of all of these tests has been first, to eliminate what was considered an undesirable stall characteristic of the basic airplane; second, to obtain satisfactory power plant cooling and operation; and third, a thorough check on the aerodynamic characteristics of the ship.

The results of the flying that has been accomplished on the Model 19L as finally modified are contained briefly in this report.

Admitted November 24, 1950.

Case No. 10930-Y
Garrett vs. Consolidated
Def EXHIBIT RRR
Date ______ No. ______ IDENTIFICATION
Date Nov 23 1950 No. RRR IN EVIDENCE
Clerk, U. S. District Court, Sou. Dist. of Calif.
Deputy Clerk

"LUFTFAHRTFORSCHUNG" (1938) pp. 604-618
(REFER EXHIBIT #22)

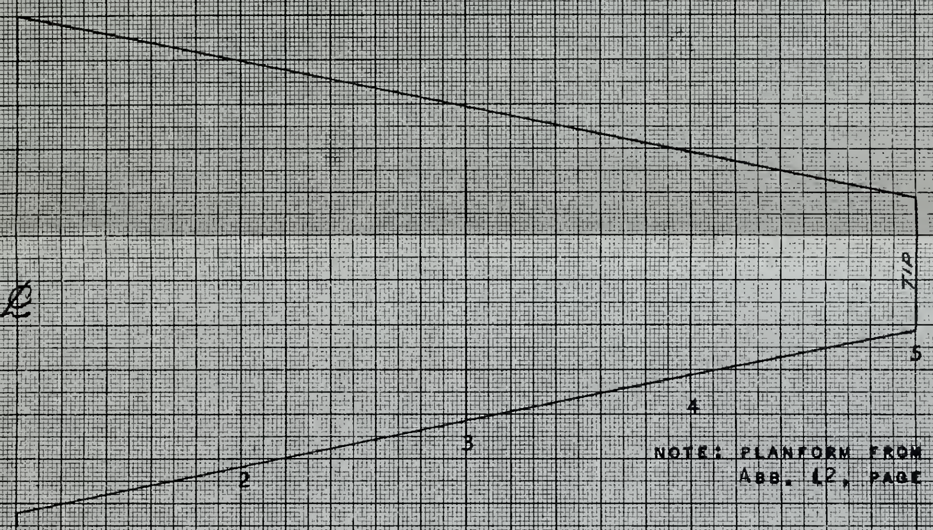

NOTE: PLANFORM FROM ABB. 12, PAGE 612

SECTION	1	2	3	4	5
LOCATION % SEMI-SPAN	0	25	50	75	100
MEAN CAMBER % OF CHORD	0	2	4	6	6
THICKNESS RATIO % OF CHORD	21	18	15	12	9

LINEAR DISTRIBUTION

MEAN CAMBER % OF CHORD	0	0.5	1.3	2.7	6
THICKNESS RATIO % OF CHORD	21	20	18.5	15.6	9

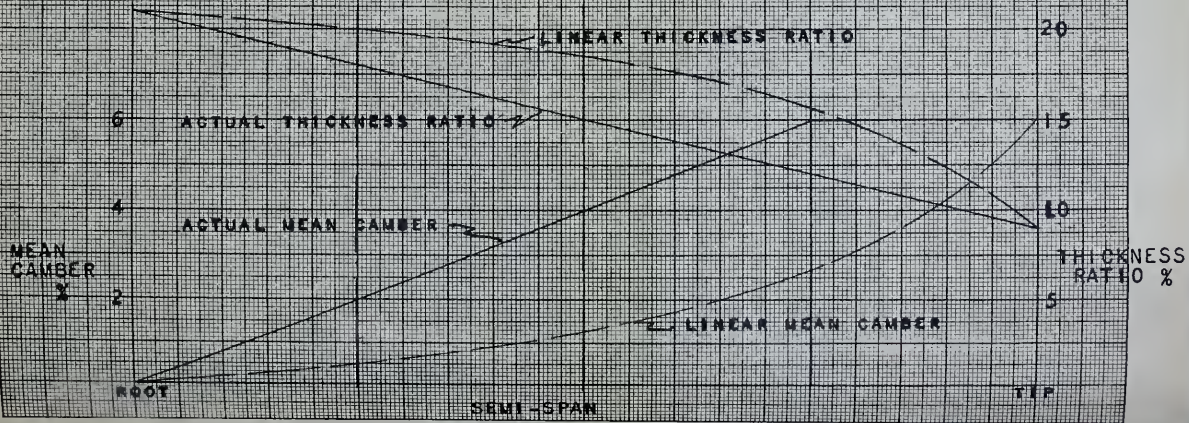

SECTION DERIVED FROM FIG. 4

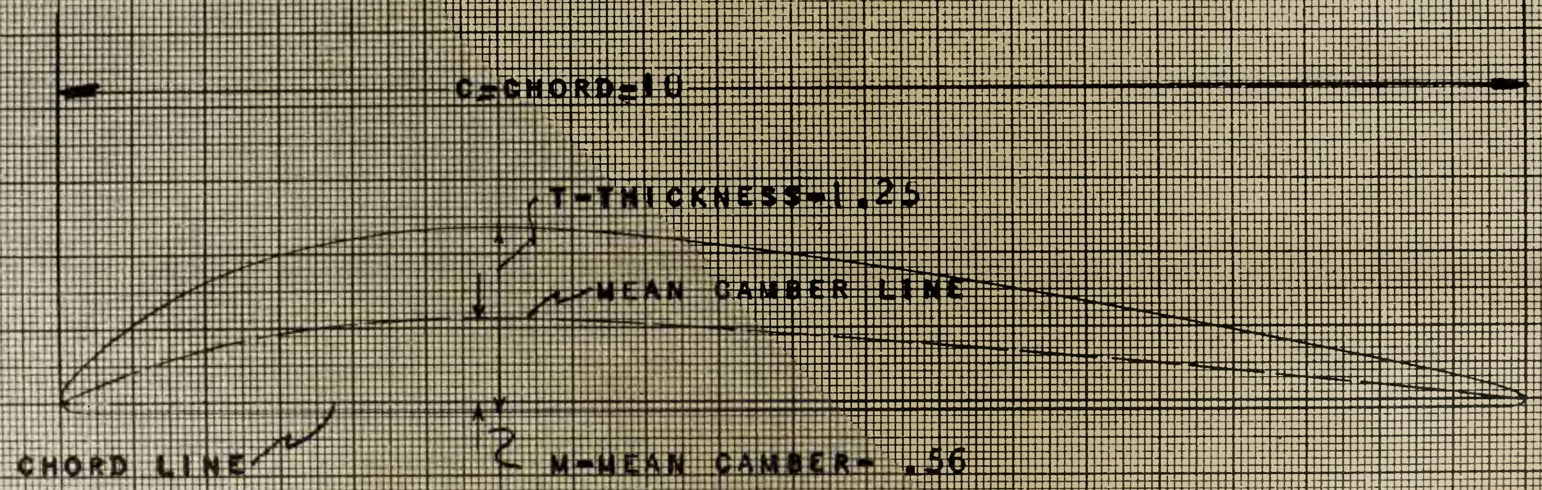

FIGURE 4

U.S. PATENT #1,547,644 - CRONSTEDT

MEAN CAMBER = M/C = 5.6% (OF CHORD)

THICKNESS RATIO = T/C = 12.5% (OF CHORD)

SECTION DERIVED FROM FIG. 5

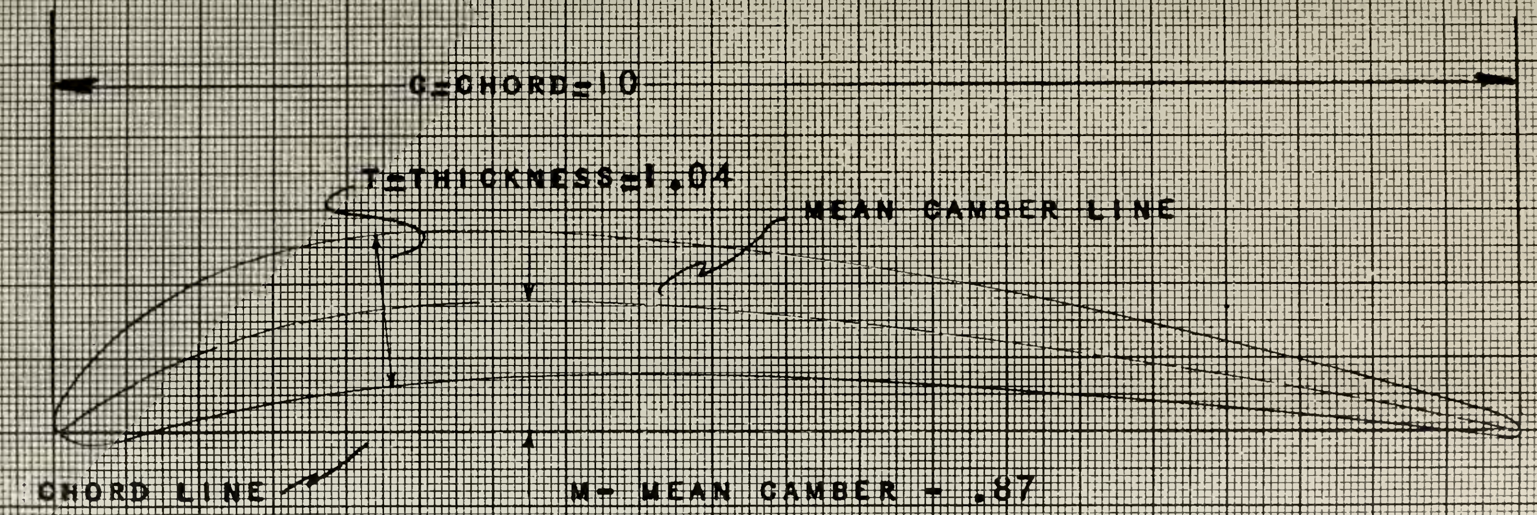

FIGURE 5

U.S. PATENT #1,547,644 - CRONSTEDT

MEAN CAMBER = M/C = 8.7% (OF CHORD)

THICKNESS RATIO = T/C = 10.4% (OF CHORD)

SECTION DERIVED FROM FIG. 3

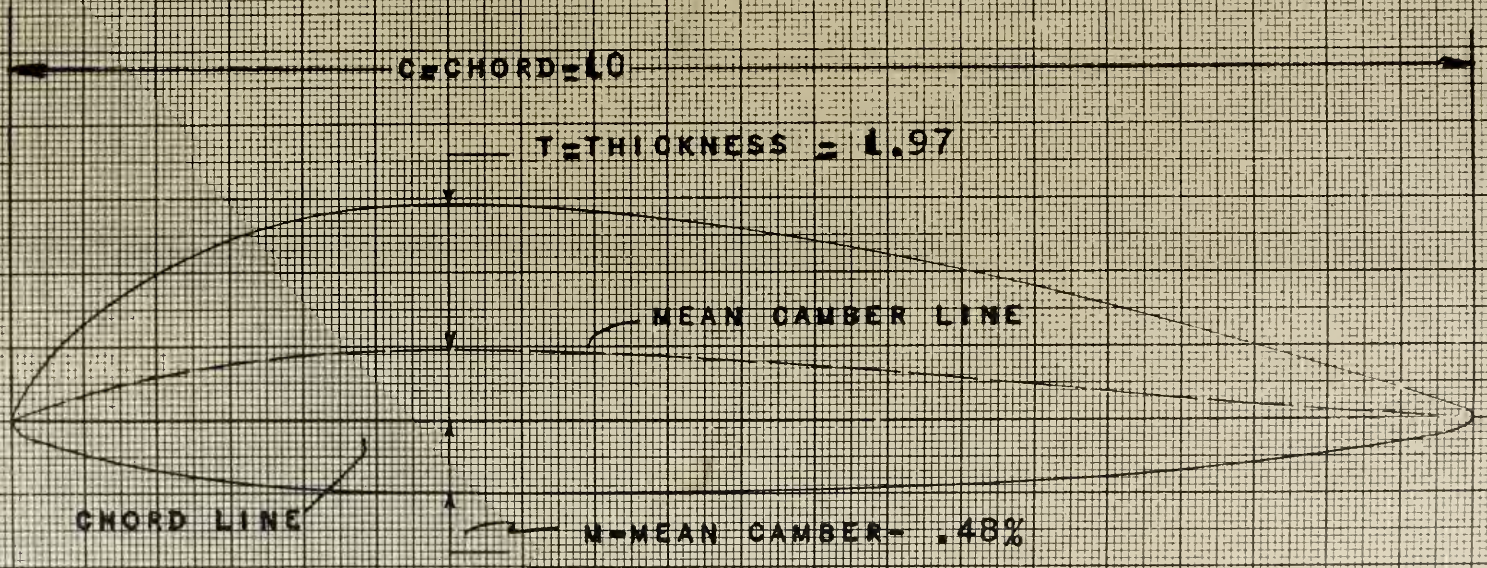

FIGURE 3

US. PATENT #1,547,644 - CRONSTEDT

MEAN CAMBER = M/C = 4.8% (OF CHORD)

THICKNESS RATIO = T/C = 19.7% (OF CHORD)

U.S. PATENT #1,547,644 - CRONSTEDT

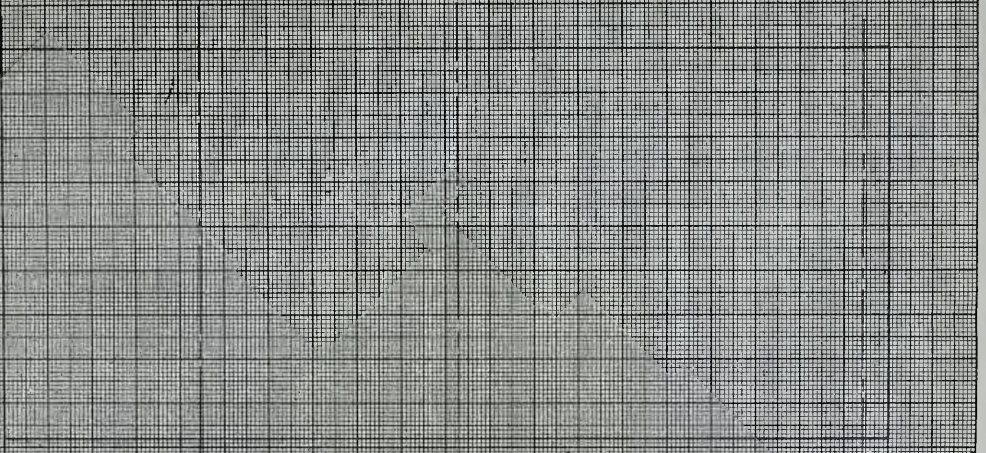

1 (FIG. 3) 2 (FIG. 4) 3 (FIG. 5)

NOTE: PLANFORM DERIVED FROM FIGS. 1 AND 2 OF PATENT

SECTION	1	2	3
LOCATION % OF SEMISPAN	22.5	51.5	97.0
MEAN CAMBER % OF CHORD	4.8	5.6	8.7
THICKNESS RATIO % OF CHORD	19.7	12.5	10.4

LINEAR DISTRIBUTION

MEAN CAMBER % OF CHORD	4.8	6.3	8.7
THICKNESS RATIO % OF CHORD	19.7	16.2	10.4

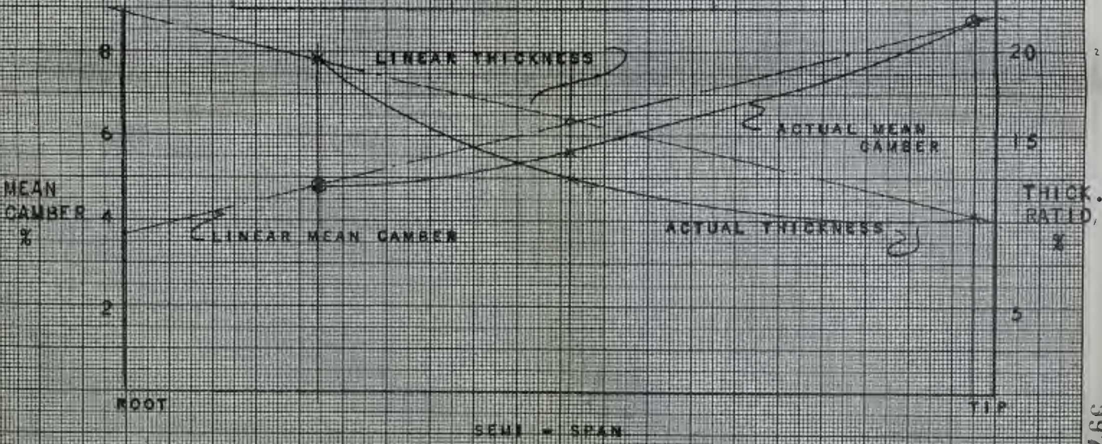

Admitted November 24, 1950.

Farbell vs Consol Vultee et al
Defts EXHIBIT 222
Date........ No. .... IDENTIFICATION
Date NOV 27 1950 No. 222 IN EVIDENCE
Clerk, U. S. District Court, Sou. Dist. of Calif.
E Muntrom Jr Deputy Clerk.

C = CHORD

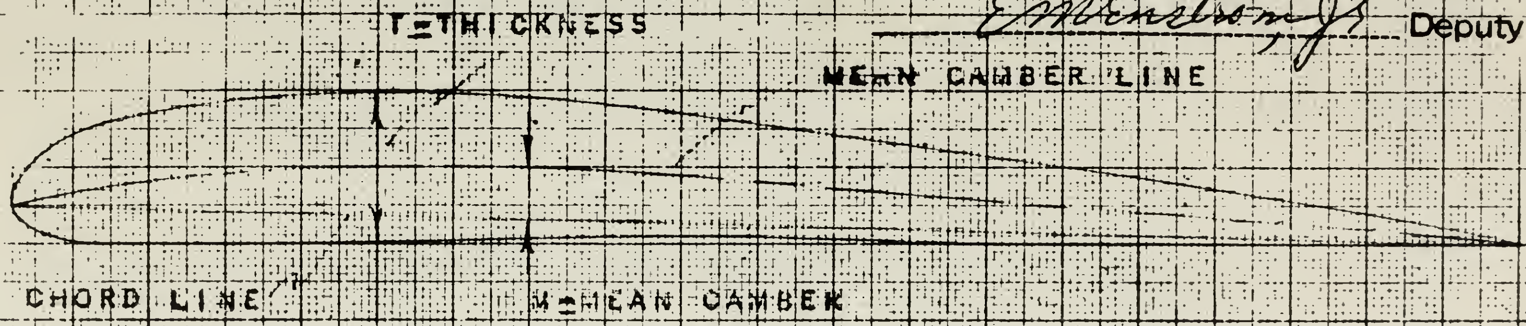

C W 19

MEAN CAMBER = M/C = 3.4% (OF CHORD)

THICKNESS RATIO = T/C = 10% (OF CHORD)

$t/c = \frac{4.10}{40.93c} = 0.100 = 10.0\%c$

$m/c = \frac{1.4}{40.93c} = 0.034 = 3.4\%c$

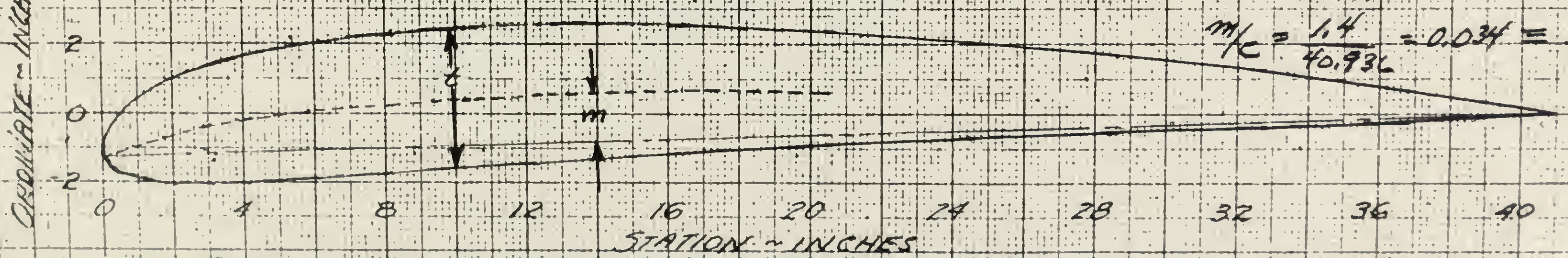

SECTION DERIVED FROM ORDINATES GIVEN ON CURTISS-WRIGHT DWG. NO. 19-03-220

DEFENDANTS' EXHIBITS REFERRED TO IN ANSWER TO INTERROGATORY XVII

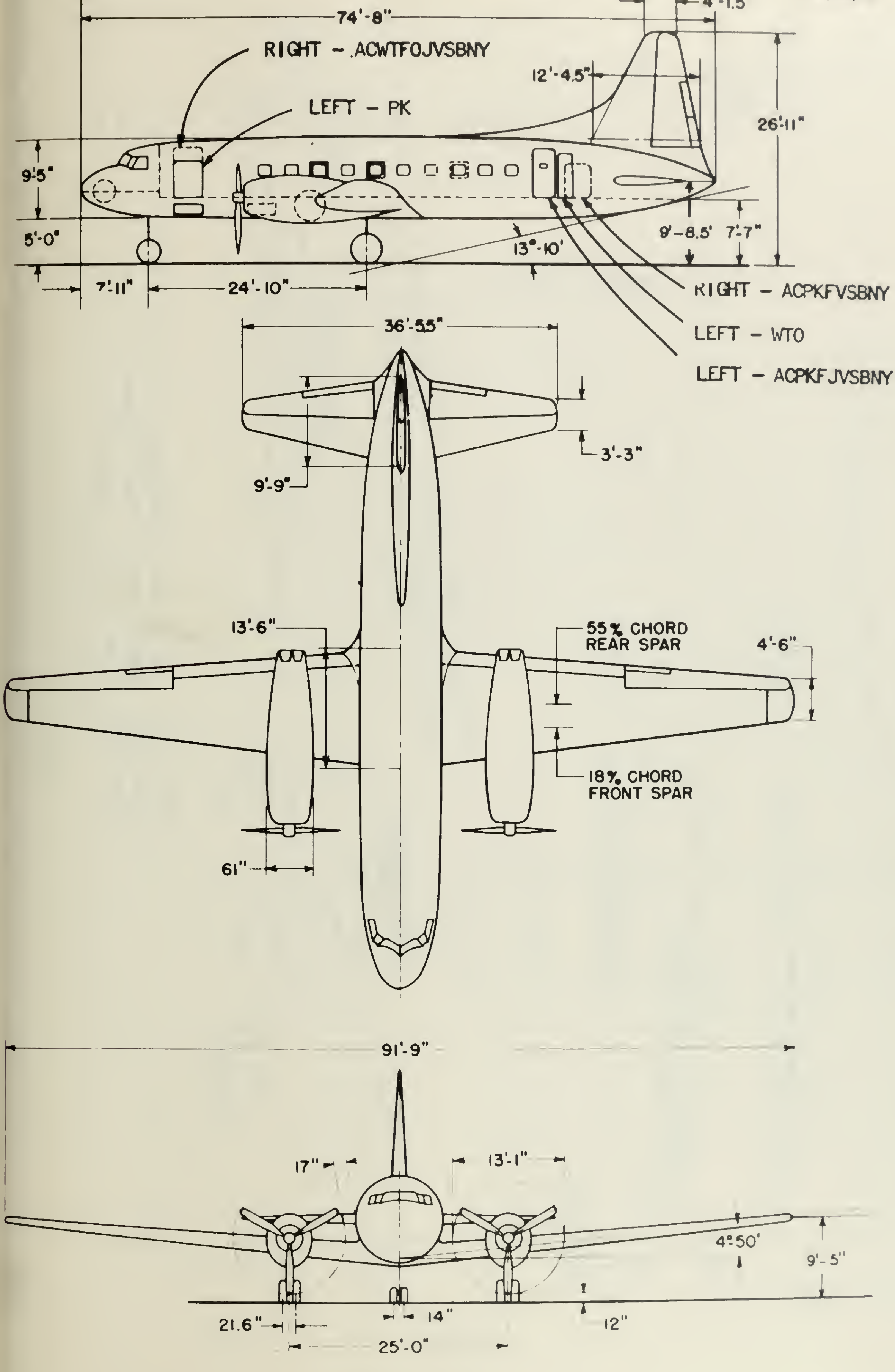
74'-8"
4'-1.5"
RIGHT - ACWTFOJVSBNY
LEFT - PK
12'-4.5"
26'-11"
9'-5"
5'-0"
9'-8.5' 7'-7"
13°-10'
7'-11"
24'-10"
RIGHT - ACPKFVSBNY
LEFT - WTO
LEFT - ACPKFJVSBNY
36'-5.5"
3'-3"
9'-9"
13'-6"
55% CHORD
REAR SPAR
4'-6"
18% CHORD
FRONT SPAR
61"
91'-9"
17"
13'-1"
4°50'
9'-5"
21.6"
14"
12"
25'-0"

THREE VIEW

CONVAIR 440 - ENGINEERING DATA BOOK

GENERAL WING DIMENSIONS

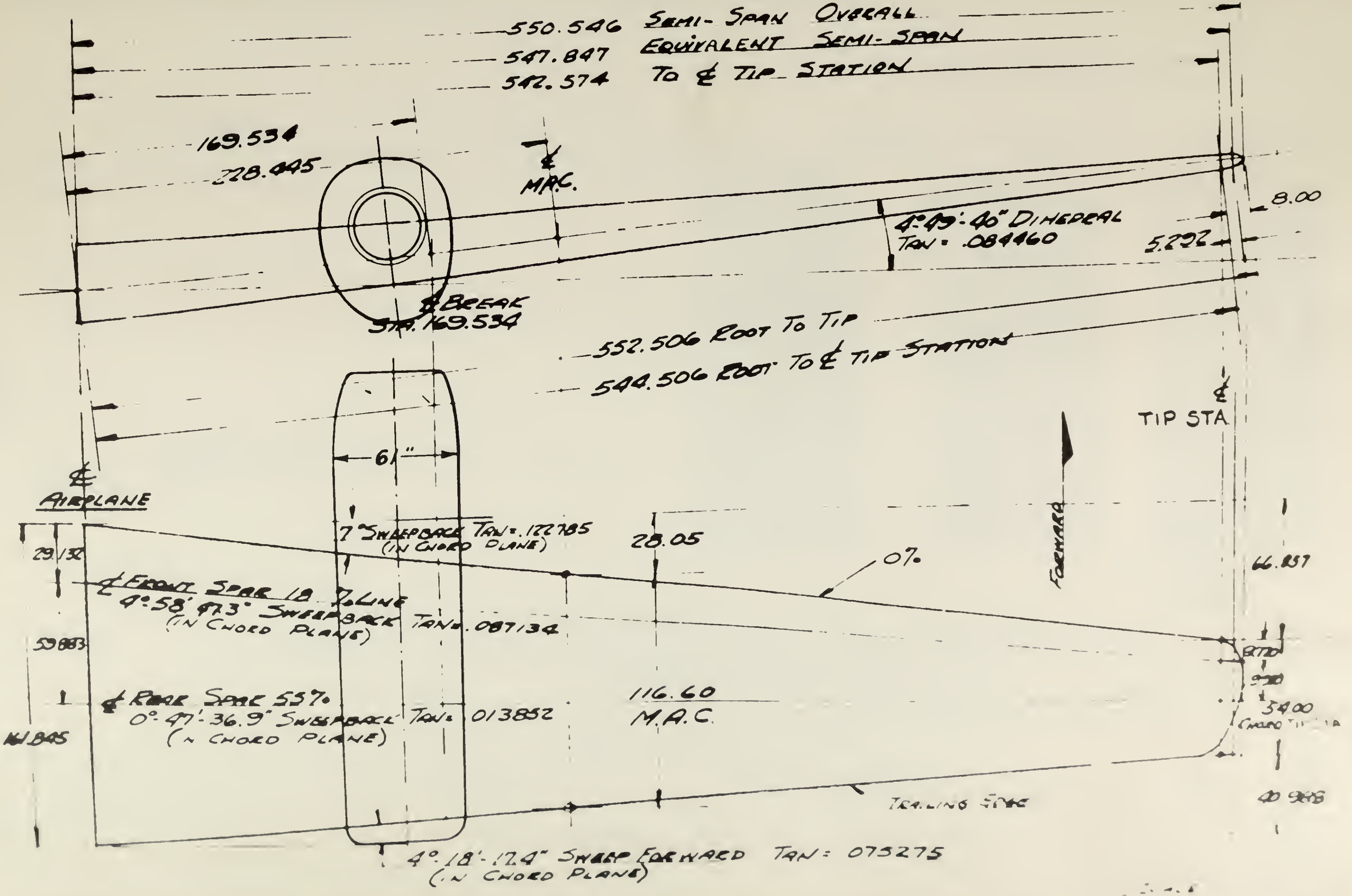

EXHIBIT

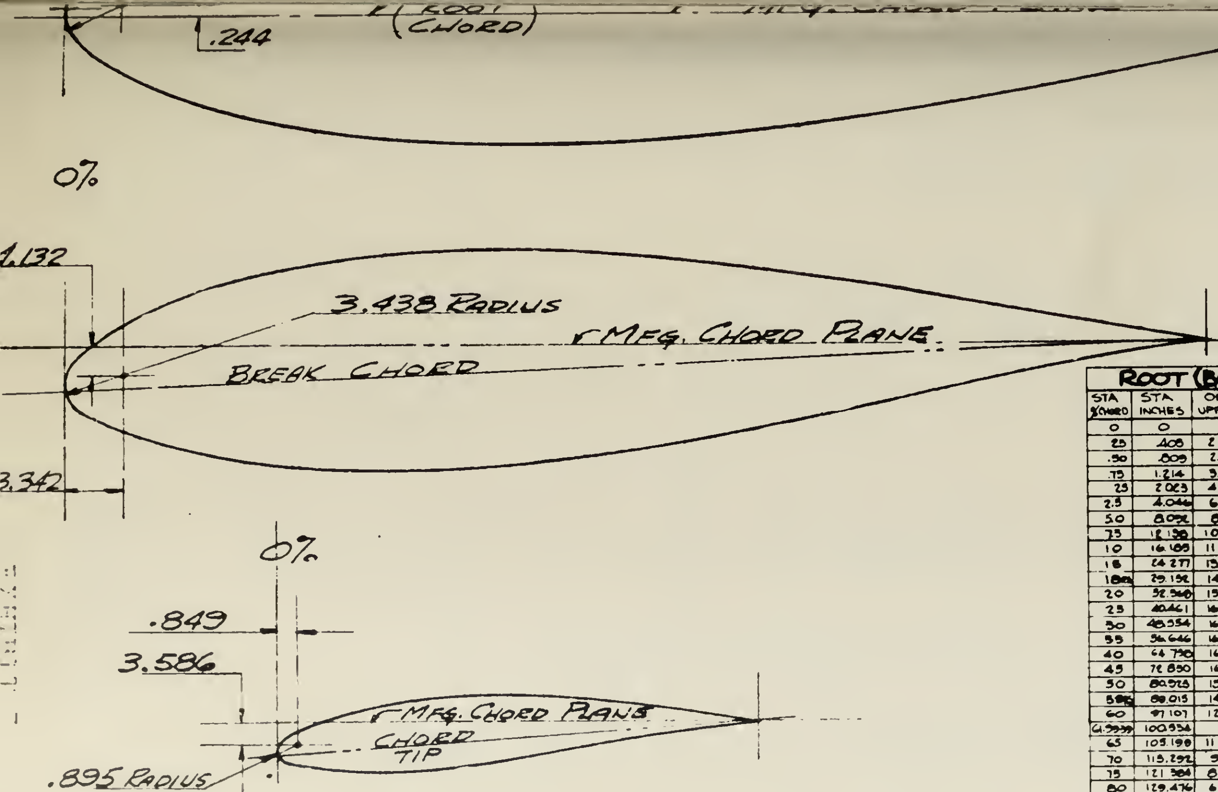

"ALL ORDINATES GIVEN FROM MFG. CHORD PLANE"

N.A.C.A. 63,4-120

ROOT (BASIC)			
STA %CHORD	STA INCHES	ORD UPPER	ORD LOWER
0	0	—	0
.25	.408	2.232	-1.738
.50	.809	2.997	-2.367
.75	1.214	3.600	-3.166
1.25	2.023	4.300	-4.048
2.5	4.046	6.102	-5.388
5.0	8.092	8.307	-7.610
7.5	12.138	10.064	-9.244
10	16.185	11.468	-10.820
15	24.277	13.680	-12.512
18a	29.152	14.681	-13.402
20	32.360	15.245	-13.900
25	40.461	16.325	-14.844
30	48.554	16.879	-15.320
35	56.646	16.982	-15.320
40	64.738	16.660	-14.947
45	72.830	16.040	-14.270
50	80.923	15.165	-13.360
55a	89.015	14.066	-12.288
60	97.107	12.768	-11.016
61.9999	100.334		
65	105.198	11.505	-9.625
70	113.292	9.787	-8.100
75	121.384	8.244	-6.774
80	129.476	6.689	-5.382
85	137.568	5.119	-4.000
90	145.661	3.508	-2.648
95	153.753	1.836	-1.340
100	161.845	-	-

N.A.C.A. 63,4-419

BREAK (169.534)			
STA. %CHORD	STA INCHES	ORD. UPPER	ORD. LOWER
0	0	—	-4.937
.25	.321	-2.481	-5.796
.50	.641	-1.941	-6.319
.75	.962	-1.306	-6.741
1.25	1.603	-.793	-7.556
2.5	3.207	+.557	-8.562
5.0	6.415	2.366	-9.650
7.5	9.620	4.161	-10.519
10	12.827	5.302	-11.209
15	19.240	7.648	-12.189
18a	23.088	8.665	-12.392
20	25.653	9.253	-12.801
25	32.067	10.451	-13.099
30	38.480	11.281	-13.097
35	44.893	11.608	-12.795
40	51.307	11.670	-12.157
45	57.720	11.477	-11.361
50	64.133	11.084	-10.420
55a	70.547	10.488	-9.365
60	76.960	8.690	-8.205
61.9999	79.518		
65	83.374	8.730	-6.974
70	89.787	7.762	-5.751
75	96.200	6.709	-4.565
80	102.614	5.600	-3.481
85	109.027	4.484	-2.441
90	115.440	3.179	-1.480
95	121.854	1.809	-.647
100	128.267	—	—

N.A.C.A. 63,4-515

TIP (544.506)			
STA. %CHORD	STA. INCHES	ORD UPPER	ORD LOWER
0	-	-	-3.875
.25	.135	-3.000	-4.135
.50	.270	-2.800	-4.300
.75	.405	-2.640	-4.417
1.25	.675	-2.310	-4.600
2.5	1.350	-1.855	-4.875
5.0	2.700	-1.060	-5.170
7.5	4.050	-.480	-5.355
10	5.400	+.125	-5.477
15	8.100	1.028	-5.625
18a	9.720	1.469	-5.649
20	10.800	1.755	-5.632
25	13.500	2.285	-5.598
30	16.200	2.682	-5.445
35	18.900	2.945	-5.195
40	21.600	3.085	-4.865
45	24.300	3.145	-4.475
50	27.000	3.115	-4.045
55a	29.700	3.017	-3.587
60	32.400	2.852	-3.095
61.9909	33.477	—	
65	35.100	2.659	-2.595
70	37.800	2.385	-2.107
75	40.500	2.100	-1.640
80	43.200	1.790	-1.200
85	45.900	1.460	-.805
90	48.600	1.092	-.465
95	51.300	.665	-.181
100	54.000	—	—

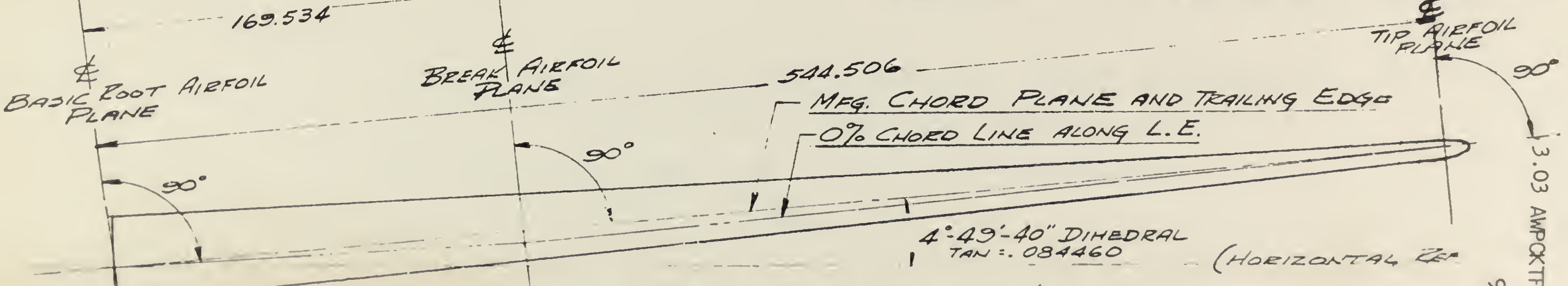

— VIEW LOOKING AFT AT L.H. WING. —

3.03 AWPCKTFOJVSBNY
9-19-46R

RELATION BETWEEN ROOT, BREAK AND TIP CHORD PLANES

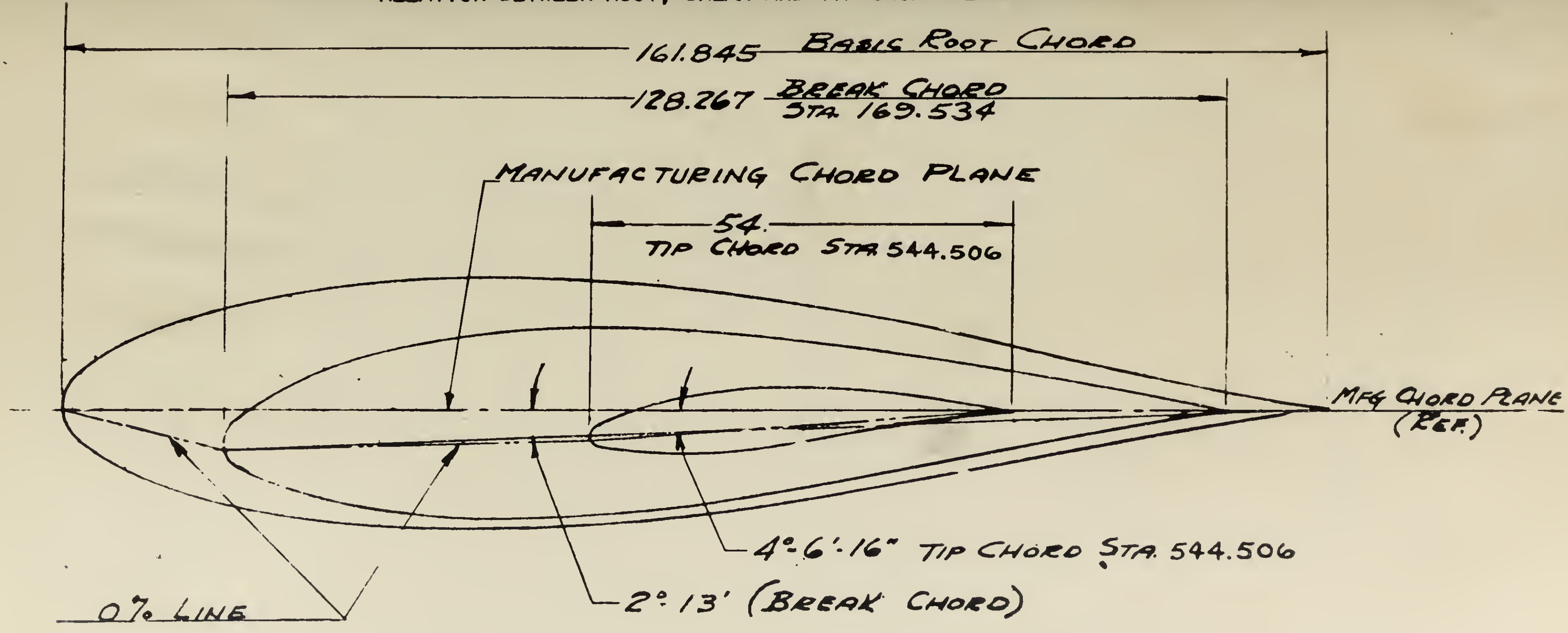

VIEW SHOWING RELATION BETWEEN ROOT, BREAK, AND TIP CHORD PLANES AND MANNER IN WHICH THE DEGREE OF WASHOUT IN WING IS MEASURED.

INCIDENCE ANGLE 4° REF.

EXHIBIT 4

3.0201 AWPCKTFOJVSBNY
9-19-46R

Consolidated Vultee Aircraft Corporation
San Diego Division

Page 10
Report No. ZD-240-040
Model 240
Date

3.0 Characteristics

3.5 Dimensions and Areas:

3.5.1 Wing Group:

Airfoil Section Designation:

Root	NACA 63.4—120
30.7% Semispan	NACA 63.4—419
Tip	NACA 63.4—515
Aerodynamic Washout	1° 12′
Wing Area	817 sq. ft.
Span (overall)	91 ft. 9 in.
Root Chord	13 ft. 6 in.
Tip Chord	4 ft. 6 in.
Taper Ratio (approximate)	3:1
Incidence Root	4°
Dihedral (reference Plane)	4° 50′
Sweepback (at 40% chord)	2° 30′
Aspect Ratio	10
Mean Aerodynamic Chord (true)	9 ft. 8.6 in.

3.5.3 Body Group:

Maximum Fuselage Cross Section:

Height	9 ft. 5 in.
Width	9 ft. 5 in.
Length, overall	74 ft. 8 in.
Height over tail (3-point position)	26 ft. 11 in.
Thread of main wheel	25 ft. 0 in.